ISSN: 2707-1146
e-ISSN: 2709-4189

NATURE & SCIENCE

International Scientific Journal







Nature & Science

International Scientific Journal

Volume: 8 Issue: 5

2026

International Indexing

© The Author(s) 2026. This is an open access journal under the CC BY-NC 4.0 license.

nature.science2000@aem.az
info@aem.az
aem.az/en

Founder

Researcher Mubariz HUSEYINOV, Azerbaijan Science Center / Azerbaijan
https://orcid.org/0000-0002-5274-0356
mubariz.6808@gmail.com

Editor-in-Chief

Elshad Gurbanov
Baku State University, Azerbaijan / Doctor of Biological Sciences, Professor
elshadqurbanov@bsu.edu.az
ORCID ID: 0000-0003-4627-3760
Scopus ID: 25227176700
Google Scholar: Profile

Editors

Ilham Shahmuradov
Institute of Genetic Resources MSERA, Azerbaijan / Doctor of Biological Sciences, Professor
ORCID ID: 0000-0001-5533-5906
Scopus ID: 7801464329
Google Scholar: Profile

Esmail Doustkhah
Istinye University, Türkiye / PhD in Chemistry, Assistant Professor
ORCID ID: 0000-0003-1459-1756
Scopus ID: 55785922800
Google Scholar: Profile

Abdallah Tageldein Mansour
King Faisal University, Saudi Arabia / PhD, Associate Professor
ORCID ID: 0000-0002-5963-5276
Scopus ID: 57191991437
Google Scholar: Profile

Victor Khrustalev
RUDN University, Russia / Doctor of Chemical Sciences, Professor
ORCID ID: 0000-0001-8806-2975
Scopus ID: 35466863600
Google Scholar: Profile

Rashid Iqbal
The Islamia University of Bahawalpur, Pakistan / PhD in Agronomy, Assistant Professor
ORCID ID: 0000-0003-0473-889X
Scopus ID: 57205928539
Google Scholar: Profile

Turkan Hasanova
Baku State University, Azerbaijan / PhD in Agricultural Sciences, Associate Professor
ORCID ID: 0000-0002-5040-2599
Scopus ID: 59834498300
Google Scholar: Profile

Assistant editors

Assoc. Prof. Dr. Vusala ISAGOVA, Institute of Geography, MSERA / Azerbaijan
https://orcid.org/0009-0005-5736-5515

Assoc. Prof. Dr. Lala BUNYATOVA, Sumgait State University / Azerbaijan
https://orcid.org/0000-0002-9140-745X

Dr. Rana KHANKISHIYEVA, Institute of Physics, MSERA / Azerbaijan
https://orcid.org/0000-0002-4532-9913

Researcher Gulnar ALIYEVA, Azerbaijan Science Center / Azerbaijan
https://orcid.org/0009-0004-1769-777X

Language editor

Prof. Dr. Azad MAMMADOV, Azerbaijan University of Languages / Azerbaijan
https://orcid.org/0000-0002-8357-1356

Editorial Board

Prof. Dr. Irada HUSEYNOVA, Institute of Molecular Biology, MSERA / Azerbaijan
Prof. Dr. Aziz SANCAR, University of North Carolina at Chapel Hill / USA
Prof. Dr. Yusuf BOZKURT, Mersin University / Türkiye
Prof. Dr. Nazim MURADOV, University of Central Florida / USA
Prof. Dr. Vagif FARZALIYEV, Institute of Chemistry of Additives named of Academician A.M.Guliyev / Azerbaijan
Prof. Dr. Gheorghe DUCA, Institute of Chemistry / Moldova
Prof. Dr. Namig MUSTAFAYEV, Azerbaijan State Agrarian University / Azerbaijan
Prof. Dr. Hasil FATALIYEV, Azerbaijan State Agrarian University / Azerbaijan
Prof. Dr. Mehmet KARATAŞ, Necmettin Erbakan University / Türkiye
Prof. Dr. Ibrahim MAMMADOV, Baku State University / Azerbaijan
Prof. Dr. Rinat ISKAKOV, Satbayev University / Kazakhstan
Assoc. Prof. Dr. Dunya BABANLI, Azerbaijan State Oil and Industry University / Azerbaijan
Assoc. Prof. Dr. Gunay MAMMADOVA, Institute of Geography, MSERA / Azerbaijan
Assoc. Prof. Dr. Fuad RZAYEV, Living Systems Research Institute, MSERA / Azerbaijan
Assoc. Prof. Dr. Ramil SADIGOV, Azerbaijan State University of Economics / Azerbaijan
Assoc. Prof. Dr. Svetlana GORNOVSKAYA, Bila Tserkva National Agrarian University / Ukraine
Dr. Aamir RAINA, Aligarh Muslim University / India
Dr. Bakhtiyor GANIYEV, Bukhara State University / Uzbekistan
Dr. Tohir BOZOROV, Chinese Academy of Sciences (CAS) / China
Dr. Muhammad Kashif KHAN, Sogang University / South Korea
Dr. Muhammad MADNEE, The Islamia University of Bahawalpur / Pakistan
Dr. Firoz Ahmad ANSARI, CCRUM-Drug Standardization Research Institute / India
Dr. Mahmuod Abubakar BASHIR, Aliko Dangote University of Science and Technology / Nigeria
Dr. Junaid AHMAD, University of Rome Tor Vergata / Italy

NATURE & SCIENCE
October 2026, Volume 8, Issue 5, pp. 7–20
DOI: https://doi.org/10.36719/2707-1146/68/7-20

Acacia nilotica Biochar Improves Sandy Soil Structure and Stimulates Root Development in Muscat Grape

Ghulam Murtaza[1], Muhammad Usman[2], and Rashid Iqbal[3*]

Abstract. *The effectiveness of biochar as a soil amendment is well recognized for improving soil fertility and plant root architecture. However, its beneficial effects on root development in perennial woody species require further investigation. In this 14-week greenhouse experiment, we evaluated the effects of Acacia nilotica-derived biochar on soil physical properties and Muscat grape growth. Muscat grape plants were grown in sandy soil amended with four biochar rates, 4%, 8%, 12%, and 16%, based on dry soil weight. Soil properties and root traits were then assessed. The results showed that adding 16% biochar to sandy soil reduced soil bulk density by 41%, increased total porosity by 51%, and improved water holding capacity by 1.11 times compared with sandy soil without biochar. Biochar incorporation also reduced soil acidity and improved soil buffering capacity, resulting in a more favorable soil pH several months after application. In addition, biochar stimulated fine root development, significantly increasing root length, root crossings, and root forks while reducing average root diameter. Overall, Acacia nilotica wood waste can be converted into valuable biochar for improving sandy soil quality and promoting grape root development. This approach supports waste recycling, improves soil physical conditions, enhances grape growth, and contributes to circular economy-based agriculture. Therefore, Acacia nilotica-derived biochar can be recommended as a promising soil amendment for Muscat grape cultivation, particularly in sandy soils where improved water retention and root growth are needed.*

Keywords: *Acacia bark-biochar, Muscat grape, Ultisol soil, root structure, soil amendment*

Introduction

Biochar is a stable carbon-rich material produced through the thermal decomposition of biomass under limited oxygen conditions (Yuan et al., 2026). Its application as a soil amendment has received increasing attention because it can improve soil water retention, nutrient availability, cation exchange capacity, porosity, and overall soil fertility (Liu et al., 2023). These benefits are especially important in sandy soils, which often have low organic matter, weak nutrient retention, poor aggregation, and limited water holding capacity. By improving soil structure and resource availability, biochar can create a more favorable root zone environment and support plant growth (Wang et al., 2024a).

[1]School of Ecology and Environmental Sciences, Yunnan University, Kunming, Yunnan, China
[2]School of Agriculture and Biology, Shanghai Jiao Tong University, Shanghai, China
[3]Department of Agronomy, Faculty of Agriculture and Environment, The Islamia University of Bahawalpur, Bahawalpur, Pakistan
[*]Corresponding author. E-mail: rashid.iqbal@iub.edu.pk
Received: 19 April 2026; Accepted: 21 September 2026; Published online: 25 October 2026
© The Author(s) 2026. This is an open access article distributed under the terms of the Creative Commons Attribution-NonCommercial 4.0 International License (CC BY-NC 4.0).

Plant roots are the primary interface for water and nutrient acquisition, and their architecture strongly determines plant establishment, stress tolerance, and productivity (Abubakar et al., 2023). Biochar can influence root growth indirectly by improving soil aeration, water availability, nutrient retention, and microbial activity. It may also affect root traits directly through changes in rhizosphere chemistry and root-soil contact (Wang et al., 2024b). Root length, surface area, diameter, branching, crossings, and forks are important indicators of how efficiently plants explore the soil and acquire resources (Zeng et al., 2024). However, most biochar studies have focused mainly on soil chemical properties (Jin et al., 2026), aboveground biomass, or crop yield, while root architectural responses have received comparatively less attention.

This knowledge gap is more evident in perennial woody crops, including grapevine (Su et al., 2023), where root development plays a long-term role in water uptake, nutrient acquisition, canopy growth, and productivity. In grapevines, the balance between aboveground growth and root system development is critical for plant performance, especially in sandy soils with poor water and nutrient retention (Fu et al., 2026; Hou et al., 2026). Although biochar has been widely evaluated in annual crops and short-term soil fertility studies (Suo et al., 2026), its role in modifying fine root development and root system architecture in perennial fruit crops remains insufficiently understood. Muscat grape is an economically important grape cultivar cultivated for fresh consumption and juice production. It can adapt to warm growing conditions, but its growth and productivity can be constrained by poor soil structure and low water retention, particularly in sandy soils (Li et al., 2022). Improving root zone conditions may therefore support better root proliferation, resource uptake, and plant establishment. *Acacia nilotica* wood waste is produced in considerable quantities and can be converted into biochar, offering a sustainable option for soil improvement and biomass waste management. Therefore, this study evaluated the effects of *Acacia nilotica*-derived biochar applied at different rates on sandy soil physical properties and root architecture of Muscat grape under greenhouse conditions. We hypothesized that biochar incorporation would improve soil structure, reduce bulk density, increase porosity and water holding capacity, and promote finer and more extensive root development. The study aimed to clarify whether biochar-mediated changes in sandy soil properties can enhance root traits in Muscat grape and provide a sustainable strategy for grape cultivation in low-fertility sandy soils.

Materials and Methods

Experimental Design and Relationship Between Pot and Column Experiments

Two complementary greenhouse experiments were conducted to evaluate the effect of *Acacia nilotica*-derived biochar on sandy soil properties and Muscat grape root development. The pot experiment was designed to assess plant growth, root architecture, and soil physical traits under a wider root zone condition. The column experiment was designed to provide a more vertically constrained rooting environment, allow controlled drainage, support leachate collection, and evaluate root development and pH changes under conditions that better represented downward root exploration. Both experiments used the same biochar rates, irrigation regime, fertilization practice, and ambient greenhouse conditions to ensure comparability between the two systems.

Biochar Treatments and Application Rate

Acacia nilotica-derived biochar was incorporated into sandy soil at 0, 4, 8, 12, and 16% on a dry weight basis. The 0% treatment served as the control. These relatively high biochar rates were selected because sandy soil has low organic matter, weak aggregation, poor nutrient retention, and limited water holding capacity. Therefore, a broad biochar gradient was required to detect clear changes in soil physical properties and root architectural responses. The highest rate was included to determine whether great improvement in porosity and water retention could support root development or whether excessive biochar addition might restrict root penetration by altering pore space and aeration.

Pot Experiment

In the pot experiment, Moscatello grape plants were grown individually in 6.1 L pots filled with the prepared biochar and soil mixtures. The experiment was arranged in a randomized complete block design with five treatments and six replications. Each replicate contained one pot, and each pot was considered the experimental unit for statistical analysis. When two plants were present in one pot, plant-level measurements were averaged before analysis so that the pot remained the experimental unit.

Column Experiment

In the column experiment, white polyethylene columns were filled with the same five biochar and soil mixtures used in the pot experiment. Fine wire mesh was fixed at the bottom of each column to prevent soil loss while allowing free drainage. One Moscatello plant was established in each column. The column experiment was maintained under the same greenhouse conditions, irrigation schedule, and fertilization regime as the pot experiment. Each column was considered the experimental unit for statistical analysis. At the end of the experiment, all plants were harvested destructively for root and aboveground trait measurements.

Irrigation and Fertilization Management

Plants were maintained under greenhouse conditions with an air temperature of 17 to 27 °C. Irrigation was applied through drip irrigation three times daily. The irrigation volume was adjusted according to plant growth stage, increasing from 120 mL day^{-1} during early growth to 240 mL day^{-1} during intermediate growth and 360 mL day^{-1} during the final growth period. Plants received a weekly nutrient solution containing nitrogen, phosphorus, potassium, and trace elements. The same irrigation and fertilization practices were applied to all treatments in both pot and column experiments.

Quantification of Soil Characteristics

A digital laboratory thermometer with a stainless-steel probe was employed to measure the soil temperature in pots monthly, precisely at a depth of 15 cm. Subsequently, in the column investigation, irrigation was manually initiated for 30 minutes, and leachate was collected monthly to assess the pH level during three months. A 50 mL sample of exudates was extracted from the lower section of each column and subsequently transported to the laboratory for pH measurement at ambient temperature utilizing a pH meter. Soil samples collected from pots evaluated soil physical properties, including water holding capacity (WHC), porosity, and bulk density. The gravimetric analysis of soil moisture was performed on the composite samples collected from each plot following the assessment. The samples were subjected to air-drying and thoroughly blended.

To avoid the loss of biochar or soil, the soil samples, each weighing 50 g, were carefully weighed and placed into funnels lined with filter paper. Deionized water was used to saturate all filter sheets. After that, 50 mL of water was incrementally added to every soil sample. The leachate water was collected in a beaker for 30 minutes until there was no more drainage at room temperature. To reduce water loss through evaporation, a plastic wrap was placed over the funnel top. The soil water holding capacity was calculated using a known volume of leachate water, as described by Yin et al. (2022).

$$\mathrm{WHC} = \frac{\text{added total water} - \text{volume of water run down}}{Soil\ sample\ dry\ weight} \times 100\% \qquad (1)$$

At the end of the trial, the bulk density of soil was measured using a single pooled sample from every treatment. The calculation of total porosity was performed using the bulk densities of soil, as expressed using the following equation:

$$\mathrm{P} = \frac{\text{Volume of voids}}{Total\ volume} \times 100\% \qquad (2)$$

The P denotes the total porosity. This equation can also be transformed into:

$$p = (1 - \frac{BD}{PD}) \times 100\% \quad (3)$$

The PD and BD represent the particle density and bulk density, respectively. The calculation of the density of soil particles (PD) can be determined using the following method:

$$PD = \frac{\text{Sample mass}}{Sample\ volume} \times 100\% \quad (4)$$

Nonetheless, for every soil sample, the density of soil particles is always presumed to be 2.65/g cm^{-3}. This allows us to compute total porosity in the following way:

$$p = (1 - \frac{BD}{2.65/g\ cm{-}3}) \times 100\% \quad (5)$$

Root Structure Determination

The roots in the pots were segregated by bisecting the containers from both sides. In the research column, columns were systematically arranged, and roots were meticulously extracted by hand. Subsequently, the roots were submerged in tap water, cleansed with a moderate water flow, and then soaked in deionized water until they were prepared for scanning. The overall root length, specific root length, average root diameter, crossing number, and root volume were quantified utilizing a root scanner and WinRHIZO software.

Data Analysis

Data from the pot and column experiments were analyzed separately. For the pot experiment, the pot was considered the experimental unit. For the column experiment, the column was considered the experimental unit. Plant measurements taken from more than one plant within the same pot were averaged before statistical analysis. Data were analyzed using the GLIMMIX procedure in SAS. Treatment effects were tested using Type III fixed effects, and means were separated using the Tukey Kramer test at $p \leq 0.05$. Diagnostic plots were used to verify normality and homogeneity of variance.

Results and Discussion

Assessment of Soil Characteristics

The data obtained from the initial two determinations indicated A negative relationship between applied biochar rate and soil temperature (Table 1). Nevertheless, third measurement exhibited a declining pattern, albeit without any statistically significant difference observed between the groups. The findings were consistent with previous research in which soil thermal conductivity underwent a considerable reduction of 7.5% and 3.5% with 9 Mg $ha^{-1}yr^{-1}$ and 4.5 Mg $ha^{-1}yr^{-1}$, respectively, when the biochar amount increased (Al-Issa et al., 2026). The observed negative relationship between applied biochar rate and soil temperature can be attributed to biochar's ability to alter soil physical properties, particularly its thermal conductivity and WHC. Biochar's porous structure can reduce soil thermal conductivity, leading to decreased heat transfer and a more stable soil temperature (Alsanhani, 2026). Additionally, biochar can increase soil water retention, which can also contribute to a more stable soil temperature. The reduction in thermal conductivity with increasing biochar amount is consistent with previous research, suggesting that biochar can effectively insulate the soil and reduce temperature fluctuations (Ameen et al., 2026). This mechanism can have implications for plant growth, microbial activity, and overall soil health. The lack of statistically significant differences in the third measurement may be due to various factors, such as changes in environmental conditions or experimental variability (Arif et al., 2025). This finding was similarly in line with the observed reduction in the bulk density of soil. According to other study findings, biochar's application

can effectively manage high temperatures of the soil, resulting in a decrease in temperature during periods of higher soil temperature and an increase in temperature during periods of low soil temperature (Bashir & Mahmud, 2025). The capacity of soil daily average temperature and diurnal range to be adjusted was predominantly within a range of 0.4 and 0.8 °C, respectively. The mechanism by which biochar regulates the temperature of the soil can be comprehended by the combined effect of alterations in soil reflectance and thermal conductivity.

Table 1
Soil temperature was monitored sequentially throughout June, July, and August

Application rate of biochar, %	20 June	20 July	20 August
0	25.9[a]	29.8[a]	31.3[a]
4	25.6[ab]	29.2[ab]	31[a]
8	24.3[c]	29.2[ab]	30.8[a]
12	24.8[bc]	28.9[b]	30.8[a]
16	24.5[c]	29[ab]	30.9[a]

Table 2 indicates a decrease in soil bulk density, along with a gradual rise in total porosity and WHC as the biochar application rate escalated. The use of biochar markedly diminished bulk density and enhanced soil porosity (Etik, 2025). Increasing biochar concentration in soils resulted in decreasing soil bulk density. Higher amount of biochar can be reasoned to affect soil bulk density by four primary mechanisms, (i) densification by small biochar particles occupying soil pores or by slaking/dispersion of aggregates causing fewer macropores between aggregates, (ii) dilution by soil volume occupied by a lower density material, (iii) increase in macropores between aggregates; and, (iv) introduction of accommodation pores between (large) biochar particles and the soil matrix (Faiyue et al., 2026).

Consequently, wood-based biochar substantially influences soil porosity in contrast to manure-derived biochar, which possesses notable ash content. A notable positive correlation between the biochar application rate and water-holding capacity was seen when the acacia-biochar treatment dosage was below 16% can be attributed to the increased porosity and surface area provided by the biochar. As the biochar application rate increases, the number of pores and surface area available for water retention also increases, leading to improved water-holding capacity. This can have beneficial effects on plant growth, especially in water-limited environments, by reducing soil moisture fluctuations and improving drought tolerance. The optimal application rate of 16% or lower may be related to the specific properties of the acacia-biochar and the soil type, highlighting the importance of considering these factors when applying biochar as a soil amendment. The water-holding capacity of soil supplemented with 16% biochar was 53%, whereas pure sandy-soil had a water-holding capacity of just 29%. Applying biochar resulted in a substantial rise of over 51% in water-holding capacity than the control group. Soil water holding capacity was enhanced by 1.3% through amount for each 1% biochar application over the agriculturally applicable range up to 16% biochar dose, because a higher amount of biochar addition was the reason for improvement. It was attributed to the internal porosity of biochar (biochar pore size <10 μm), which determines its ability to store water in the soil. This is because biochar replenishes water as it is removed by gravity, trapping water in pores, reducing hydraulic conductivity, and increasing water retention. According to the findings, the water-holding capacity of loamy sand soil that was mixed with various proportions of pinewood-derived biochar exhibited a positive relationship with the percentage of biochar treatment for biochar levels that were below 10% (Fatima et al., 2024). Furthermore, it was observed that the rise in water-holding

capacity per unit of biochar was higher when the amount of biochar was below 10%. However, it remained constant at 12% when the amount of biochar was over 10%. The observed trend can be attributed to the saturation of soil pores. At lower biochar application rates (below 10%), biochar effectively increases soil porosity, providing additional sites for water retention and significantly improving water-holding capacity. However, as the application rate exceeds 10%, soil pores become saturated, and additional biochar does not provide further significant increases in water-holding capacity. The constant 12% increase at higher rates suggests a threshold beyond which additional biochar does not provide proportional benefits, likely due to the existing pores being filled and excess biochar not contributing to further improvements in soil structure. Therefore, it has been proposed that a 10% amendment enhances the water retention capacity of a 1% biochar sample. A study found that standard deviation exhibited minimal variation in biochar rates up to 20%, but gradually rose as the biochar amendment level increased (Gavin et al., 2026).

Table 2

Measurement of soil qualities obtained from the soil that remains after harvesting

Application rate of biochar, %	Total porosity, %	Bulk density gcm^{-3}	Water holding capacity %
0	46	1.51	29
4	55	1.31	35
8	61	1.10	41
12	63	1.03	47
16	68	0.91	53

The water-holding capacity (WHC) (n = 3) and bulk density were assessed from un-sieved soil specimens at the end of trial. Total porosity was determined from bulk densities, assuming a particle density of 2.66 g/cm³ for soil minerals. Three replicate specimens from every treatment pool were utilized to assess statistical uncertainty.

Alteration of biochar has two impacts on soil water holding capacity. Firstly, biochar possesses the ability to retain water within its internal pores, so directly enhancing the moisture content of the soil. Previous research on straw-derived biochar verified that pores ranging in diameter from 0.1 to 10 μm in biochar increase the amount of water available to plants. Moreover, other parameters, including hydrophilic functional groups and total pore volume on the biochar surface, could potentially enhance soil water-holding capacity. However, it is essential to note that these benefits may be constrained due to the minimal quantity of biochar incorporated into the soil. Table 2 demonstrates that the incorporation of *Acacia*-biochar particles can decrease the total bulk density of sandy soils. According to a study, small particles of biochar had a greater impact on reducing the sandy soil's bulk density, but larger biochar particles had a greater impact on reducing the bulk density of loamy sand soil (Haq et al., 2022). Murtaza et al. (2024) assert that decreasing the particle size of biochar may improve water retention; however, this may lead to a drop in saturated water outflow. Murtaza et al. (2021) indicated that the variations in bulk density observed throughout the incubation period following biochar application did not consistently demonstrate statistical significance. The alterations in the bulk density of mixed soil can be ascribed to the comparatively low bulk density of biochar. The study provided data on soil physical parameters and biochar, demonstrating that biochar often results in a decrease in soil bulk density of 3–3%, an increase in porosity of 15–60%, and an improvement in wet aggregate stability of 5% to 230%. Biochar demonstrates a superior ability to improve the properties of sandy soils relative to clay soils (Molua & Nwachuku, 2026).

There is a clear correlation between biochar's influence on soil physical qualities and Moscatello's growth. The penetration depth and the availability of water and air in the root zone primarily depend

on the soil's physical makeup. Furthermore, it may affect the soil's ability to adjust to pH alterations, permeability during expansion, cation retention, aggregation capacity, and dynamics (Nepal et al., 2025). Table 3 displays the leachate's pH values. The pH value of the soil utilized in the present research was 5.8. The measurements conducted in May showed a positive correlation between the amount of biochar and the leachate pH. The leachate pH was reduced during the July evaluation, which can be attributed to the utilization of N fertilizer. The leachate pH rose during the September evaluation, mainly due to irrigation. The leachate pH treated with biochar after four months ranged from 6.51 to 6.93. The pH, which is 6.9, was close to the optimal pH for Moscatello growth. After five months, the pH of the leachate from the control treatment soil started to stabilize at approximately 6.6, but the pH of the leachate from the altered soil reached a stable level of around 7.1. The increase in pH in the biochar-treated soil to around 7.1 may be due to the biochar's ability to neutralize soil acidity and release basic cations. This pH shift can have implications for nutrient availability and microbial activity, potentially contributing to the observed positive effects on plant growth. The stable pH levels in both treatments suggest that the soils had reached a new equilibrium, with the biochar-treated soil maintaining a slightly higher pH. This finding matches a multitude of research studies thathave demonstrated the positive impact of biochar on the pH levels of acidic soils (Rai et al., 2026).

Furthermore, the pH level of the soil may influence nutrient availability. The optimal phosphorus availability is observed at a pH of roughly 6.5. Phosphorus converts insoluble aluminum/phosphorus minerals at low pH, whereas it generates calcium-phosphate solid minerals at elevated pH levels. Furthermore, acidic soils have diminished the availability of magnesium, calcium, and potassium as a result of leaching (Shoukat, 2025). The findings of three measurements suggest that the pH of the leachate in the control had an increasing tendency over time.

Conversely, the pH levels of the biochar treatments remained consistent. The results indicated that the incorporation of biochar ameliorated soil acidity and augmented the soil's capacity to stabilize pH levels. The incorporation of biochar in acidic soils primarily improves their pH buffering capacity by facilitating the deprotonation and protonation of oxygenated functional groups inherent in the biochar (Suyanto et al., 2026). The functional groups containing oxygen can receive and donate protons via a conjugation reaction at lower pH values and a dissociation reaction at higher pH (Wijyanti, 2025).

Table 3
The soil pH was monitored monthly from May to September 2023 using leachate in column research

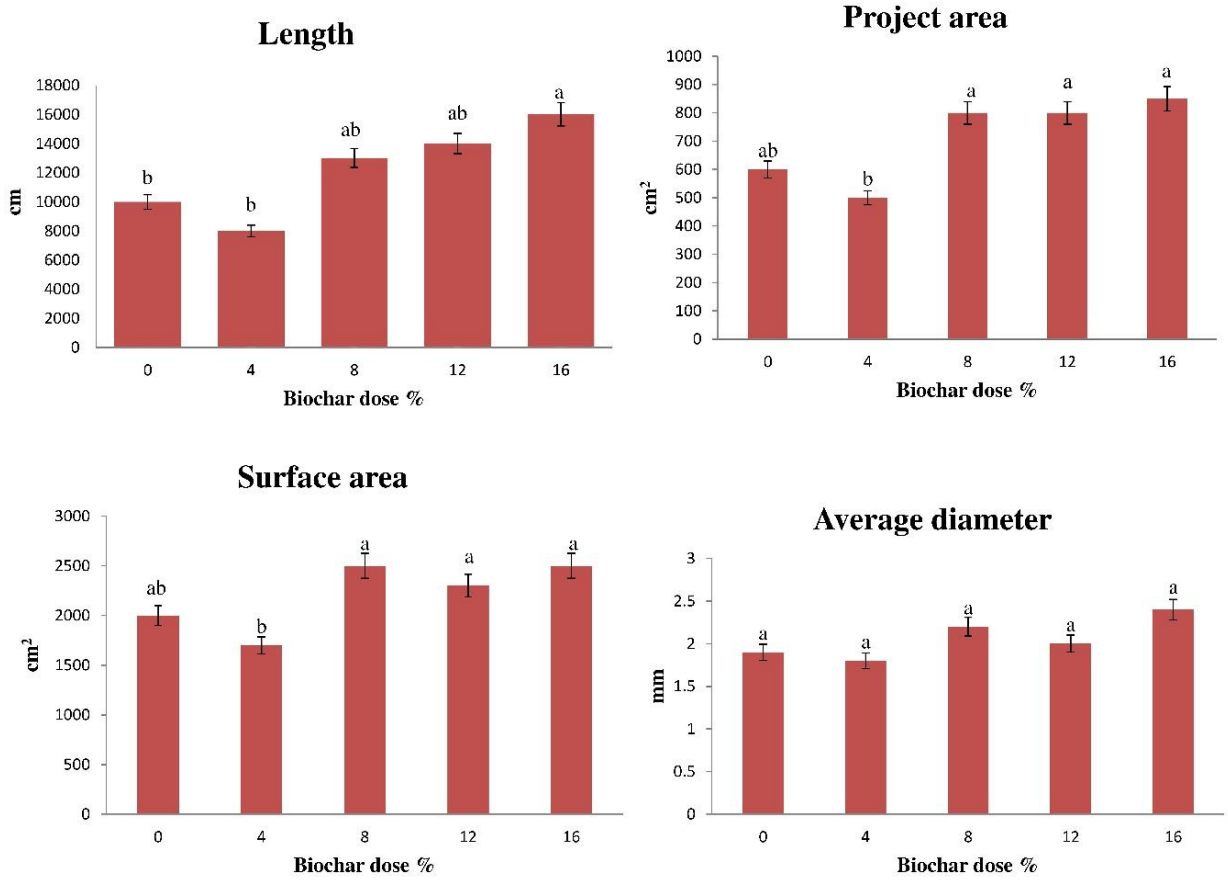
Application rate of biochar, %	20 May	20 July	20 September
0	5.69^{d}	4.93^{c}	6.31^{b}
4	6.51^{c}	6.39^{b}	6.77^{ab}
8	6.84^{b}	6.87^{ab}	6.93^{a}
12	6.84^{b}	7.19^{a}	6.98^{a}
16	6.93^{a}	7.13^{a}	6.91^{a}

a Least square means denoted by identical letters are not substantially different ($P \leq 0.05$) as determined by the Tukey–Kramer test.

Root Architecture Assessment

The results from pot experiment indicated that use of biochar led to a significant increase in several plant attributes, including root surface area, projected area, length, crossings, and fork numbers, can be ascribed to biochar's capacity to enhance soil physical and chemical characteristics. The porous structure of biochar and its elevated cation exchange capacity (CEC) improve soil aeration, water retention, and nutrient availability, hence fostering a more conducive environment for root development. Moreover, biochar can enhance advantageous microbial activity, facilitating plant growth and root development. The augmented root characteristics are likely attributable to the synergistic impacts of enhanced soil conditions, elevated nutrient availability, and advantageous microbial interactions, hence improving plant growth and productivity (Yousaf et al., 2025).

However, no distinction was noted between the groups with 0% and 4% biochar amendment. The 8%, 12%, and 16% biochar treatments did not demonstrate any statistically significant differences (Figure 1). The research demonstrated a significant increase in biomass, root volume, and arbuscular mycorrhizal colonization rate in corn following the application of wood-derived biochar (Infurna et al., 2023). The root growth enhancement could be achieved by improving soil physicochemical qualities. Previous studies have indicated that using biochar-based materials can potentially enhance root growth. Moreover, roots are capable of infiltrating the pores of biochar.



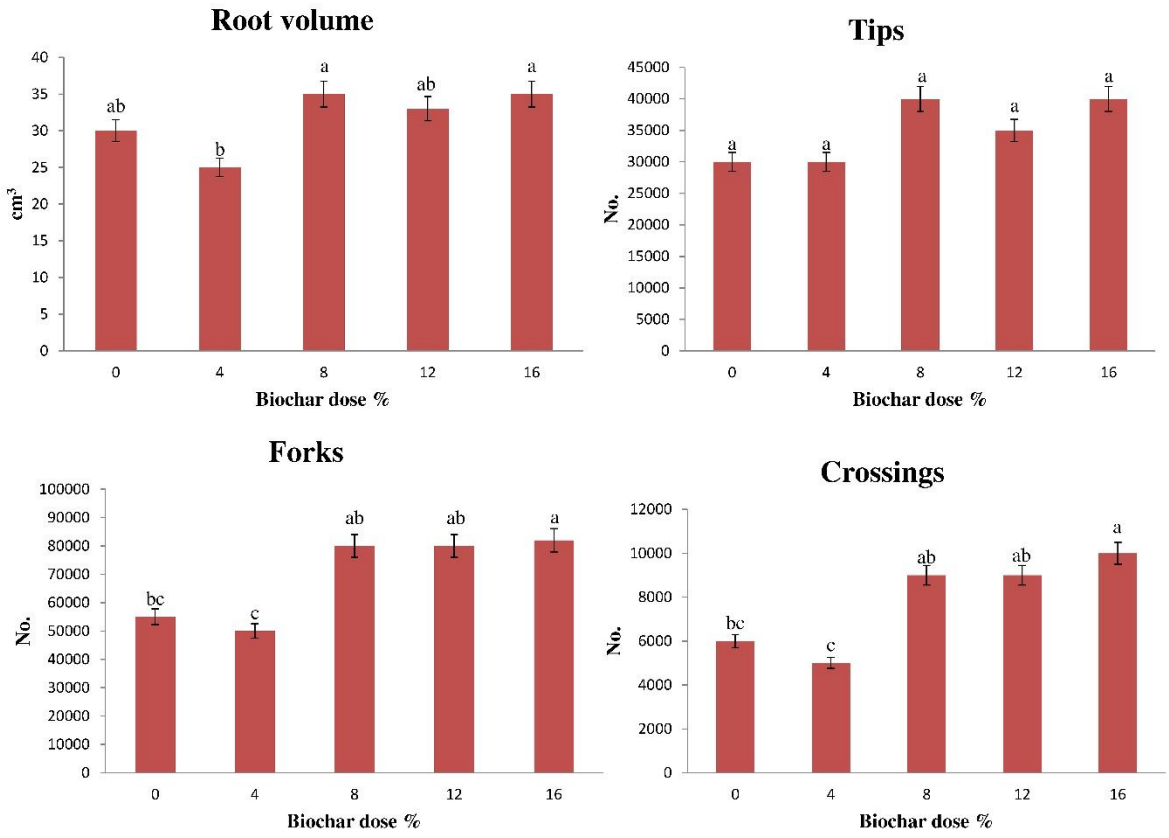


Figure 1

Root characteristics obtained from a pot study using the WinRhizo program. Bars with similar letters indicate no significant difference in least-squares means according to the Tukey–Kramer test ($P \leq 0.05$).

The fundamental properties of Moscatello, identified in the column study, are illustrated in Figure 2. No statistically significant variations were seen in project size, root volume, and surface area among the treatments. The average diameter, root length, number of crossings, forks, and root tips demonstrated a substantial increase following a 12% biochar treatment. The control group yielded the lowest values. Significantly, in the control sample, the root length had a similar surface area, albeit it possessed a more pronounced average diameter compared to the other treatments. The control group exhibited increased root thickness, while roots of Moscatello from various treatments displayed a finer texture. Alternatively referred to as feeder roots, fine roots serve as functional elements and play a crucial role in the acquisition of resources. Hence, the utilization of biochar has been found to facilitate the growth of feeder roots, consistent with the results of our experiments. The decrease in root diameter can be attributed to increased root occupancy of the soil pore space (Gaurav et al., 2025). The 12% biochar treatment resulted in the maximum number of root tips, higher root lengths, and a higher number of root crossings and forks. Nonetheless, no statistically significant difference in root size was seen across all other treatments. The treatments did not affect the root volume, surface area, or projected area. Soil mechanical resistance, encompassing bulk density, moisture content, and texture, is a primary factor affecting root growth. Sandy soil presents a considerable impediment to root development due to its low compressibility, inadequate structure, and high bulk density. Nevertheless, a certain number of these qualities might be counteracted by biochar improvement.

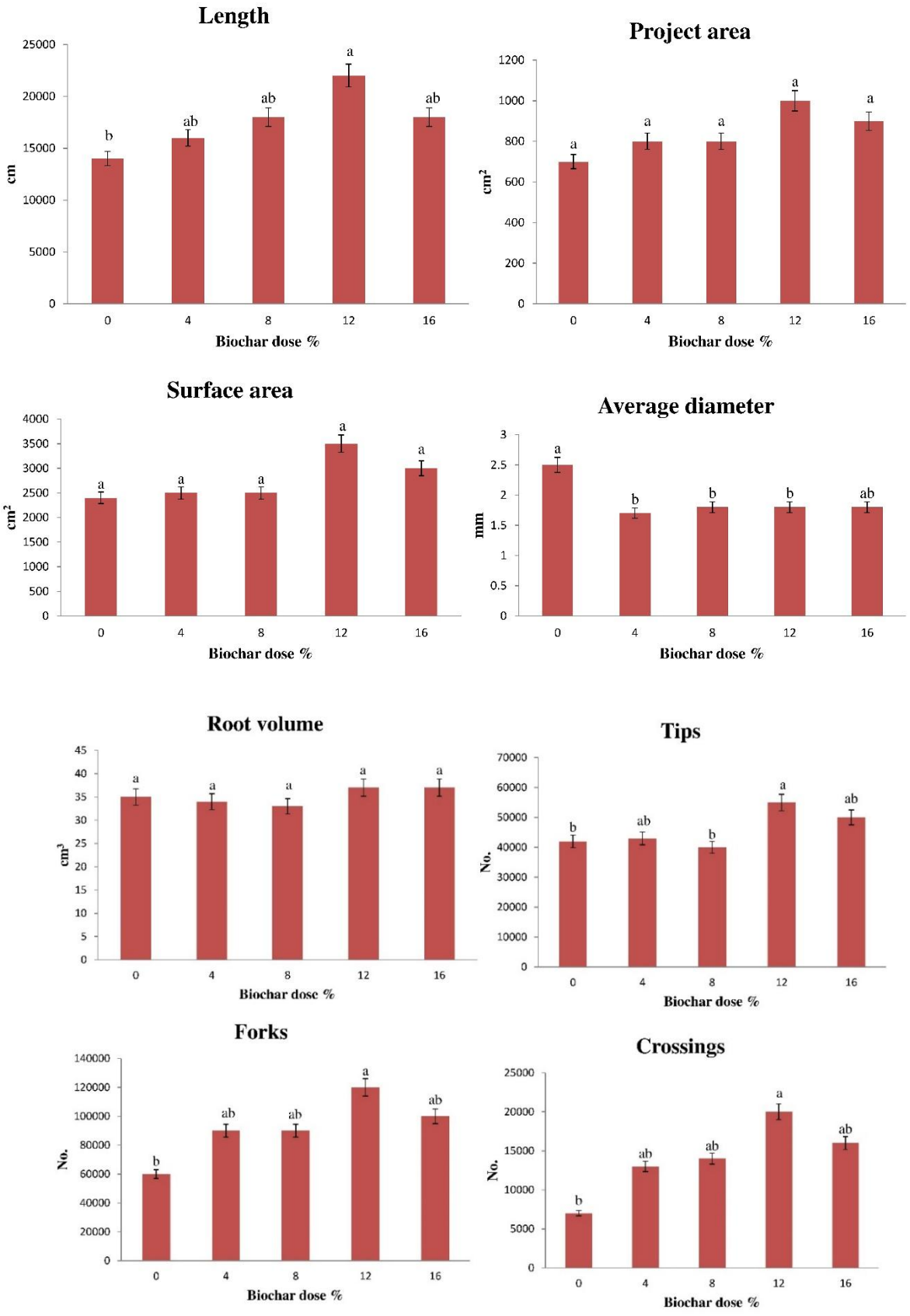


Figure 2

Characteristics of Moscatello plant taken from columns. The presence of bars with similar letters suggests that the least squares means do not exhibit a statistically significant difference (P≤0.05) as determined by the Tukey-Kramer test.

Conclusion

Biochar amendment markedly improved soil physical properties, including soil thermal regulation, bulk density, pH buffering, and water retention capacity. The reduction in bulk density enhanced soil aeration and porosity, creating better conditions for root growth. Biochar application also increased root length, root surface area, projected area, crossings, and forks. In contrast, plants grown without biochar showed shorter and thicker roots, suggesting that biochar promoted the formation of finer and more elongated roots. Therefore, if economically feasible, biochar can serve as an effective management strategy for Muscat grape cultivation, especially in sandy soils with low nutrient availability and poor water holding capacity. Acacia wood waste can also be converted into value-added biochar, improving soil quality and root architecture while supporting waste recycling and the circular economy. Further field studies are needed to evaluate biochars from different feedstocks, application rates, and crop growth stages.

Funding: Not applicable.

Author Contributions: G.M., M.U. designed and conceived the study idea. G.M. completed the experiments. R.I. analysed the data and performed visualizations and statistical data analysis. G.M., M.U. wrote the original draft. R.I. reviewed and edited the manuscript. All authors made valuable revisions and edited the manuscript and approved the last version.

Data Availability Statement: All the raw data in this research can be obtained from the corresponding authors upon reasonable request.

Permission

Permissions or Licenses were obtained to collect the Muscat grape variety known as "Moscatello", which has been extensively cultivated. The commercial nursery in Bahawalpur supplied tissue-cultured vines one month old. The department provided the biochar generated through the pyrolysis of *Acacia nilotica* before starting the research.

Ethics declarations

Ethics approval and consent to participate

This study does not include human or animal subjects.

Consent for publication

Not applicable.

Clinical trial number

Not applicable.

Statement on guidelines

All experimental studies and experimental materials involved in this research are in full compliance with relevant institutional, national and international guidelines and legislation.

Conflict of Interest

The authors stated that they had no interest which might be perceived as posing a conflict or bias. R.I. is an Editor of the journal. He was not involved in the editorial evaluation or publication decision concerning this manuscript.

References

Abubakar, A. S., Wu, Y., Chen, F., Zhu, A., Chen, P., Chen, K., Qiu, X., Huang, X., Zhao, H., Chen, J., & Gao, G. (2023). Comprehensive Analysis of WUSCEL-Related Homeobox Gene Family in Ramie (*Boehmeria nivea*) Indicates Its Potential Role in Adventitious Root Development. *Biology, 12*(12), 1475. https://doi.org/10.3390/biology12121475

Al-Issa, T. A., Alomari, L. M., & Omari, H. J. (2026). Lettuce nutrition and minerals acquisition by the addition of biochar and nitrogen fertilization under greenhouse conditions. *International Journal of Agriculture and Biosciences, 15*(4), 1484–1495. https://doi.org/10.47278/journal.ijab/2026.060

Alsanhani, A. N. (2026). Bridging food security through agricultural development. *Plant Crop Letters, 7*, 38–43. https://doi.org/10.65822/j.pcl/2026.22

Ameen, M., Zulifqar, A., Shoukat, A., & Saqib, Z. A. (2026). Chromium removal from contaminated water using thiourea-modified biochar and zinc nanoparticle-enhanced biochar. *Trends in Animal and Plant Sciences, 7*, 52–59. https://doi.org/10.62324/TAPS/2026.007

Arif, A. H., Riaz, A., & Akhlaq, A. (2025). Global sustainable agriculture: Challenges, strategies, and future pathways. *Science & Society Insights, 4*, 1–13. https://doi.org/10.65822/j.sasi/2025.29

Bashir, H., & Mahmud, M. (2025). Next-generation irrigation strategies: Enhancing water productivity in crops under changing climates. *Plant Crop Letters, 4*, 11–18. https://doi.org/10.65822/j.pcl/2025.21

Etik, N. S. (2025). Granulated and enriched compost enhances growth and yield of multiple leafy vegetable species. *Plant Crop Letters, 2*, 45–51. https://doi.org/10.65822/j.pcl/2025.11

Faiyue, B., Thepthida, M., Krongsawaskul, P., Umnajkitikorn, K., & Assawincharoenkij, T. (2026). Rice husk biochar mitigates saltwater intrusion stress in rice (*Oryza sativa* L.) by regulating symplastic and apoplastic sodium transport. *International Journal of Agriculture and Biosciences, 15*(1), 175185. https://doi.org/10.47278/journal.ijab/2025.155

Fatima, M., Nazim, M., Haq, T. U., Sadiq, Q.-U.-A., Hussain, A., & Ali, M. (2024). Exploring the synergistic effect of animal manure and biochar to improve maize growth and productivity under water deficit condition. *Agrobiological Records, 17*, 83–90. https://doi.org/10.47278/journal.abr/2024.026

Fu, J., Fu, X., Wang, P., Fu, Y., & Chen, C. (2026). Ultrasonic degradation of *Dendrobium officinale* polysaccharide: Kinetics, structural modification, and its impact on wheat starch digestibility. *Food Research International, 231*, 118776. https://doi.org/10.1016/j.foodres.2026.118776

Gaurav, S., Diptanu, B., Mehta, C. M., Prasann, K., Nishihara, E., Inubushi, K., Sudo, S., Hayashida, S., Patra, P. K., Minkina, T., & Rajput, V. D. (2025). Effects of biochar amendment at various soil depths on maize roots and growth indices. *Scientific Reports, 15*(1), 26310. https://doi.org/10.1038/s41598-025-09218-1

Gavin, C., Barzallo, D., Carrasquero, E., Yugsan, F., & Palmay, P. (2026). Rice husk biochar outperforms compost and biol for chive growth and yield in pot trials (*Allium schoenoprasum*). *International Journal of Agriculture and Biosciences, 15*(1), 364–372. https://doi.org/10.47278/journal.ijab/2025.201

Haq, A. U., Majeed, A., Ilahi, F., Kareem, A., & Murtaza, A. (2026). Nano-biopesticides and integrated pest management: Emerging technologies, mechanisms, and pathways to sustainable agriculture. *Plant Crop Lett, 6*, 61–77. https://doi.org/10.65822/j.pcl/2026.14

Hou, Q., Nethmini, R. T., Qi, F., Pan, L., Shi, X., Huang, L., He, Q., Chen, Q., Li, X., Jiang, G., Ke, D., & Li, N. (2026). Biogeography and community stability of leaf endophytic diazotrophs in

mangrove *Kandelia obovata*. *Communications Biology, 9*, 976. https://doi.org/10.1038/s42003-026-10168-1

Infurna, G., Caruso, G., & Dintcheva, N. T. (2023). Sustainable materials containing biochar particles: A review. *Polymers, 15*, 343.

Jin, Z., Wang, H., Pang, B., Li, S., Xu, M., & Shen, A. (2026). Biomimetically-engineered FRP composites: Integration of nanostructured resin matrix with hybrid fiber networks towards ultrahigh chemical stability and mechanical strengthening. *Advanced Composites and Hybrid Materials*, *9*, 286. https://doi.org/10.1007/s42114-026-01823-6

Li, Q. Y., Dou, Z. M., Chen, C., Jiang, Y. M., Yang, B., & Fu, X. (2022). Study on the effect of molecular weight on the gut microbiota fermentation properties of blackberry polysaccharides in vitro. *Journal of Agricultural and Food Chemistry, 70*(36), 11245–11257. https://doi.org/10.1021/acs.jafc.2c03091

Liu, J., Wang, Y., Li, Y., Peñuelas, J., Zhao, Y., Sardans, J., Tetzlaff, D., Liu, J., Liu, X., Yuan, H., Li, Y., Chen, J., & Wu, J. (2023). Soil ecological stoichiometry synchronously regulates stream nitrogen and phosphorus concentrations and ratios. *CATENA, 231*, 107357. https://doi.org/10.1016/j.catena.2023.107357

Molua, C. O., & Nwachuku, D. N. (2026). Integrated assessment of soil–plant–water interactions in tropical agroecosystems using geophysical and remote sensing approaches. *Agrobiological Records, 24*, 111–122. https://doi.org/10.47278/journal.abr/2026.029

Murtaza, G., Ahmed, Z., Usman, M., Tariq, W., Ullah, Z., Shareef, M., & Ditta, A. (2021). Biochar-induced modifications in soil properties and its impacts on crop growth and production. *Journal of Plant Nutrition, 44*, 1677–1691.

Murtaza, G., Ahmed, Z., Valipour, M., Ali, I., Usman, M., Iqbal, R., & Tariq, A. (2024). Recent trends and economic significance of modified/functionalized biochars for remediation of environmental pollutants. *Scientific Reports, 14*, 217.

Nepal, A., Shah, S., & Rai, R. (2025). Factors for the consideration to the establishment of commercial fruit orchards in the mid-hills of Nepal. *Trends in Animal and Plant Sciences, 6*, 23–34. https://doi.org/10.62324/TAPS/2025.077

Rai, S., Nepal, A., & Rai, R. (2026). Detection and prevention of fungal pathogens in horticultural and kiwifruit products: A comprehensive review. *Agrobiological Records, 23*, 1–24. https://doi.org/10.47278/journal.abr/2026.001

Shoukat, A. (2025). Nanofertilizers and stress management: Emerging opportunities for climate-resilient farming. *Agrobiological Records, 22*, 73–88. https://doi.org/10.47278/journal.abr/2025.050

Su, M., Tang, T., Tang, W., Long, Y., Wang, L., & Liu, M. (2023). Astragalus improves intestinal barrier function and immunity by acting on intestinal microbiota to treat T2DM: A research review. *Frontiers in Immunology, 14*, 1243834. https://doi.org/10.3389/fimmu.2023.1243834

Suo, C., Zhang, L., Liang, Q., Chen, C., Qiu, L., Li, Z., Zhang, X., Xu, X., Qi, X., Chen, X., Feng, J., & Yang, X. (2026). Discovery of farnesal from a wild cucumber landrace enables eco-compatible biopesticide development against aphids. *Nature Communications*, 17, 5693. https://doi.org/10.1038/s41467-026-72502-9

Suyanto, A., Radian, R., Palupi, T., & Masulili, A. (2026). Encapsulated phosphorus-enriched biochar improves rice productivity in alluvial soil. *International Journal of Agriculture and Biosciences, 15*(4), 1518–1535. https://doi.org/10.47278/journal.ijab/2026.064

Wang, F. (2024b). Research on engineering characteristics of magnesium phosphate cement solidified copper-contaminated soil. *Journal of Shenyang Jianzhu University (Natural Science), 40*(2), 313–321. https://doi.org/10.11717/j.issn:2095-1922.2024.02.14

Wang, F., Zhang, J., Zeng, Y., Wang, H., Zhao, X., Chen, Y., Deng, H., Ge, L., Dahlgren, R. A., Gao, H., & Chen, Z. (2024a). Arsenic mobilization and nitrous oxide emission modulation by different nitrogen management strategies in a flooded ammonia-enriched paddy soil. *Pedosphere, 34*(6), 1051–1065. https://doi.org/10.1016/j.pedsph.2023.09.008

Wijyanti, A. (2025). Optimizing vegetative development of papaya seedlings using rice husk charcoal and indigenous microorganism fertilizer. *Science & Society Insights, 1*, 8–16. https://doi.org/10.65822/j.sasi/2025.02

Yin, M., Li, X., Liu, Q., & Tang, F. (2022). Rice husk ash addition to acid red soil improves the soil property and cotton seedling growth. *Scientific Reports, 12*, 1704. https://doi.org/10.1038/s41598-022-05199-7

Yousaf, A., Rasul, F., Hayat, M. K., & Arshad, F. (2025). Mitigating heavy metal uptake in wastewater-irrigated radish (*Raphanus sativus* L.) through biochar and L-methionine application. *Trends in Animal and Plant Sciences, 7*, 136–159. https://doi.org/10.62324/TAPS/2026.015

Yuan, J., Liu, Y., He, Q., Wen, H., Li, Z., Lin, R., Chu, T., Peng, C., Zheng, C., Chen, H., & Tan, Y. (2026). Phosphorus-modified biochar from *Salvia miltiorrhiza* dregs: Synthesis, characterization, and dual-functional synergy for heavy metal immobilization and soil fertility augmentation. *Biochar, 8*, 30. https://doi.org/10.1007/s42773-025-00540-5

Zeng, Y., Wang, H., Hu, J., Zhang, J., Wang, F., Wang, T., Zhou, Q., Dahlgren, R. A., Gao, M., Gao, H., & Chen, Z. (2024). Illuminated fulvic acid stimulates denitrification and As(III) immobilization in flooded paddy soils via an enhanced biophotoelectrochemical pathway. *Science of the Total Environment, 912*, 169670. https://doi.org/10.1016/j.scitotenv.2023.169670

NATURE & SCIENCE
October 2026, Volume 8, Issue 5, pp. 21–27
DOI: https://doi.org/10.36719/2707-1146/68/21-27

Soil Organic Matter and Its Fractions at Different Stages of Soil Salinization, as well as Their Resistance to Decomposition in Relation to Soil Bioactivity

Turkan Hasanova[1*], Tariverdi Islamzade[2,3], Gunay Mammadova[3,4], and Muhammad Mubashar Zafar[5]

Abstract. *The aim of the study was to conduct a comparative assessment of key biological activity indicators in soils with varying degrees of salinity. The research objectives included determining the decomposition rates of plant OM and cellulose, the intensity of soil respiration, and analyzing the total number of microorganisms and bacterial populations in the upper humus horizon of the saline soils. The stabilization process is closely linked to high soil moisture, elevated silt and clay content, and rising nitrogen levels. While rapid changes occur in the surface soil layers (0–10 cm), deeper layers respond much more slowly, retaining specific carbon structures. Ultimately, ecological restoration promotes effective soil carbon sequestration, although this effect is unevenly distributed and concentrated primarily in the surface layer. Based on the results obtained, it was established that the molecular structures of carbon are positively correlated with soil depth, and the dynamics of recovery change in the opposite direction. In both models developed, the processing of the topsoil is clearly separated from the processing of the deeper layers, indicating a noticeable vertical stratification: the topsoil responds more quickly to revegetation than the deeper soil.*

Keywords: *decomposition, microorganisms, soil bioactivity, polysaccharides, phyto-organic nutrient, ecological restoration*

Introduction

Chemical composition and the degree of salinity are key factors influencing the functional activity of soils, determining their natural fertility, productivity, biodiversity, and ecosystem stability. The basis for the biodiagnostic assessment of lowland soils with varying degrees of salinity is biological activity defined as the aggregate of biological processes characterizing the scale and direction of matter and energy transformation in terrestrial ecosystems, as well as the intensity of organic matter (OM) decomposition and synthesis. The biodiagnostics of soil condition using biological activity indicators represents an important area of scientific research. Soil respiration, measured as O_2 consumption or CO_2 production, is an important and informative indicator of OM recycling and soil activity (Acevedo & Govan, 2026; Swaminathan et al., 2021). The biodiagnostics of soil condition using biological activity indicators represents an important area of scientific research. Soil respiration, measured as O_2 consumption or CO_2 production, is an important and informative indicator of OM recycling and soil activity (Acevedo & Govan, 2026; Swaminathan et al., 2021).

[1]Faculty of Ecology and Soil Science, Baku State University, PhD in Agrarian Sciences, Baku, Azerbaijan
[2]Department of Agrarian Sciences, Faculty of of Agriculture and Engineering, Lankaran State University, PhD in Agrarian Sciences, Lankaran, Azerbaijan
[3]Institute of Geography Public Legal Entity, PhD in Agrarian Sciences, Baku, Azerbaijan
[4]Faculty of Chemistry and Ecology, Sumgait State University, PhD in Agrarian Sciences, Sumgait, Azerbaijan
[5]University of Agriculture Faisalabad, PhD in Plant Molecular Biology, Faisalabad, Pakistan
[*]Corresponding author. E-mail: turkanhesenova@mail.ru
Received: 13 May 2026; Accepted: 5 October 2026; Published online: 25 October 2026
© The Author(s) 2026. This is an open access article distributed under the terms of the Creative Commons Attribution-NonCommercial 4.0 International License (CC BY-NC 4.0).

The decomposition of cellulose and plant material in general allows for an assessment of decomposition intensity a process considered a natural ecosystem attribute that is sensitive to changes in ecosystem functioning and involves the breakdown of residues and the transfer of OM and nutrients within the soil (Sadigov et al., 2025a; Mirzezadeh et al., 2025). Determining microbial counts by inoculating soil suspensions onto solid culture media enables the identification of biological activity patterns. Soil respiration and microbial counts serve as indicators of potential soil biological activity, measured under optimal conditions for a specific biological process. In contrast, the breakdown of cellulose and plant material indicates actual soil biological activity, reflecting the activity occurring under field conditions (Hasanova et al., 2026a; Nasirova et al., 2026).

Materials and Methods

Four sites with varying degrees of salinity in the Mil-Mugan Plain of Azerbaijan, located in close proximity to one another under similar climatic conditions, were selected as experimental sites. The research was conducted from September 2023 to September 2024. The degree and chemical composition of soil salinity were determined using the classical method of water extract analysis. Aqueous extract analysis method: slightly saline (salt content 0.23%), sulfate type ($Cl:SO_4 \leq 0.3$); moderately saline (0.6%), chloride type ($Cl:SO_4 \geq 2.5$); highly saline (2.18%), sulfate type ($Cl:SO_4 \leq 0.3$); very highly saline (4.95%), sulfate-chloride type ($Cl:SO_4$=2.5–1.0). According to soil maps, the experimental plots are situated on meadow and saline-meadow soils-including areas with saline marsh patches as well as on clay and heavy-clay soils (Hasanova & Mammadova, 2023; Hasanova et al., 2026a). Key physicochemical soil parameters were determined using standard methods: chemical composition and salinity were assessed via water extraction, OM content was determined by calcining soil samples, and soil acidity was measured using a pH meter directly on the experimental plots. The soils of the experimental plots are similar in terms of OM content and total water-holding capacity. To assess the decomposition rate, we employed soil exposure methods using filter paper samples and hay bags techniques frequently used in studies evaluating soil activity and metabolism (Bashir et al., 2021; Hasanova et al., 2026b).

Bags containing a specific amount of plant material or filter paper are placed in the soil for a set period. The decomposition rate is calculated as the daily mass loss per gram of OM ($mg \cdot g^{-1} \cdot 24 \cdot h^{-1}$). The decomposition of standardized, homogeneous material enables a comparison of the decomposition capacity of plant material across different soil types with specific compositions and structures. The method of exposing filter paper samples to the soil is used to assess the decomposition rate of pure cellulose and serves as an indicator of the cellulolytic activity of microorganisms, whereas the method of exposing bags allows for the assessment of the decomposition rate of plant OM as a whole and reflects the degradative activity. Samples of filter paper and vegetables material were in the soils of the experimental plots in the post-vegetation period (September – November 2023) and growing season (June – September 2024) periods. Since the regime of CO_2 in soil air is more dynamic than O_2, which is related to several sources of its entry into the gas phase and high solubility in the water environment, we estimated soil respiration as the amount of $\mu l O_2 h^{-1} \cdot g^{-1}$. One of the study's objectives was to demonstrate the respiratory potential of the different soil types rather than to measure O_2 consumption under actual natural conditions. Laboratory measurements were conducted using a volumetric respirometer with 25 ml flasks, following the standard method, at three temperatures (8, 18, and 25 °C) and a moisture content of 60% of the soil's total water capacity a level commonly used in such studies. Microorganisms in the soils of the experimental plots were quantified using 1:10,000 dilutions of soil suspensions plated on solid culture media (Swaminathan et al., 2021; Li et al., 2023). Meat-peptone agar was used to isolate and quantify the total bacterial count, while *Azotobacter* numbers were assessed by culturing on nitrogen-free media. Statistical analysis of all obtained results was performed using STATISTICA version 10 (Ismayilova et al., 2025a; Verdiyeva et al., 2026).

Results and Discussion

The obtained data indicate that the decomposition rates of plant OM in the soils of each of the four experimental plots varied significantly (t-test, $p < 0.05$) during both the growing season and the autumn (Tunlid et al., 2022). In all experimental plot soils, the decomposition rate increased markedly under conditions favorable for active microbiological activity and biochemical processes, as well as under the temperature and moisture conditions characteristic of the growing season. During this period, the decomposition rate of hay and filter paper more than doubled in moderately and highly saline soils. It has been established that the rate of phyto-organic decomposition is inversely proportional to salinity (Ismayilova et al., 2025b; Mammadova et al., 2026a; Sadigov et al., 2025b).

The highest values were observed in the soil of the slightly saline site during the growing season, whereas the lowest decomposition rates during this period were observed in the soil of the highly saline site. A similar inverse relationship regarding decomposition rates along the salinity gradient was evident in autumn: the most intense decomposition of phyto-organic matter occurred in the slightly saline site, while the lowest rate was observed in the highly saline soil. Across all experimental sites, the rate of cellulose decomposition also decreased along the soil salinity gradient during both the growing and post-growing seasons (Shukurov et al., 2025; Mammadova et al., 2026c). The dry conditions typical of an arid climate characterized by high air temperatures and low summer precipitation during the sample exposure period were similar across the adjacent experimental plots. All soils in the experimental plots were similar in terms of total water-holding capacity and OM content (Table 1).

This enabled us to track the influence of salinity on the decomposition rate of phyto-organic nutrients while keeping the effects of climatic conditions and other soil physicochemical parameters constant. The data confirmed that the higher the soil salinity level, the lower the rate of phyto-organic nutrient decomposition (Mammadova et al., 2025; Mammadova et al., 2026b). Soil respirometer measurements were obtained at temperatures of 25 °C, 18 °C, and 8 °C. A temperature of 25 °C proved optimal for soil biological activity across all experimental plots and closely approximates the natural growing season in the study area. A temperature of 18 °C proved critical for moderately, strongly, and very strongly saline soils, with no O_2 consumption observed. For soils in the slightly saline plot, no O_2 consumption was observed at a temperature of 8 °C. The respiration rate of the studied soils at 25 °C varied significantly along the salinity gradient ($p < 0.05$, t-test). The maximum rate was observed in the moderately saline soil (3.586 ± 0.173 $\mu l O_2 h^{-1} \cdot g^{-1}$ dry mass), a value slightly higher than that of the slightly saline soil. Respiration rates were virtually identical in the highly and very highly saline soils ($p < 0.05$, t-test). At 18 °C, O_2 consumption was observed only in samples from the slightly saline soil site (2.045 $\mu l O_2 h^{-1} \cdot g^{-1}$ dry mass); the respiration rate was lower than at 25 °C ($p < 0.05$, t-test).

According to previous studies on saline soils in the lowlands of the Republic of Azerbaijan, low concentrations of readily soluble salts up to 1 mol eq. per 100 g of soil have a positive effect on the functioning of microbial communities; the higher the concentration, the greater the vitality of the microorganisms. This is clearly reflected in the respiration rate of moderately saline soils, where peak O_2 consumption values are observed, whereas the salinity levels found in the third and fourth study sites prove detrimental to microbial activity. Analysis of the number of microorganisms isolated by plating diluted soil suspensions showed that the total number of microbial cells, as well as the number of nitrifying bacteria per gram of soil in each of the four experimental plots, decreased along the salinity gradient.

It was found that the number of colony-forming units for both the total microbial population and nitrogen-fixing bacteria was more than five times higher in soil samples from the slightly saline plot than in soils with moderate or high salinity. Low salt concentrations have no negative effect on the functioning and total biomass of soil microorganisms, while high salt concentrations can cause osmotic stress, limiting the growth and activity of microbial communities (Mammadova et al., 2025).

The decomposition rate of plant OM and cellulose in the soils of experimental plots under natural conditions serves as an indicator of their actual biological activity. It was found that, given identical natural hydrothermal conditions and similar OM content and soil water-holding capacity, the decomposition rate of plant OM and cellulose decreases along the salinity gradient. Data obtained via respirometer and microbial counts indicate the potential biological activity of the soils, as measurements were taken under artificially optimized conditions. O_2 consumption potential was found to be quite high in soils with low salinity levels. The total number of microorganisms including both the total count and specific nitrogen-fixing bacteria was more than five times higher in slightly saline soils than in moderately saline soils. Evidently, the salt concentration in moderately saline soils does not critically inhibit microbial activity, allowing the microbes to exhibit high activity potential despite lower population numbers.

This is corroborated by data showing maximum respiration rates in moderately saline soils with low bacterial populations. High and very high salinity levels proved detrimental to the soil's biological activity potential, affecting both respiration rates and total microbial counts. To evaluate the relationship between soil organic matter (SOM) composition, thermal stability, and environmental factors (EF) at different restoration stages and soil depths, redundancy analysis (RDA) was conducted (Figure 1). In Figure 1a, the first two axes explain 28.48% of the total variance, with RDA1 dominating at 26.47% and RDA2 accounting for 2.01%. Ordination revealed a clear spatial division of soil samples according to RDA1, based on the chronological sequence of restoration.

Early recovery samples (5 years, pink/red) clustered on the positive side of RDA1, showing strong positive correlations with labile OM, soil depth, and pH. Conversely, late recovery samples (30 years, in green) clustered on the negative side of RDA1, which was largely driven by recovery age (years) and soil water content (SWC). The refractory OM and recalcitrant OM vectors indicated longer recovery stages, suggesting accumulation of stable organic components over time accompanied by an increase in silt + clay content and NH_4^+-N.

In Figure 1b, the RDA models the shifts in specific carbon functional traits (aliphatic and aromatic carbon, polysaccharides, and the decomposition resistance index) in response to environmental drivers. The first two canonical axes captured 25.96% of the total structural variance (RDA1: 25.62%, RDA2: 0.34%).

Mirroring the trends in the fraction analysis, the polysaccharides and the recalcitrant index vectors pointed in the direction of the late-stage restoration plots (30 years), aligning closely with the long-term increase in years, SWC, and nitrogen availability NH_4^+-N and NO_3^+-N. On the other hand, aliphatic C and aromatic C molecular structures were positively aligned with soil depth, shifting opposite to the restoration timeline. Notably, in both models, the 0–10 cm surface soil layer (demarcated by the dashed ellipses) clustered distinctly away from the deeper core layers, highlighting a profound vertical stratification where topsoil’s exhibit an accelerated response to vegetation restoration compared to subsoils.

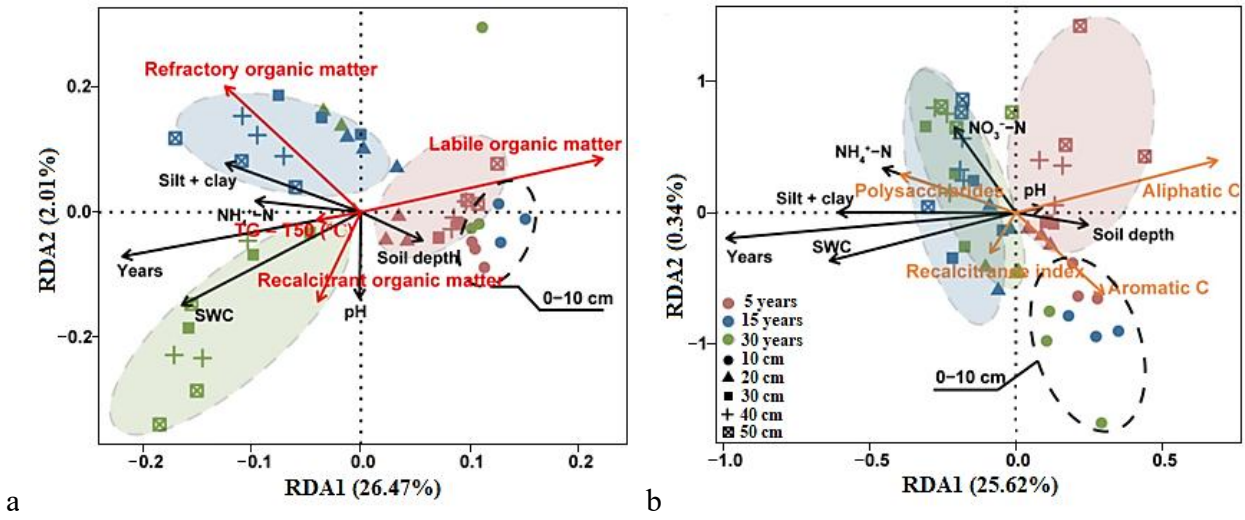


Figure 1

RDA analysis of SOM composition and EF at various stages of restoration: (a) OM fractions in relation to EF and the thermal stability index; (b) aliphatic and aromatic carbon, polysaccharides, and the decomposition resistance index in relation to EF

Table 1

Physicochemical properties, rates of decomposition of plant OM and cellulose, and soil respiration rates in the soils of experimental plots

The degree of soil salinity in experimental sites	OM, %	Maximum capillary water capacity, ml/g	pH	Soil texture
Slightly saline	7.74	0.38	7.1	middle to heavy loamy soils
Medium saline	5	0.35	6.2	middle to heavy loamy soils
Highly saline	7.48	0.39	4.6	loamy and heavy loamy soils
Very saline	7.44	0.4	6.0	loamy and heavy loamy soils
		Samples of hay		
	September–November 2023		June–September 2024	
The degree of soil salinity in experimental sites	Number of samples	Average decomposition rate $X \pm Sx$	Number of samples	Average decomposition rate $X \pm Sx$
Slightly saline	14	4.25 ± 0.27	24	5.51 ± 0.12
Medium saline	19	2.67 ± 0.26	21	5.31 ± 0.17
Highly saline	20	1.28 ± 0.13	15	4.49 ± 0.16
Very saline	19	0.86 ± 0.07	8	2.63 ± 0.44
		Samples of filter paper		
	September–November 2023		June–September 2024	
The degree of soil salinity in experimental sites	Number of samples	Average decomposition rate $X \pm Sx$	Number of samples	Average decomposition rate $X \pm Sx$
Slightly saline	29	11.12 ± 0.22	21	10.07 ± 0.02
Medium saline	23	0.22 ± 0.03	20	3.13 ± 0.12
Highly saline	21	0.16 ± 0.03	13	3.84 ± 0.15
Very saline	22	0.10 ± 0.01	23	1.50 ± 0.2
		Temperature regime		
		25 °C		18 °C

The degree of soil salinity in experimental sites	Number of samples	O_2 uptake $X \pm Sx$	Coefficient of variation, %	Number of samples	O_2 uptake $X \pm Sx$	Coefficient of variation, %
Slightly saline	30	3.025 ± 0.126	18.6	23	2.045 ± 0.086	18.4
Medium saline	30	3.586 ± 0.173	21.5	24	0	–
Highly saline	33	2.168 ± 0.131	30.7	12	0	–
Very saline	31	1.886 ± 0.096	22.7	10	0	–

Conclusion

Slightly saline soils have the highest potential activity. They hold more than five times the number of microbes and nitrogen-fixing bacteria than moderately saline soils. Moderately saline soils have fewer microbes, but those microbes are highly efficient. They can still achieve maximum respiration rates because the salt level is not yet critical. High and very high saline soils are toxic. The extreme salt levels severely damage both the microbe populations and their ability to breathe. Overall, while low-to-moderate salt levels change how microbes behave, high salt levels destroy the soil's biological life.

Acknowledgement
The authors express their gratitude for the support of the scientific and technological research project to the Institute of Geography Public Legal Entity, Lankaran State University. They also thank the Baku State University's Faculty of Ecology.

Conflict of Interest
The authors declare no competing interests that could be perceived as influencing the research or its publication. T.H. is an Editor of the journal, while G.M. is a member of the Editorial Board. Neither T.H. nor G.M. was involved in the editorial evaluation or publication decision concerning this manuscript.

References

Acevedo, M., & Govan, J. E. (2026). Organic nanoagriculture: The use of natural nanomaterials for sustainable agriculture. *Sustainability*, *18*(15), 7705. https://doi.org/10.3390/su18157705

Bashir, O., Ali, T., Baba, Z. A., & Bhat, R. A. (2021). Soil organic matter and its impact on soil properties and nutrient status. *Microbiota and Biofertilizers*, *2*(1), 128–139. https://doi.org/10.1007/978-3-030-61010-4_7

Hasanova, T. A., Jafarov, A. M., Huseynova, S. M., Isagova, V. G., Mammadova, G. I., Madnee, M., & Asgarova, G. F. (2026a). Modeling humus stocks and introducing a saturation coefficient to assess soil organic carbon capacity in forest soils of the Sheki-Zagatala Region, Azerbaijan. *International Journal of Agriculture and Biosciences, 15*(5), 2134–2146. https://doi.org/10.47278/journal.ijab/2026.116

Hasanova, T., & Mammadova, G. (2023). The impact of changes in soil moisture indicators on biological activity in recent years on the southern slope of the Greater Caucasus. *Nature & Science*, *5*(3), 7–12. https://doi.org/10.36719/2707-1146/30/7-12

Hasanova, T., Mammadova, G., Tsitsiagi, M., & Lapitov, N. (2026b). Modelling moisture dynamics of agricultural steppe soils in the Greater Caucasus. *Nature & Science*, *8*(4), 5–12. https://doi.org/10.36719/2707-1146/67/5-12

Ismayilova, A. A., Mirzezadeh, R. I., Bunyatova, L. N., Mammadova, G. I., Hasanova, T. A., Asgarova, G. F., & Madnee, M. (2025a). Biomass and enzymatic activity assessment of the coniferous-deciduous forests in Azerbaijan. *SABRAO Journal of Breeding and Genetics*, *57*(6), 2584–2595. https://doi.org/10.54910/sabrao2025.57.6.31

Ismayilova, A., Shukurov, S., Hasanaliyeva, L., Osmanova, S., Asgarova, G., & Hasanova, T. (2025b). Modern soil cover of natural cenoses and agrocenoses landscapes of the Kur-Araz plain. *Advances in Biology and Earth Sciences*, *10*(2), 314–325.

https://doi.org/10.62476/abes.102314

Li, Q., Wang, L., & Fu, Y. (2023). Transformation of soil organic matter subjected to environmental disturbance and preservation of organic matter bound to soil minerals: a review. *Journal of Soils and Sediments,* 23, 1485–1500. https://doi.org/10.1007/s11368-022-03381-y

Mammadova, G., Salimova, Sh., Aliyeva, G., Isagova, V., & Hasanova, T. (2026a). Modern approaches in the study of soil bioactivity in Katekh and Garakli village (Azerbaijan) irrigated alluvial meadow and mountain forest brown soils. *Bulgarian Journal of Agricultural Science, 32*(2), 278–285. https://doi.org/10.61308/sp7p2257

Mammadova, R., Hasanova, T., & Aliyeva, M. (2025). Ecological state of modern soil cover in agrocenoses of the Greater Caucasus Sheki region. In T. Cherniavska (Ed.), *Ecological systems modeling* (pp. 57–73). Scientific Route OÜ. https://doi.org/10.21303/978-9908-9706-6-0.ch3

Mammadova, G. I., Bunyatova, L. N., Gahramanova, A. Y., Isaqova, V. G., Fatdayeva, A. K., Alakbarli, G. Y., & Hasanova, T. A. (2026b). Environmental pollution in soil, plant leaves, and roots using bioindication in hazelnut fields. *SABRAO Journal of Breeding and Genetics, 58*(3), 1436–1444. https://doi.org/10.54910/sabrao2026.58.3.46

Mammadova, G. I., Salimova, Sh. J., Jafarov, A. M., Huseynova, S. M., Isayeva, K. K., Isagova, V. G., & Hasanova, T. A. (2026c). Rocky soil compositions influence on the microorganisms and vegetation at the Sheki-Zagatala Economic Region, Azerbaijan. *SABRAO Journal of Breeding and Genetics, 58*(3), 1407–1414. https://doi.org/10.54910/sabrao2026.58.3.43

Mirzezadeh, R. I., Ramazanova, F. M., Hasanova, T. A., Mammadova, G. I., & Asgarova, G. F. (2025). Assessment of variations caused by biological activities in the Greater Caucasus forest soils used for agriculture. *SABRAO Journal of Breeding and Genetics*, *57*(4), 1634–1643. https://doi.org/10.54910/sabrao2025.57.4.29

Nasirova, A. I., Isagova, V. G., Mirzezadeh, R. I., Gahramanova, A. Y., Bunyatova, L. N., Mammadova, G. I., Hasanova, T. A., Asgarova, G. F., & Mammadova, R. N. (2026). Changing the biological activity of soil in sunflower crops. *Comptes Rendus De L Academie Bulgare Des Sciences, 79*(1), 145–156. https://doi.org/10.7546/CRABS.2026.01.18

Shukurov, S. Kh., Ismayilova, A. A., Sadigov, R. A., Javanshir, M. K., Hasanova, T. A., & Asgarova, G. F. (2025). Determination of soil salinization by hyperspectral remote sensing in the Shirvan Plain. *International Journal of Advances in Applied Sciences*, *14*(3), 662–670. https://doi.org/10.11591/ijaas.v14.i3.pp662-670

Swaminathan, C., Nivetha, D., & Pandian, K. (2021). Soil organic matter decomposition-roles, factors and mechanisms. *Latest Trends in Soil Sciences*, *1*(1), 1121–1129. https://doi.org/10.22271/int.book.33

Sadigov, R. A., Nazarova, K. M., Garayeva, I. E., Mammadova, G. I., Hasanova, T. A., & Madnee, M. (2025a). Modern research on the use of alternative energy resources in Azerbaijan. *International Journal of Advances in Applied Sciences*, *14*(3), 907–915. https://doi.org/10.11591/ijaas.v14.i3.pp907-915

Sadigov, R. A., Farman, N. A., Mammadova, G. I., Isagova, V. G., Hasanova, T. A., & Madnee, M. (2025b). Current state of production of alternative energy on the Absheron Peninsula. *International Journal of Applied Power Engineering*, *15*(1), 37–45. https://doi.org/10.11591/ijape.v15.i1.pp37-45

Tunlid, A., Floudas, D., Op De Beeck, M., Wang, T., & Persson, P. (2022). Decomposition of soil organic matter by ectomycorrhizal fungi: Mechanisms and consequences for organic nitrogen uptake and soil carbon stabilization. *Frontiers in Forests and Global Change,* 5, 934409. https://doi.org/10.3389/ffgc.2022.934409

Verdiyeva, F. B., Abdullayeva, R. K., Ismayilzadeh, N. N., Fatdayeva, A. K., Mammadova, G. I., Hasanova, L. U., Asgarova, G. F., & Hasanova, T. A. (2026). Biosynthesis of seeds and bioecological parameters of gray-meadow soils by remote sensing (Republic of Azerbaijan) under wheat crops. *International Journal of Agriculture and Biosciences, 15*(4), 126–137. https://doi.org/10.47278/journal.ijab/2026.075

NATURE & SCIENCE
October 2026, Volume 8, Issue 5, pp. 28–33
DOI: https://doi.org/10.36719/2707-1146/68/28-33

Biotechnological Evaluation of Fungal Strains Isolated from Extreme Habitats Based on Their Enzymatic and Antimicrobial Properties

Lala Bunyatova[1], Parvin Omar[1*], and Aida Gahramanova[1]

Abstract. *This scientific investigation focuses on obtaining, cataloging in a culture collection, and biotechnologically evaluating fungal isolates retrieved from diverse ecological niches characterized by extreme environmental stress in Azerbaijan. These habitats encompass petroleum-contaminated soils, high-salinity terrains, mineralized thermal springs, and humid subtropical forest ecosystems. A total of 76 fungal isolates (comprising 64 micromycetes and 12 macromycetes) were successfully derived into pure cultures using approved protocols and methods. The enzymatic potential of these isolates—specifically hydrolytic (endo-1,4-β-glucanase, protease, pectinase, amylase, xylanase, lipase) and oxidative (laccase, peroxidase) activities—was evaluated. The enzymatic activities were assessed using spectrophotometric methods, while antimicrobial effects were evaluated through agar block and disc diffusion assays. Furthermore, their antagonistic effects against clinically relevant human pathogens (Escherichia coli, Pseudomonas aeruginosa, Staphylococcus aureus, and Candida albicans) were thoroughly examined, leading to the identification of potent producing strains. Systematic optimization of environmental factors and growth media parameters yielded an 11–20% enhancement in target metabolite biosynthesis.*

Keywords: *extreme habitats, micromycetes, hydrolases, oxidases, antimicrobial potency, metabolic regulation, bioprocess optimization, microbial biotechnology*

Introduction

In the contemporary era, the exponential expansion of the global population necessitates innovative microbiological strategies to address critical challenges in food security, sustainable bioenergy supplies, healthcare, and pharmaceutical raw material generation (Kutu et al., 2019). Current forecasts project that agricultural and food demand will experience a nearly twofold increase in the upcoming decades (Pobiega et al., 2024). Consequently, discovering biologically active natural resources with enhanced biosynthetic capabilities represents a key priority in modern bioprocess engineering (Rappaport & Oliverio, 2023).

Compared to conventional plant and animal bioresources, micromycetes offer substantial advantages, including rapid growth kinetics, short generation cycles, and the capacity to bioconvert low-cost industrial by-products into valuable biomass and bioactive compounds (Pobiega et al., 2024).

[1]Sumgait State University, PhD in Biology, Sumgait, Azerbaijan
[*]Corresponding author. E-mail: parvin.omar@sdu.edu.az
Received: 8 June 2026; Accepted: 14 September 2026; Published online: 25 October 2026
© The Author(s) 2026. This is an open access article distributed under the terms of the Creative Commons Attribution-NonCommercial 4.0 International License (CC BY-NC 4.0).

Despite the vast species diversity of the kingdom Fungi, only a minor fraction has been harnessed for industrial applications Extremophilic micromycetes, which have evolved specialized physiological machinery to thrive under severe environmental conditions (such as heavy metal toxicity, hypersalinity, thermal stress, and extreme pH levels), serve as an extraordinary reservoir for stable functional enzymes and bioactive molecules (Rappaport & Oliverio, 2023; Mirzezade & Mammadova, 2026).

The territory of Azerbaijan exhibits remarkable physiogeographic and geochemical diversity (Mammadova et al., 2026a). Unique ecological niches—including hydrocarbon-polluted soils across the Absheron Peninsula, mineralized thermal springs, hypersaline inland lakes, and the humid subtropical forest ecosystems of Hirkan National Park—provide ideal environments for the evolution of specialized microflora. Fungal strains retrieved from these extreme habitats possess high physiological resilience, making their extracellular enzymes and secondary metabolites highly valuable for bioprocess development (Mammadova et al., 2026b; Mammadova et al., 2026a).

The primary goal of this research is the isolation of micromycete and macromycete strains from extreme Azerbaijani habitats, comprehensive profiling of their enzymatic and antimicrobial characteristics, and the assessment of their biotechnological application prospects.

Materials and Methods

Environmental samples were gathered from distinctive stressed habitats in Azerbaijan, including petroleum-hydrocarbon-contaminated soils, hypersaline soil-water environments, thermal mineral springs, and humid subtropical forest ecosystems located within Hirkan National Park.

A total of 100 specimens were collected per designated sampling site, cataloged, and conveyed to the laboratory within 2–6 hours for subsequent processing. During the isolation phase, 10% (w/v) soil suspensions were formulated in sterile distilled water and allowed to stand at ambient temperature for 2 hours. Serial dilutions (undiluted, 10^{-1}, and 10^{-2}) were subsequently inoculated onto solid growth media, specifically malt extract agar (MEA) and Sabouraud dextrose agar. Following an incubation period of 2–3 days, colonies were differentiated according to their macro-morphological traits, transferred onto fresh nutrient media, and sequentially subcultured to yield axenic biomass. Culture purity was routinely confirmed via optical microscopy (OMAX 40X–2500X), and taxonomic identification was executed using established mycological keys and authoritative determinative manuals (White et al., 1990).

Isolation and Cultivation: Pure fungal cultures were isolated by serial dilution plating on Czapek-Dox, Wort Agar, and Meat-Peptone Agar nutrient media.

Protease Activity Assay: Extracellular proteolytic activity was determined spectrophotometrically using hemoglobin as a substrate, following the principles of Anson's method.

Carbohydrase Analysis: Endo-1,4-β-glucanase and amylase activities were evaluated spectrophotometrically by measuring released reducing sugars via the Somogyi-Nelson colorimetric technique (Vermelho & Couri, 2013).

Oxidoreductase Determination: Laccase and peroxidase activities were quantified spectrophotometrically based on the oxidation rates of ABTS and guaiacol substrates (Bourbonnais & Paice, 1990).

Antimicrobial Potency Evaluation: Antagonistic performance against target microbial pathogens was evaluated using agar block assays and disc diffusion methods (Danquah et al., 2022).

Biometric and Statistical Processing: All analytical trials were conducted in 4 to 6 replicates, and the quantitative data were processed using standard statistical techniques (White et al., 1990).

Results and Discussion

Investigations yielded a total of 76 pure fungal isolates, consisting of 64 micromycetes and 12 macromycetes. Physiological profiling revealed that 75% of the micromycetes belonged to the mesophilic group, whereas 25% exhibited thermotolerant characteristics, retaining growth capacity at elevated temperatures (Table 1).

Table 1
Temperature tolerance of micromycetes isolated from diverse biotopes

No.	Collection site	Thermotolerants (II)*	Mesophiles (I)*	Total Isolated Strains (pcs) 4
1	Petroleum-contaminated soils	5	11	16
2	High-humidity subtropical forests	4	9	13
3	Thermal springs	3	3	6
4	Lake Masazir (Saline environment)	4	9	13
Total	All habitats	16	32	48

**Note.* Group I represents mesophilic strains, and Group II represents thermotolerant strains.

In order to select the most relevant micromycete and macromycete strains, their enzymatic activities were evaluated according to internationally recognized methods. We selected the strains with the highest activity based on enzymatic activity analyses using determinative agents (Ismayilova et al., 2025a). The end of the tests and determinative methods revealed that (Kirk et al., 2008).

Selected High-Yielding Producer Strains:

- Hydrolytic Enzymes: *Aspergillus candidus* (Mazsazir Lake), *Chaetomium thermophile* (thermal springs), *Penicillium resticulosum* (Mazsazir Lake), *Humicola lanuginose* (thermal springs), and *Mucor hiemalis* (oil-contaminated soil) were selected as prominent producers of hydrolytic enzymes.
- Complex Enzymatic System: *Bjerkandera adusta* demonstrated strong, balanced expression of both hydrolytic and oxidative enzyme complexes (subtropical forests).
- Oxidases: *Trametes hirsuta* displayed remarkable potential for laccase and peroxidase production (subtropical forests).
- Endoglucanase: *Trichoderma viride* demonstrated high cellulolytic activity (subtropical forests).

Screening of the isolated strains for extracellular enzyme production yielded the following results:

- Hydrolytic and oxidative activities were detected in 25.0% to 73.4% of the micromycetes.
- Enzymatic activities were identified in 25.0% to 100% of the macromycete isolates.

Table 2
The characteristics of fungi based on their fermentative activity

No.	Enzymes	Number of isolated/active		Percentage in total (%)	
1	Endoglucanase	64/39	12/12	60.9	100
2	Protease	64/47	12/10	73.4	83.3
3	Pectinase	64/35	12/ 8	54.7	66.7
4	Amylase	64/36	12/7	56.3	58.3
5	Xylanase	64/27	12/12	42.2	100
6	Lipase	64/35	12/3	54.7	25.0
7	Laccase	64/19	12/9	29.7	75.0
8	Peroxidase	64/16	12/9	25.0	75.0

MACROMUCOTES
MICROMUCOTES

Antimicrobial Activity Analysis
Additionally, we tested the most promising producers in terms of antimicrobial activity using the disk diffusion method and methods that have been adopted globally in laboratory protocols based on antagonistic capabilities against pathogenic test organisms (Barabadi et al., 2022).

The results of the tests revealed that:
53.1% of micromycete isolates and 58.3% of macromycete isolates exhibited noticeable antimicrobial effects against test strains (Table 3).

The most pronounced antagonistic action was observed in cultures of *Aspergillus flavus* (Masazir Lake), *Chaetomium globosum* (oil-contaminated soil), *Penicillium chrysogenum* (Thermal springs), *Penicillium citrinum* (Thermal springs), *Trametes hirsuta*, and *Trichoderma viride* (subtropical forests).

Table 3
Antimicrobial activity characteristics of the isolated strains

No.	Sampling location	Isolated /Active strains		Percentage of strains in total (%)	
		Micromycetes	Macromycetes	Micromycetes	Macromycetes
1	Petroleum-contaminated soils	21/14	0	66.7	0
2	Lake Masazir (Saline environment)	17/9		52.9	
3	Thermal springs	9/4		44.4	
4	High-humidity subtropical forests	17/7	12/6	41.2	58.3
	Total	64/34	12/6	100/53.1	100/58.3

Optimization of Cultivation Parameters
To enhance the biosynthesis of targeted enzymes and secondary metabolites in selected producer strains, culture conditions were systematically adjusted. Although an organism's genetic framework fundamentally governs the biosynthesis of any cellular metabolite, environmental parameters are equally critical in determining metabolic yields. Accordingly, this phase of the study focused on

defining the optimal growth medium to maximize the fermentative activity of the selected high-producing strains (Abdel-Azeem et al., 2020).

We systematically optimized key nutritional and physical parameters—specifically carbon and nitrogen substrates, cultivation modes, incubation temperature, pH levels, inoculum preparation protocols, and propagation period (Ismayilova et al., 2025b). The findings revealed that while certain regulatory conditions for fermentative expression were uniform across all evaluated fungal strains, other parameters exhibited distinct strain-specific variations (Abdel-Azeem et al., 2020).

Influence of Carbon Source: A positive correlation was identified between the degree of polymerization of the carbon substrate and extracellular enzyme secretion (Mammadova et al., 2026).
Role of Nitrogen Origin: Nitrate nitrogen sources were more effective for micromycete growth, whereas ammonium nitrogen compounds favored macromycetes.
Biosynthetic Yields: Optimization strategies resulted in a 15–20% increase in target product yield for Group 1 strains and an 11–17% increase for Group 2 strains.

Mechanistic evaluations confirmed that protease expression is operates via a constitutive pathway, whereas cellulase biosynthesis is inducible and regulated through catabolite repression.

Conclusion

The empirical findings expand current scientific understanding regarding the physiological and biosynthetic capabilities of fungal strains isolated from extreme environments. Promising strains—such as *Trichoderma viride*, *Trametes hirsuta*, *Aspergillus candidus*, and *Penicillium* species—represent valuable bioresources for the industrial-scale formulation of commercial enzyme preparations and bioactive compounds.

1. A total of 76 pure fungal cultures (64 micromycetes and 12 macromycetes) were isolated from stressed ecological habitats in Azerbaijan, with 25% of the micromycetes classified as thermotolerant, while mesophiles accounted for 75% and true thermophiles were not detected.
2. Hydrolytic and oxidative enzyme activities were observed in 25.0–73.4% of micromycetes and 25.0–100% of macromycetes.
3. Over 50% of the isolates demonstrated antimicrobial inhibition against pathogenic *E. coli*, *P. aeruginosa*, *S. aureus*, and *C. albicans* strains.
4. Modulation of growth parameters enhanced target metabolite accumulation by 11–20%.
5. Regulatory pathways (constitutive vs. inducible) and substrate dependencies governing fungal enzyme expression were established.
6. Optimization of cultivation parameters to enhance fermentative expression yielded a 15–20% increase in output, whereas refining the conditions for antimicrobial activity produced an 11–17% enhancement.

Conflict of Interest

The authors declare no competing interests that could be perceived as influencing the research or its publication. L.B. is an Assistant Editor of the journal. She was not involved in the editorial evaluation or publication decision concerning this manuscript.

References

Abdel-Azeem, A. M., El-Mansy, S. A., Abo Nahas, H. H., Mousa, M. K., Gandal, H. E., Hamdy, S. E., El-Ansary, M. M., & Abdel-Azeem, M. A. (2020). Thermophilic Chaetomium in biotechnology. In A. Abdel-Azeem (Ed.), *Recent developments on genus Chaetomium* (pp. 421–439). Springer. https://doi.org/10.1007/978-3-030-31612-9_16

Barabadi, H., Mohammadzadeh, A., Vahidi, H., Rashedi, M., Saravanan, M., Talank, N., & Alizadeh, A. (2022). Penicillium chrysogenum-derived silver nanoparticles: Exploration of their antibacterial and biofilm inhibitory activity against the standard and pathogenic Acinetobacter baumannii compared to tetracycline. *Journal of Cluster Science*, 33, 1929–1942. https://doi.org/10.1007/s10876-021-02121-5

Bourbonnais, R., & Paice, M. G. (1990). Oxidation of non-phenolic substrates by laccase from Trametes versicolor in the presence of aminobenzotriazole. *FEBS Letters, 267*(1), 99–102.

Danquah, C. A., Minkah, P. A. B., Junior, I. O. D., Amankwah, K. B., & Somuah, S. O. (2022). Antimicrobial compounds from microorganisms. *Antibiotics, 11*(3), 285. https://doi.org/10.3390/antibiotics11030285

Ismayilova, A. A., Mirzezadeh, R. I., Bunyatova, L. N., Mammadova, G. I., Hasanova, T. A., Asgarova, G. F., & Madnee, M. (2025a). Biomass and enzymatic activity assessment of the coniferous-deciduous forests in Azerbaijan. *SABRAO Journal of Breeding and Genetics, 57*(6), 2584–2595. https://doi.org/10.54910/sabrao2025.57.6.31

Kirk, P. M., Cannon, P. F., Minter, D. W., & Stalpers, J. A. (2008). *Dictionary of the fungi* (10th ed.). CABI Publishing.

Kutu, F. R., Mokase, T. J., Dada, O. A., & Rhode, O. H. J. (2019). Assessing microbial population dynamics, enzyme activities and phosphorus availability indices during phospho-compost production. *International Journal of Recycling of Organic Waste in Agriculture, 8*(1). https://doi.org/10.1007/s40093-018-0231-9

Mammadova, G. I., Bunyatova, L. N., Gahramanova, A. Y., Isaqova, V. G., Fatdayeva, A. K., Alakbarli, G. Y., & Hasanova, T. A. (2026a). Environmental pollution in soil, plant leaves, and roots using bioindication in hazelnut fields. *SABRAO Journal of Breeding and Genetics, 58*(3), 1436–1444. https://doi.org/10.54910/sabrao2026.58.3.46

Mammadova, G. I., Salimova, S. J., Jafarov, A. M., Huseynova, S. M., Isayeva, K. K., Isagova, V. G., & Hasanova, T. A. (2026b). Rocky soil composition influences on the microorganisms and vegetation at the Sheki-Zagatala Economic Region, Azerbaijan. *SABRAO Journal of Breeding and Genetics, 58*(3), 1407–1414. https://doi.org/10.54910/sabrao2026.58.3.43

Mammadova, G., Hasanova, T. A., Jafarov, A. M., Huseynova, S. M., Isagova, V. G., Madnee, M., & Asgarova, G. F. (2026). Modeling humus stocks and introducing a saturation coefficient to assess soil organic carbon capacity in forest soils of the Sheki-Zagatala region, Azerbaijan. *International Journal of Agriculture and Biosciences, 15*(5), 2134–2146. https://doi.org/10.47278/journal.ijab/2026.116

Mirzezade, R. I., & Mammadova, G. (2026). Soil protection: A strategic priority of the Soil Museum. *Nature & Science*, *8*(3), 5–11. https://doi.org/10.36719/2707-1146/66/5-11

Pobiega, K., Sękul, J., Pakulska, A., Latoszewska, M., Michońska, A., Korzeniowska, Z., Macherzyńska, Z., Pląder, M., Duda, W., Szafraniuk, J., Kufel, A., Dominiak, Ł., Lis, Z., Kłusek, E., Kozicka, E., Wierzbicka, A., Trusińska, M., Rybak, K., Kot, A. M., & Nowacka, M. (2024). Fungal proteins: Sources, production and purification methods, industrial applications, and future perspectives. *Applied Sciences, 14*(14), 6259. https://doi.org/10.3390/app14146259

Rappaport, H. B., & Oliverio, A. M. (2023). Extreme environments offer an unprecedented opportunity to understand microbial eukaryotic ecology, evolution, and genome biology. *Nature Communications*, 14, 4959. https://doi.org/10.1038/s41467-023-40657-4

Vermelho, A. B., & Couri, S. (2013). *Methods to determine enzymatic activity*. Bentham Science Publishers. https://doi.org/10.2174/97816080530011130101

White, T. J., Bruns, T., Lee, S., & Taylor, J. (1990). Amplification and direct sequencing of fungal ribosomal RNA genes for phylogenetics. In *PCR protocols: A guide to methods and applications* (pp. 315–322). Academic Press.

NATURE & SCIENCE
October 2026, Volume 8, Issue 5, pp. 34–39
DOI: https://doi.org/10.36719/2707-1146/68/34-39

Navigating Transformative Agricultural Technologies on the Path to Food System Transformation

Tinatin Mshvidobadze

Abstract. *Modern agriculture encompasses various existing or emerging technologies, such as robotics, nanotechnology, synthetic proteins, cellular agriculture, gene-editing technologies, artificial intelligence, blockchain, and machine learning, which can have a significant transformative impact on the future of agricultural and food systems. These technologies underpin concepts such as vertical farming, digital agriculture, the bioeconomy, circular agriculture, and aquaponics. Examples of these concepts include different strands of agroecology, such as permaculture, regenerative agriculture, and ecological intensification, which may themselves require the use of various technologies and often incorporate indigenous knowledge. These approaches can also be connected to and integrated with digital technologies. This requires responsible innovation processes that entail anticipating the potential impacts of agricultural technologies through inclusive processes, as well as responding to emerging outcomes and adjusting the direction and course of transition pathways. This paper emphasizes the need to pay greater attention to the inclusion and exclusion effects associated with agricultural technologies and to anticipate their potential impacts through inclusive processes.*

Keywords: *agricultural technologies, innovation systems, food system, sustainability transitions, agricultural innovation*

Introduction

Technology is most commonly believed to cre-ate advantages for large-scale production (i.e., economies of scale), associated with notions of modernization, advancement, improvement auto-mation, physical capital, and digital processes. Historically, agricultural technology developed in the industrialized West and is thus suitable for large areas of monocropping using labor-saving technologies. This was especially true of Green Revolution technology, which was an adaptation of the modern agricultural technology used in Western countries.

Agricultural technology has largely been capital-intensive and labor-saving, and more recently it has moved toward genetic modifiation. Its effects in the West have produced monocropped patterns of land use, and agriculture has developed as an indus-try requiring large transportation networks and supply chains, finding ways to produce vegetables and fruits that will withstand mechanical harvest-ing and transportation over long distances. Pro-cessed and ready-to-eat foods have also been one of the outcomes of the agricultural technologies that have been developed over the past 50 or 70 years. Simultaneously, there is a move in industrialized countries to reclaim local crops and farms in order to produce crops and fresh food locally.

Gori State University, Doctor of Technical Sciences, Gori, Georgia
E-mail: tinikomshvidobadze@gmail.com
Received: 22 April 2026; Accepted: 27 August 2026; Published online: 25 October 2026
© The Author(s) 2026. This is an open access article distributed under the terms of the Creative Commons Attribution-NonCommercial 4.0 International License (CC BY-NC 4.0).

This paper examines issues related to the development of agriculture—specifically, the implications of associated narratives regarding inclusion and exclusion, their potential impact, and how mission-oriented agricultural innovation systems can responsibly organize the transition toward sustainable agriculture.

Materials and Methods

This article employs descriptive, analytical, and explanatory methods to highlight key issues relevant to the study. To formulate the concept, the views of various researchers were cited, serving as a basis for illustrating the arguments and conclusions. Within the framework of innovative agricultural systems, the primary objective is to propose methods and ideas regarding how such a process can be organized responsibly. The paper provides an overview of frequently used methods and formal frameworks, such as technological innovations across various sectors of agriculture. These methods are primarily applied to synthetic data, generating a wide range of solutions.

Results and Discussion

Significant technological progress is currently being observed in the agricultural sector across fields such as robotics, nanotechnology, gene technologies, artificial intelligence and machine learning, energy production, and many other areas (De Clercq et al., 2018).

Future agriculture and food systems—some of which are already developing and operating, though not yet implemented on a full scale—encompass concepts such as vertical farming, digital agriculture, the bioeconomy, circular agriculture, and aquaponics (Hermans, 2018).

These technologies have the potential to radically impact the processes of food production, processing, trade, and consumption. These include technologies such as gene editing, synthetic food production (e.g., synthetic protein), lab-grown meat—or cellular agriculture technologies—microalgae bioreactors, drones, the Internet of Things (IoT), robotics and sensors associated with precision farming technologies, 3D food printing, artificial intelligence and machine learning, as well as blockchain.

Some authors view the use of technologies as part of the digital revolution in agriculture, which could ultimately lead to "Agriculture 5.0". Influential international organizations working in the fields of food and nutrition security—such as the World Bank, FAO, and OECD—discuss the potential of agricultural technologies and the global landscape in this regard in their recent reports (Jouanjean, 2019).

Currently, significant financial resources are being spent worldwide on the development and implementation of Agriculture technologies. For instance, investments are being made in large-scale digital transformation research and innovation programs, such as the DigiScape platform and Food Agility Hub in Australia; the #DigitAg program in France; and the "Internet of Food and Farming" program, along with Digital Innovation Hubs (or SmartAgriHubs), in the European Union (Klerkx et al., 2010). Research institutes such as Wageningen University and Research (Netherlands) and AgResearch (New Zealand) maintain strategic investment programs addressing "Protein Transitions" and "New Zealand's Bioeconomy in the Digital Age," respectively. Organizations such as CGIAR and CSIRO collaborate on initiatives like "Wild Futures," which focus on technologies that accelerate innovation within food systems to achieve the Sustainable Development Goals (Herrero et al., 2019).

In terms of diversity, the coexistence of agricultural and food systems is possible. However, when there is no longer room for diversity and certain systems assume a dominant and hegemonic position, this can give rise to inequality and injustice—outcomes that are undesirable from the perspectives of human well-being and ecosystem integrity and sustainability.

Different agricultural technologies—and the systemic concepts upon which they are based and which they encompass (or exclude)—follow distinct trajectories. They shape the development path of agricultural and food systems through the technologies, markets, institutional arrangements, and values they integrate, as well as the transformative outcomes they aim to achieve (Kanger & Schot, 2019). Precision agriculture (PA) represents a transformative approach to modern farming, leveraging advanced technologies such as GPS-guided machinery, drones, and remote sensing to optimize agricultural practices (Fig. 1) (Gebbers & Adamchuk, 2010).

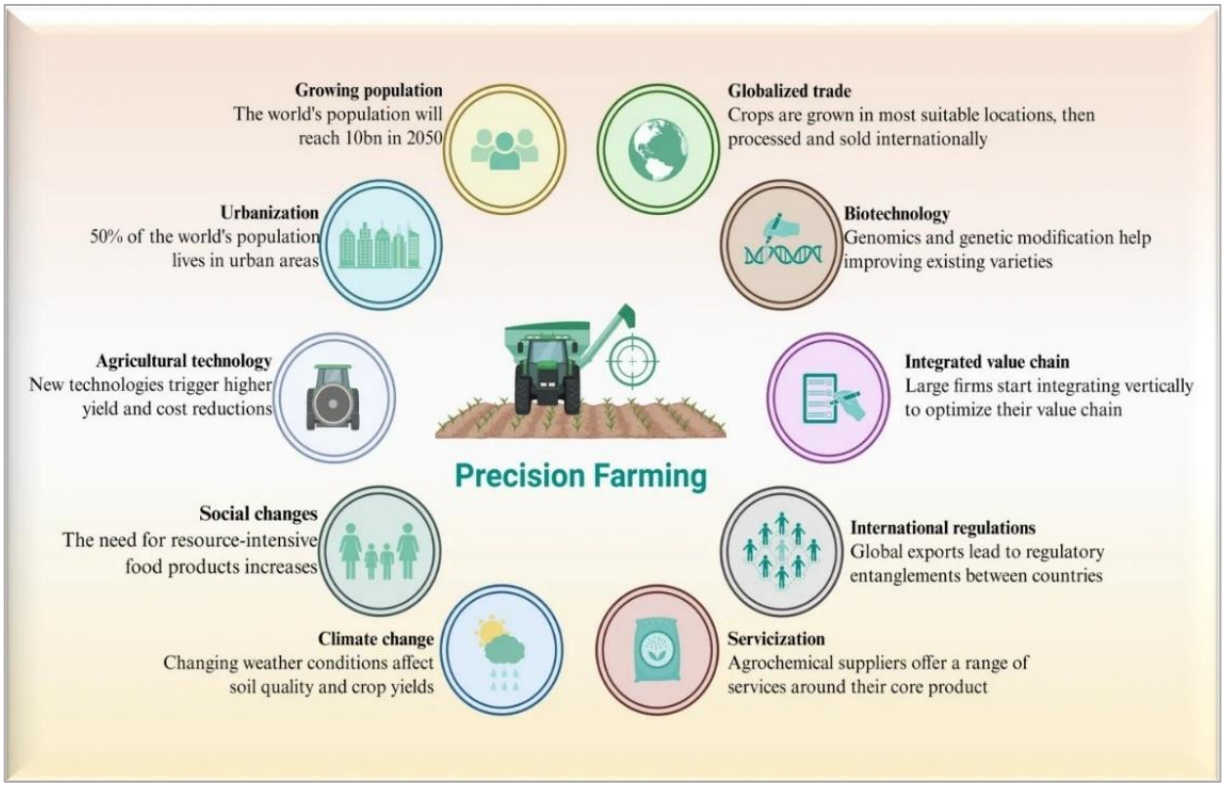


Figure 1
Precession agriculture as one of the modern agricultural technologies (www.biorender.com)

Recent advances in biotechnology and genetic engineering have revolutionized agriculture by developing drought-resistant crops, CRISPR-edited varieties, and genetically modified organisms (GMOs), each playing a critical role in enhancing food security under climate change (Fig. 2). Drought-resistant crops, such as Water Efficient Maize for Africa (WEMA) and drought-tolerant wheat, are engineered to thrive in water-scarce conditions by modulating genes like OsNAC9 in rice and ZmPYL in maize, improving water-use efficiency by up to 30% (Varshney et al., 2021).

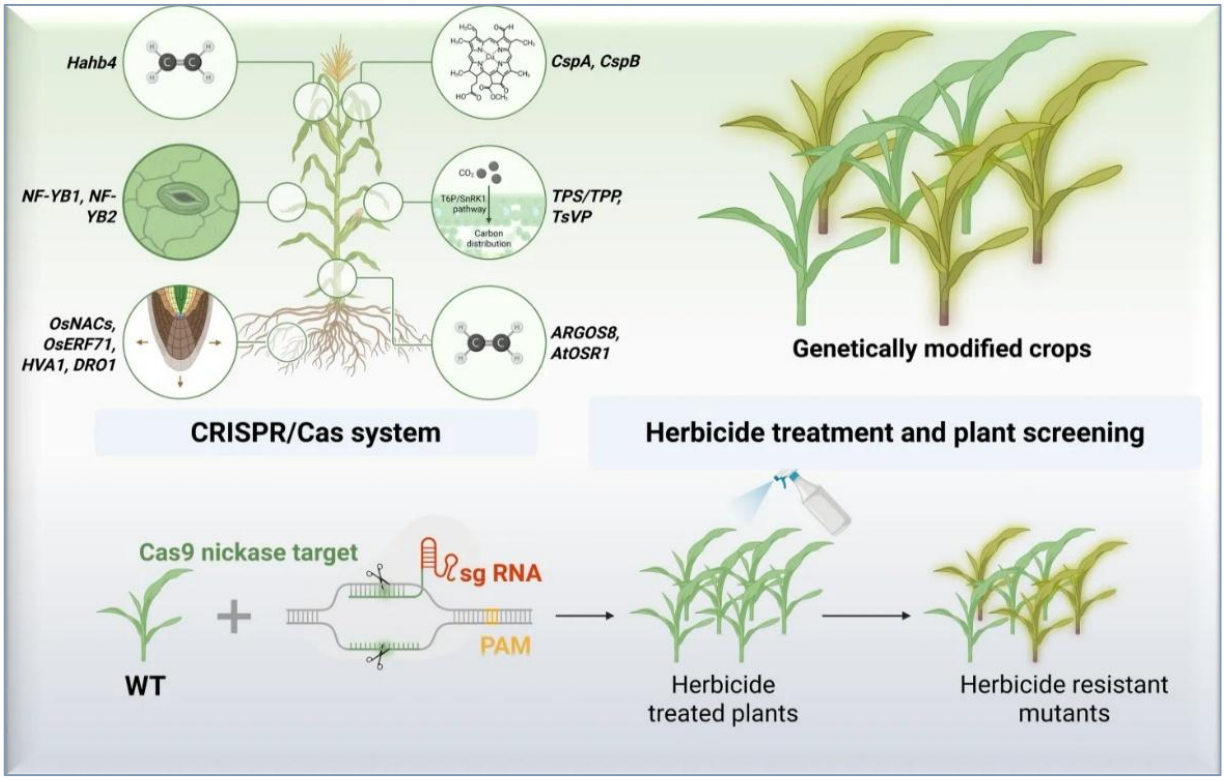


Figure 2
Techniques involved in the biotechnological and genetic engineering for the efficient agriculture production

Moreover, scaling up could lead to unforeseen and unpredictable consequences. Outcomes may also vary across different contexts—for instance, when considering the disparities between developed and developing nations. This is because technology is not context-neutral and is linked to specific configurations of economic power.

Organizing Transition Processes in Agricultural Innovation Systems

It is widely acknowledged that transition processes involve transformative events leading to new technological and economic systems. These processes include co-evolution (where technologies develop alongside and in interconnection with societal structures), selection (where some technologies fail to achieve dominant status), and stabilization/institutionalization (where certain technologies evolve into new dominant models and their corresponding social, market, or political structures) (El Bilali, 2018).

This implies that the ongoing processes of adopting and scaling up agricultural technologies likely involve active interaction between various technologies and the underlying concepts upon which they are based (agricultural and food systems). Such interaction can be "passive"—occurring through the dynamics of competition in global markets—or "active"—taking place through cooperation, competition, or "co-opetition" (a combination of cooperation and competition) among innovators (Planko et al., 2019).

Agricultural innovation systems often foster the development of specific sets of technologies, yet the underlying values upon which these technologies are based remain unclear. Furthermore, it is uncertain how they contribute to shaping sustainability-oriented transition processes—specifically, whether they reinforce existing technological and economic paradigms or facilitate "deep transitions". Despite the adoption of sustainable development principles and a focus on critical policy issues such as food and nutritional security, the primary goal of dominant and influential groups within

agricultural innovation systems—the constellation of business, scientific, governmental, and civil society actors that create and disseminate innovations—in many countries is to boost agricultural productivity and growth through a modernization pathway that perpetuates existing practices of food production, trade, and consumption (Pigford et al., 2018).

It is worth noting that a number of countries are adopting "mission-oriented" approaches within their agricultural innovation systems; with a view toward future food systems, these approaches focus on issues such as food and nutritional security and environmental sustainability. For instance, the Netherlands has adopted the "circular agriculture" paradigm and is investing in the "protein transition" (Pyett et al., 2019). Nicaragua places great emphasis on agroecology, while New Zealand has recently focused on developing a "digital bioeconomy".

Conclusion

When shaping future visions, it is essential to consider how agricultural technologies interact with one another and with concepts of sustainable agriculture—such as agroecology or regenerative farming—and what this implies for the future of agricultural and food systems. Naturally, it is difficult to fully foresee the consequences of the large-scale adoption of new technologies. The degree of reflexivity is of crucial importance in strategies aimed at implementing socio-technical transformations. It is important to consider the context and acknowledge that technologies are not universal (as the experience of the "Green Revolution" has already demonstrated); rather, they evolve and become integrated into diverse socio-economic, cultural, and political environments.

Declaration of Competing Interests

The author declares that they have no known competing financial interests or personal relationships that could have appeared to influence the work reported in this paper.

References

De Clercq, M., Vats, A., & Biel, A. (2018, 11–13 February). *Agriculture 4.0: The future of farming technology*. World Government Summit. Dubai, United Arab Emirates.

El Bilali, H. (2018). Transition heuristic frameworks in research on agro-food sustainability transitions. *Environment, Development and Sustainability, 22*, 1693–1728. https://doi.org/10.1007/s10668-018-0290-0

Gebbers, R., & Adamchuk, V. I. (2010). Precision agriculture and food security. *Science, 327*(5967), 828–831. https://doi.org/10.1126/science.1183899

Hermans, F. (2018). The potential contribution of transition theory to the analysis of bioclusters and their role in the transition to a bioeconomy. *Biofuels, Bioproducts and Biorefining, 12*(2), 265–276. https://doi.org/10.1002/bbb.1861

Herrero, M., Thornton, P., Mason-D'Croz, D., & Palmer, J. (2019). *Transforming food systems under a changing climate: Future technologies and food systems innovation for accelerating progress towards the SDGs—Key messages*. CGIAR Research Program on Climate Change, Agriculture and Food Security (CCAFS).

Jouanjean, M. (2019). Digital opportunities for trade in the agriculture and food sectors. *OECD Food, Agriculture and Fisheries Papers*, 122. OECD Publishing. https://doi.org/10.1787/91c40e07-en

Kanger, L., & Schot, J. (2019). Deep transitions: Theorizing the long-term patterns of socio-technical change. *Environmental Innovation and Societal Transitions, 32*, 7–21. https://doi.org/10.1016/j.eist.2018.07.006

Klerkx, L., Aarts, N., & Leeuwis, C. (2010). Adaptive management in agricultural innovation systems: The interactions between innovation networks and their environment. *Agricultural Systems, 103*(6), 390–400. https://doi.org/10.1016/j.agsy.2010.03.012

Pigford, A. E., Hickey, G. M., & Klerkx, L. (2018). Beyond agricultural innovation systems? Exploring an agricultural innovation ecosystems approach for niche design and development in sustainability transitions. *Agricultural Systems, 164*, 116–121. https://doi.org/10.1016/j.agsy.2018.04.007

Planko, J., Chappin, M. M. H., Cramer, J., & Hekkert, M. P. (2019). Coping with coopetition—Facing dilemmas in cooperation for sustainable development: The case of the Dutch smart grid industry. *Business Strategy and the Environment, 28*(5), 665–674. https://doi.org/10.1002/bse.2271

Pyett, S., de Vet, E. W. M. L., Trindade, L. M., van Zanten, H. H. E., & Fresco, L. O. (2019). *Chickpeas, crickets, and chlorella: Our future proteins*. Wageningen Food & Biobased Research.

Varshney, R. K., Barmukh, R., Roorkiwal, M., Qi, Y., Kholova, J., Tuberosa, R., Reynolds, M. P., Tardieu, F., & Siddique, K. H. M. (2021). Breeding custom-designed crops for improved drought adaptation. *Advanced Genetics, 2*(3), e202100017. https://doi.org/10.1002/ggn2.202100017

NATURE & SCIENCE
October 2026, Volume 8, Issue 5, pp. 40–60
DOI: https://doi.org/10.36719/2707-1146/68/40-60

Current Understanding of PGPR–Plant Interaction under Salt Stress Environment: A Review

Shafeequr Rahman Khan[1], Saba Siddiqui[1*], Iqbal Ahmad[2], Firoz Ahmad Ansari[3], and Sheeba Khan[4]

Abstract. *Soil salinity is a serious environmental problem which affects agricultural production globally, especially in arid and semi-arid areas. Soluble salt accumulation may affect water uptake, induce ionic toxicity, decrease nutrient availability and increase reactive oxygen species (ROS) production that leads to damage to cellular components and affects normal physiological functioning. Traditional breeding has developed salt-tolerant crops, but long breeding cycles, high costs, and genotype–environment interactions limit its efficiency. Plant growth-promoting bacteria (PGPB) offer an eco-friendly alternative for improving crop performance under salinity. They enhance salt tolerance through complementary mechanisms, including phytohormone regulation, osmolyte accumulation, exopolysaccharide production, nutrient acquisition, and balanced Na^+/K^+ uptake. PGPB also promote proline and glycine betaine accumulation, supporting osmotic adjustment, membrane stability, and cellular protection. Together, these microbial activities help plants maintain ionic and physiological balance, reduce salt-induced damage, and sustain growth under saline conditions. This review brings together the physiological responses of the crop plants to salinity and discusses both the direct and indirect mechanisms mediating salt tolerance that PGPB provide based on fundamental and contemporary (2020–2026) literature. Representative plant-bacterium associations are curated in comparative tables to showcase the taxonomic diversity and mechanisms already described, and existing knowledge gaps are highlighted, including at the field-level and in the context of multi-strain consortia. The use of PGPB is proposed as a low-cost, non-toxic, and eco-friendly solution to maintain crop productivity in salinity affected soils, and to help ensure long-term food security in the face of climatic changes.*

Keywords: *soil salinity, plant growth-promoting bacteria, reactive oxygen species, sustainable agriculture, food security*

[1]Department of Agriculture Sciences, Integral Institute of Agricultural Science and Technology, Integral University, Lucknow, Uttar Pradesh, India
[2]Department of Agricultural Microbiology, Faculty of Agricultural Sciences, Aligarh Muslim University, Aligarh, Uttar Pradesh, India
[3]Microbiology Lab, CCRUM-Drug Standardization Research Institute, Ministry of Ayush, Ghaziabad, Uttar Pradesh, India
[4]Department of Environmental Sciences, Dr. R.M.L. Avadh University, Faizabad, Uttar Pradesh, India
[*]Corresponding author. E-mail: profsaba27@gmail.com
Received: 4 June 2026; Accepted: 10 September 2026; Published online: 25 October 2026
© The Author(s) 2026. This is an open access article distributed under the terms of the Creative Commons Attribution-NonCommercial 4.0 International License (CC BY-NC 4.0).

1. Introduction

Climate change is among the most pressing environmental issues in the 21st century. However, a large amount of evidence exists that intensive agriculture and increased energy usage are significant anthropogenic drivers of global climatic changes that include higher temperatures, variability in rainfall, flooding and degradation of soils (Ansari et al., 2021; Kopittke et al., 2026). Soil salinisation is one of these consequences and is especially problematic in areas with limited water resources, such as in arid and semi-arid regions, where it further impacts agricultural sustainability (Janni et al., 2024; Shokri et al., 2024).

Salinity in soils occurs when soluble salts slowly build up in the soil profile to levels that inhibit plant growth and soil activity. There are two types of salinisation; the first is through geological and climatic processes (primary) and the second is due to human activities such as inappropriate irrigation practices, inadequate drainage, and unsuitable land-use (secondary) (Stavi et al., 2021; Hassani et al., 2021). The high concentration of soluble salts is the most typical characteristic of saline soils and can be used to determine salinity status of soil, typically by measuring the electrical conductivity of the saturated soil extract at 25 °C, with a value above 4 dS m^{-1} indicating saline soils (Liu et al., 2026).

While NaCl is generally regarded as the main salt causing salinity stress it can be other salts such as sodium sulfate that "can play a significant role in salinity" related issues. Ions like sodium (Na+), calcium (Ca2+), magnesium (Mg2+) and carbonate species can build up in the soil over time, causing fertility problems and impacting plant growth (Negacz et al., 2022). Now, it is known that salinity is one of the most significant causes of land degradation worldwide, with over 833 million hectares of agricultural land already impacted by salt and the number of such affected areas anticipated to grow with the ongoing climate change and unsustainable land management practices (Liu et al., 2026; Alhan et al., 2026).

The development and severity of soil salinity are influenced by several factors related to the environment and anthropogenic such as climate, water irrigation quality, soil properties, hydrology, topography, biological activity, and land use practice (Basak et al., 2022). Beyond soil degradation, crop productivity and economic return in saline environments has been found to be lower, with losses reported across a range of staple crops including rice, wheat, cotton and sugarcane – particularly in agricultural areas such as India (Kopittke et al., 2026; Derbew et al., 2026).

When plants encounter saline conditions, they use various adaptations to cope with the stress, typically either by avoiding the stress (to minimise the damage) or tolerating the stress (to keep growing and living normally despite the stress). Under conditions where salinity levels are high enough, however, plant growth and yields can be significantly reduced, to a higher or lower degree depending on the species and cultivars (van Zelm et al., 2020; Liu et al., 2024).

Salinity effects are of a multifaceted nature in terms of physiology and biochemistry. "A high salt concentration decreases the soil water potential to which plants" must adjust, making it harder for them to absorb water, and causing osmotic stress. With limited water supply, the shoots keep growing less and more, and the stomata begin to close, which decreases the transpiration rate and the efficiency of photosynthesis (Hasanuzzaman et al., 2023). As salinity continues, toxic ions, especially sodium and chloride are increasing in plant tissues, which alters the organisation, integrity and metabolism of cells (Tester & Davenport, 2003).

Salinity also affects uptake and uptake of mineral nutrients. The antagonistic effects of toxic ions and nutrient elements may cause deficiency of N, P, K, Ca, Mg, Fe, Cu, Zn and other plant growth elements (Dey et al., 2021). High accumulation of salt further disrupts the photosynthetic apparatus, elevates the overproduction of Reactive Oxygen Species (ROS) causing oxidative stress and

programmed cell death (PCD) in proteins, lipids, nucleic acids and cellular membranes (Hasanuzzaman et al., 2021). Salinity hence negatively impacts the plant growth from the germination to the vegetative growth stage, flowering and reproduction stage (Manono, 2025).

As saline soils are becoming more common, sustainable strategies to enhance soil productivity in saline environments have become more relevant (Xing et al., 2026). Salinity mitigation through conventional management strategies, including irrigation, drainage enhancement, soil amendment and the development of salt-tolerant cultivars, has helped reduce salinity, but can be expensive, labour intensive, location-specific and will not provide a long-term solution (Melino & Tester, 2023). To devise more effective management strategies, a better understanding of the molecular, physiological and ecological mechanisms of plant response to salinity is needed (Singh, 2022).

In the last few years, plant growth-promoting bacteria (PGPB) have gained a lot of attention in recent years as environment-friendly bioinoculants that are able to increase the resistance of plants to saline conditions (Mishra et al., 2021). They promote plant growth and productivity in a diverse range of ways such as nutrient uptake, ion homeostasis, control of phytohormone levels, water relations, antioxidant defence, and stress responsive pathways (Ilangumaran & Smith, 2017; Shahid et al., 2026). Owing to these multifaceted benefits, PGPB are increasingly considered a promising biological tool for sustainable crop production in salt-affected environments, and PGPR-based bioinoculants are also being explored in combination with mycorrhizal fungi and engineered soil microbiomes to further extend crop resilience under climate-driven salinity (Shi et al., 2026; Chanson et al., 2026; Zeng et al., 2024).

Accordingly, “this review aims to provide a comprehensive, critically referenced overview of the mechanisms through which plant growth-promoting bacteria alleviate salinity stress and enhance plant performance under saline conditions”. The review brings together literature on both the basics of stress tolerance mechanisms exerted by PGPB and more recent advances in the same field (de Andrade et al., 2023; Chakrovarty et al., 2026; Nguyen et al., 2025) and points to the potential of using these microbes in sustainable agriculture under the new challenges of increasing salinity.

2. The Plant's Response to Salinity Stress will be Physiological

As dissolved ion concentration increases in soil, soil becomes saline and can become saline, sodic or saline-sodic soil. Salinity-affected soils typically have elevated concentrations “of cations like Ca^{2+}, Mg^{2+} and Na^{+}, and anions like SO_4^{2-}, Cl^{-} and HCO_3^{-}”. Of these, the sodium and chloride ions are clearly damaging because of their toxicity to plant physiology and their ability to cause disruption of soil structure (Tester & Davenport, 2003; Ansari et al., 2024).

Plants are impacted by salinity at the morphological, physiological and biochemical level. It can inhibit seed germination, inhibit vegetative growth and affect reproductive development by osmotic stress, causing roots to have trouble absorbing water, and ionic stress, from the accumulation of toxic ions in the plant tissue. These stresses over time lead to soil erosion, reduced soil fertility and reduced yields. In addition to these primary effects, salinity also generates secondary effects, known as oxidative stress, whereby an excess of ROS damages cellular membranes, proteins and DNA. These all together effects are harmful for the growth of the plants and endanger the sustainability of agriculture in salt affected areas (Liu et al., 2026).

2.1. Disruption of Water Uptake

2.1.1. Osmotic Stress

“Osmotic stress is one of the first responses of plants to salinity. Too much salt in the soil solution decreases its water potential, decreasing the water potential gradient and making it harder for water

to enter roots". Under these conditions, plants also have a water deficit despite the presence of adequate soil water and adjust by reducing the openings of their stomata and minimising transpiration, a process that is known to help conserve water but also reduces their ability to fix carbon dioxide (CO2) (Tester & Davenport, 2003).

2.1.2. Cellular Dehydration

When the osmotic stress is continuous, the turgor pressure of the cell decreases, which will prevent it from growing. Loss of turgor manifests as leaf wilting, reduced leaf-area development, and inhibited elongation of shoots and roots. Prolonged dehydration reduces meristematic activity, which in turn slows the production of new tissues.

2.2. Rhizobacteria-Derived Biomolecules Contributing to Plant Tolerance and Resistance

2.2.1. Production of Plant Growth-Regulating Compounds

Saline "conditions cause plants to" synthesise several phytohormones, including abscisic acid "(ABA), indole-3-acetic acid (IAA), and ethylene, which regulate plant" metabolism, morphology, biomass accumulation, and physiological adjustment. Soil microorganisms can additionally modify the plant's hormonal status by releasing phytohormones or hormone-modulating enzymes of their own. "Modifications in hormonal signalling arising from plant-microbe interactions are consequently regarded as a significant mechanism contributing to plant tolerance of soil salinity" (Ilangumaran & Smith, 2017).

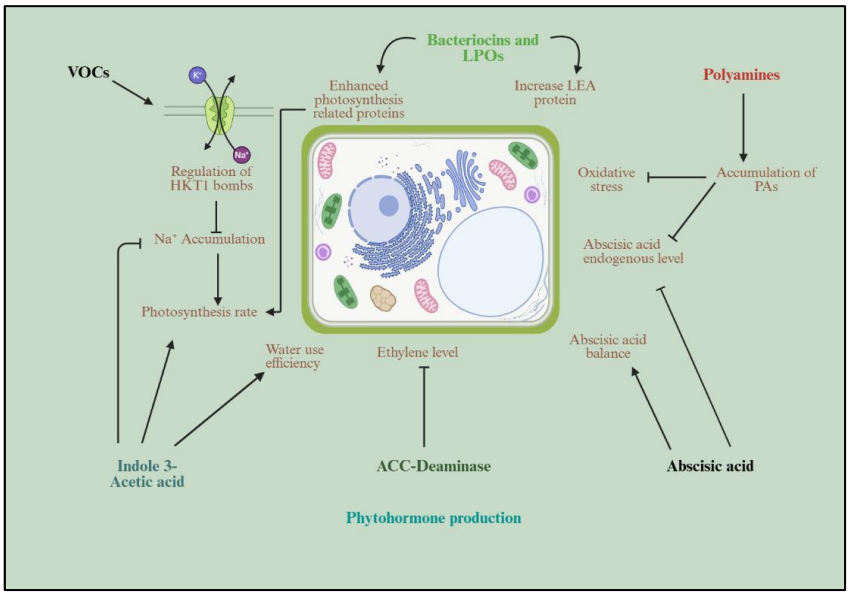


Figure 1

Molecules synthesized by plant growth-promoting bacteria (PGPB) implicated in plant salinity tolerance, including indole-3-acetic acid, ACC deaminase, abscisic acid, volatile organic compounds, polyamines, and bacteriocins/lipo-chito-oligosaccharides, and their downstream physiological effects.

Source. Original figure prepared by the authors, synthesised from the mechanistic evidence discussed in Section 2.2 (Ilangumaran & Smith, 2017, and the primary studies cited there in).

2.2.1.1. Indole-3-Acetic Acid (IAA)

Indole-3-acetic acid (IAA) is the key auxin governing plant growth and development. IAA is synthesised by rhizobacteria through several metabolic routes, many of which depend on L-tryptophan supplied by root exudates. This hormone regulates a range of plant "processes, including

cell division, cell elongation, tissue differentiation, apical dominance, phototropism, and gravitropism"; a balanced IAA concentration supports normal growth, whereas excessive levels can be inhibitory.

External "application of IAA to crops such as maize, sorghum, and pea has been shown to reduce the adverse effects of salinity stress, improving photosynthetic activity, water-use efficiency", regulation of sodium ion accumulation, and biomass. Increased auxin levels under saline conditions are considered important for supporting root and shoot growth, which are particularly sensitive to this abiotic stress.

Auxin-producing PGPB also limit the yield losses typically caused by soil salinity. Inoculation of salt-stressed cotton with the IAA/ABA-modulating strain *Pseudomonas putida Rs-198* improved germination, productivity traits, and nutrient content while lowering internal ABA synthesis (Yao et al., 2010). Comparable benefits have been reported in groundnut inoculated with halotolerant IAA-producing rhizobacteria under 100 mM NaCl, which enhanced water-status maintenance and productivity traits (Shukla et al., 2012; Ansari et al. 2019). In wheat, inoculation with the "auxin- and siderophore-producing *actinobacterium Streptomyces sp.* under saline soil conditions" increased germination rate, seedling length, biomass, and nutrient content (Sadeghi et al., 2012), while in common bean, IAA-producing *Azospirillum brasilense* and *Rhizobium etli* increased root biomass, root number, and nodulation relative to IAA-deficient mutants, directly implicating bacterial auxin in the root-developmental response (Remans et al., 2008; Ansari et al., 2023).

These findings collectively support a strong relationship between bacterial IAA production and modification of plant hormonal balance in a manner that promotes growth under saline conditions. Comparisons between externally applied IAA and auxin-deficient bacterial mutants indicate that bacterially derived auxin differentially affects root biomass, nodule formation, and basal root development during early growth stages (Ilangumaran & Smith, 2017).

2.2.1.2. Ethylene Regulation Through ACC Deaminase Activity

Ethylene is widely recognised as a stress-related hormone, and its synthesis is strongly affected by both abiotic and biotic stress. Increased ethylene levels reduce root elongation and formation and therefore have an overall negative effect on plant growth. The immediate precursor of ethylene biosynthesis, 1-aminocyclopropane-1-carboxylate (ACC), is transported to stress-affected tissue, where it is oxidised to ethylene by ACC oxidase.

PGPB can lower ethylene accumulation in plants through the production of "ACC deaminase, an enzyme that cleaves ACC into ammonia and α-ketobutyrate", which can subsequently serve as nitrogen and carbon sources for bacterial metabolism. Through this mechanism, ACC deaminase-producing rhizobacteria decrease stress-induced ethylene levels, alleviate growth inhibition, and promote overall plant development.

Multiple studies confirm that ACC deaminase-producing bacteria counteract ethylene-mediated growth suppression under saline conditions. In tomato, *Achromobacter piechaudii* reduced ethylene production and increased fresh and dry biomass and phosphorus/potassium uptake under 172 mM NaCl (Mayak et al., 2004), while ACC deaminase-deficient *Pseudomonas* mutants produced markedly poorer growth outcomes than wild-type strains in salt-stressed tomato, confirming the causal role of this enzyme (Ali et al., 2014). Halotolerant ACC deaminase-producing strains of *Brevibacterium, Bacillus,* and *Zhihengliuella* supported growth and nutrient uptake in red pepper under salt stress by suppressing ethylene synthesis (Siddikee et al., 2011), and an ACC deaminase-producing *Pseudomonas fluorescens* strain significantly improved salt tolerance and yield in groundnut compared with strains lacking this enzymatic function (Saravanakumar & Samiyappan, 2007). In *Trigonella foenum-graecum*, "ACC deaminase-containing *Bacillus subtilis* reduced

ethylene-induced damage and improved mycorrhizal colonisation and rhizobial nodulation under osmotic stress" (Barnawal et al., 2013).

Beneficial microbes that combine IAA and ACC deaminase production appear to act synergistically: "IAA stimulates cell division and root development, while ACC deaminase" prevents excessive ethylene accumulation, together sustaining plant growth under stress. Co-inoculation of tomato with ACC deaminase- and trehalose-producing *Pseudomonas* sp. UW4 synergistically protected plants against salt stress (Orozco-Mosqueda et al., 2019), and inoculation of salt-stressed chickpea (150 mM NaCl) with the "IAA- and ACC deaminase-producing Pantoea dispersa strain PSB3" improved growth and yield while reducing sodium uptake (Panwar et al., 2016).

2.2.1.3. "Abscisic Acid (ABA)" Modulation

Abscisic acid (ABA) is a key phytohormone in plant adaptation to abiotic and biotic stress, playing a significant role in "tolerance to drought, salinity, and heavy-metal toxicity". Under osmotic stress, ABA is mainly synthesised in roots and transported to aerial tissue, where it regulates stomatal closure, stimulates root growth to enhance water uptake, and helps maintain ionic balance.

PGPB influences endogenous ABA levels and thereby contributes to improved stress tolerance under saline environments. Cucumber inoculated with "*Burkholderia cepacia*, *Promicromonospora* sp., and *Acinetobacter calcoaceticus* under combined salt and drought stress" showed higher biomass, chlorophyll, water status, and downregulation of ABA-associated genes relative to non-inoculated controls (Kang et al., 2014). In soybean, halotolerant rhizobacteria reduced endogenous ABA levels and downregulated the ABA-linked GmNARK signalling pathway, increasing weight, length, and chlorophyll content under NaCl stress (Khan et al., 2019). Similarly, inoculation of maize with Kocuria rhizophila Y1 conferred protection against salinity through coordinated hormonal modulation increased IAA together with reduced ABA associated with downregulation of the ABA-biosynthesis gene ZmNCED1 and altered expression of the ion-transporter genes ZmHKT1 and ZmNHX1-3 (Li et al., 2020).

Other investigations show that specific rhizobacteria can instead increase ABA accumulation, indicating a context-dependent regulatory role. ABA-producing *Bacillus* and *Pseudomonas* strains isolated from grapevine roots reduced water loss and induced ABA accumulation together with defence-related terpene synthesis in *in vitro*-cultured *Vitis vinifera* (Salomon et al., 2014), while an ABA-, IAA-, and gibberellin-producing endophytic "*Azospirillum lipoferum* strain alleviated the effects of osmotic (drought) stress in maize, with ABA" quantitatively confirmed by GC-EIMS (Cohen et al., 2009). Collectively, this body of evidence indicates that PGPB can fine-tune ABA levels in a manner that depends on environmental conditions and host developmental stage, a nuance also emphasised in the broader synthesis by Ilangumaran and Smith (2017).

Table 1

Modulation of phytohormones (IAA, ACC deaminase, ABA) in connection with salinity tolerance (represented by PGPB)

No.	Plant host	Bacterium	Mechanism	Effect	Citation
1	*Gossypium hirsutum* L.	*Pseudomonas putida* Rs-198	IAA production; ABA suppression	Increased germination rate, productivity traits, nutrient content	Yao et al. (2010)
2	*Arachis hypogaea* L.	*Brachybacterium, Brevibacterium, Haererohalobacter* spp.	Water homeostasis; IAA accumulation	Higher productivity traits and nutrient content) (100 mM NaCl	Shukla et al. (2012)

3	*Triticum aestivum* L.	*Streptomyces* sp.	IAA and siderophore production	Increased germination, seedling length, weight, nutrient content	Sadeghi et al. (2012)
4	*Phaseolus vulgaris* L.	*Azospirillum brasilense* + *Rhizobium etli*	IAA production	Higher root weight, root number, and nodulation	Remans et al. (2008)
5	*Zea mays* L.	*Pseudomonas fluorescens* + *Enterobacter aerogenes*	ACC deaminase production	Increased height, biomass, K+/Na+ ratio, NPK uptake	Zahir et al. (2012)
6	*Trigonella foenum-graecum* L.	*Bacillus subtilis*	ACC deaminase production	Reduced ethylene damage; improved nodulation/mycorrhization under osmotic stress	Barnawal et al. (2013)
7	*Solanum lycopersicum* L.	*Achromobacter piechaudii*	ACC deaminase production	Increased fresh/dry weight, P and K uptake (172 mM NaCl)	Mayak et al. (2004)
8	*Capsicum annuum* L.	*Brevibacterium, Bacillus, Zhihengliuella* spp.	ACC deaminase production	Higher biomass and nutrient uptake (halotolerant strains)	Siddikee et al. (2011)
9	*Arachis hypogaea* L.	*Pseudomonas fluorescens*	ACC deaminase production	Increased seedling weight, height, germination	Saravanakumar & Samiyappan (2007)
10	*Solanum lycopersicum* L.	*Pseudomonas* sp. UW4	ACC deaminase + trehalose production	Synergistic protection: root/shoot length, dry weight, chlorophyll	Orozco-Mosqueda et al. (2019)
11	*Solanum lycopersicum* L.	*P. fluorescens / P. migulae* (ACC-deaminase mutants)	ACC deaminase production	Wild type > mutant for biomass, chlorophyll, flowering	Ali et al. (2014)
12	*Cicer arietinum* L.	*Pantoea dispersa* (PSB3)	IAA + ACC deaminase production	Improved yield, K+/Na+ ratio, water/chlorophyll content (150 mM NaCl)	Panwar et al. (2016)
13	*Cucumis sativus* L.	*Burkholderia, Promicromonospora, Acinetobacter* spp.	Downregulation of ABA-associated genes	Increased biomass, chlorophyll, K/P content under salt + drought	Kang et al. (2014)
14	*Glycine max* L.	*Halotolerant rhizobacteria (Bacillus/Arthrobacter* spp.*)*	Reduced ABA; downregulation of GmNARK	Increased fresh/dry weight, length, chlorophyll content	Khan et al. (2019)
15	*Zea mays* L.	*Kocuria rhizophila Y1*	HKT/NHX and ZmNCED1 gene regulation; IAA up, ABA down	Decreased Na+ accumulation; improved productivity traits	Li et al. (2020)
16	*Vitis vinifera* L.	*Bacillus* sp. + *Pseudomonas* sp.	ABA production/accumulation	Reduced water-loss rate; terpene defence synthesis	Salomon et al. (2014)
17	*Zea mays* L.	*Azospirillum lipoferum*	ABA, IAA, gibberellin production	Reversed effects of osmotic (drought) stress	Cohen et al. (2009)

This is a compilation of the authors from the primary studies mentioned in the final (Citation) column of the above table.

2.3. Ion Toxicity

Saline conditions cause the build-up of certain ions, primarily sodium (Na+) and chloride (Cl−) in the plant tissue (Tester & Davenport, 2003). Excessive absorption of these ions affects enzyme function, compromise membrane integrity and interfere with nutrient absorption, particularly "potassium (K^+) and calcium (Ca^{2+}) which are essential for protein synthesis and membrane" function. Common symptoms of ion toxicity are chlorosis, marginal necrosis and early senescence, especially on older leaves where accumulation of salts occurs.

2.4. Impairment of Photosynthesis and Growth

2.4.1. Reduced Photosynthetic Efficiency

Salinity stress affects photosynthesis by disrupting the activity of enzymes in the Calvin cycle, causing damage to the chlorophyll pigments, and damaging Photosystem II. The osmocosmosis also leads to reduced stomatal conductance which further limits the supply of CO_2 to the chloroplasts, thus further reducing the photosynthetic rate.

2.4.2. Reduced Growth and Biomass

The amount of carbohydrates produced by the plants for energy and plant structure is reduced due to less photosynthetic carbon fixing. The growth inhibition is most severe in young rapidly growing tissue (leaf tips and root tips) and the resulting decrease in assimilate production has a negative impact on both vegetative and reproductive growth, resulting in a reduction in yield.

2.5. Altered Gas Exchange

2.5.1. Stomatal Closure

When exposed to salinity, "plants close their stomata to conserve water", so less water transpires and less salt is taken up. This adaptive response is a mechanism to cope with high salinity under water limitation and is involved in maintaining water homeostasis and ion homeostasis in the cell.

2.5.2. Diffusion of Nutrients is Also Lowered and Transpiration is Reduced

Persistent stomatal closure causes reduced transpiration, which causes reduction in evaporative cooling and in the transport of nutrients in the xylem, thus increasing the deficiency of essential minerals like N, P and K, and hence further compromising the metabolic activity (Ilangumaran & Smith, 2017; Alhan et al., 2026).

2.6. Metabolic Changes & Excess Production of Reactive Oxygen Species (ROS)

2.6.1. Oxidative Stress

Overproduction "of reactive oxygen species (ROS) like superoxide radicals (O_2^-), hydrogen peroxide (H_2O_2), and hydroxyl radicals (·OH) in chloroplast, mitochondria, and" peroxisome all frequently accompany salinity stress. High levels of ROS can cause genetic damage, inactivate enzymes, and result in membrane leakage (Ilangumaran & Smith, 2017; Alhan et al., 2026).

2.6.2. The Disruption of Key Metabolic Pathways

Ionic imbalance and oxidation damage affect the most important metabolic functions such as respiration, nitrogen assimilation and hormone signal transduction. These hormonal changes, including elevated ABA and decreased levels of cytokinin, alter stress-signalling pathways and gene expression and either promote short-term survival or limit further growth (Ilangumaran & Smith, 2017; Alhan et al., 2026).

3. The Most Important "Mechanisms of Salinity Tolerance Induced by PGPB"

"The effects of salinity on physiology outlined above causes substantial losses in crop yields. But the positive effects of PGPB have been demonstrated to enhance crop growth and to reduce the adverse effects of high soil" populations. This beneficial effect is achieved by several mechanisms such as maintaining ionic balance, synthesis of stress-relieving phytohormones and improvement in nutrient-uptake efficiency. PGPB also plays a role in antioxidant enzyme activation and osmotic adjustment, which helps the plants cope with oxidative stress and cellular damage (Ilangumaran & Smith, 2017; Alhan et al., 2026).

3.1. Water Homeostasis and Accumulation of Osmolytes "To Maintain Osmotic Balance"

"Under salinity conditions, the initial physiological stress which is experienced by plants is osmotic stress. It disrupts water balance causing stomatal closure and a decrease in photosynthetic activity and gas exchange"; carbohydrate accumulation is stored in meristems and storage tissue instead of new-tissue growth, limiting plant proliferation and expansion.

In order to survive, "plants need to regulate water homeostasis and to protect the photosynthetic structures". PGPB acts in various ways to contribute to osmotic balance. The other pathway is through bacterial extracellular polysaccharide (EPS) complex, which is high-molecular weight carbohydrate producing protective biofilm around roots, which retain water in soil, improves soil structure and reduces the Na^+ uptake (Shahid et al., 2026). PGPB may also trigger the plant to produce endogenous plant osmolytes "proline, glycine betaine and soluble sugars as molecular chaperones that help in the stability of protein and cellular structures and turgor pressure. This dual physical barrier/ biochemical adjustment approach is of help to plants in the first stage when they are exposed to saline conditions. In addition, EPS" also works by binding particles together, which is essential for good soil aggregation, thereby increasing soil porosity and aeration, which is required for root growth.

Under field condition, co-inoculation of lettuce with Pseudomonas mendocina and arbuscular mycorrhizal fungus Glomus intraradices improved soil aggregate stability due to increased EPS production (Kohler et al., 2006), while Halomonas variabilis–Planococcus rifietensis improved the growth of chickpea and soil aggregation under salinity stress by increasing EPS and biofilm production (Qurashi & Sabri, 2012). EPS-producing rhizobacteria have similarly improved wheat growth and selective nutrient uptake under salt stress (Ashraf et al., 2004; Talebi Atouei et al., 2019), while co-inoculation of *alfalfa* with *Halomonas maura* and *Ensifer meliloti* increased plant biomass and leghemoglobin content through combined nodulation and EPS effects (Martínez et al., 2015), and indigenous EPS-producing rhizobacteria improved productivity traits and the K^+/Na^+ ratio in pistachio seedlings under salinity and drought (Khalilpour et al., 2021).

Salinity-induced growth reduction is also linked to "feedback inhibition of photosynthesis, and microorganisms help modulate the source-sink relationship of soluble sugars, supporting osmotic adjustment" during the osmotic phase of salinity. In Medicago ciliaris, salt tolerance conferred by *Sinorhizobium medicae* was linked to maintenance of source-sink carbohydrate and hormonal relationships during symbiotic nodulation (Ben Salah et al., 2012), and "co-inoculation of soybean with *Bradyrhizobium japonicum* 532C, *Rhizobium sp*. SL42, and *Hydrogenophaga* sp. SL48 enhanced shoot and root growth, nitrogen assimilation, and the K^+/Na^+ ratio" through improved symbiotic nodulation and source-sink balance (Ilangumaran et al., 2021). In pepper, co-inoculation with *Azospirillum brasilense* and *Pantoea dispersa* under 40-120 mM NaCl improved yield-related traits via "enhanced stomatal conductance and photosynthesis (Del Amor & Cuadra-Crespo, 2012), and inoculation with various *Bacillus* strains has similarly improved photosynthesis, stomatal conductance, productivity, and fruit quality in strawberry" (Karlidag et al., 2013).

"Plants accumulate compatible solutes commonly termed osmolytes, such as proline, glycine betaine, and trehalose" to counter osmotic imbalance. PGPB frequently synthesise osmoregulators more rapidly than plants themselves and can enhance host osmolyte content either through direct uptake of bacterial solutes or by stimulating de-novo synthesis in plant tissue. Trehalose-accumulating *Azospirillum brasilense* improved "biomass and survival in maize under water-deficit stress" (Rodríguez-Salazar et al., 2009), and osmolyte-accumulating *Bacillus* spp. together with *Paenibacillus favisporus* enhanced maize biomass, water homeostasis, and soil aggregate stability under drought-related osmotic stress (Vardharajula et al., 2011). "Co-inoculation of maize with *Rhizobium* sp. and *Pseudomonas* sp." enhanced development, biomass, and nutrient uptake through combined proline accumulation and ion/water homeostasis (Bano & Fatima, 2009), while combined endophytic and rhizospheric inoculation of rice with *Pseudomonas pseudoalcaligenes* and *Bacillus pumilus* increased plant weight and height through elevated osmoprotectant accumulation (Jha et al., 2011; Zahir et al., 2012).

Wheat inoculated with the halotolerant, osmoprotectant-accumulating strain *Bacillus aquimaris* showed increased biomass, weight, and leaf-nutrient content under saline soil (Upadhyay & Singh, 2015), while inoculation with "*Bacillus megaterium* MPP7, *Bacillus tequilensis* MPP8, and *Pseudomonas putida* MPP18 reduced electrolytic leakage and oxidative damage" through combined proline/soluble-sugar accumulation and transcriptional upregulation of the SOS-type ion-transporter genes SOS1 and SOS4 (Haroon et al., 2022). Comparable benefits from osmolyte accumulation have been reported in peak inoculated with *Acinetobacter, Enterobacter*, and *Alcaligenes* strains, where elevated osmolyte levels correlated with reduced oxidative damage (Sapre et al., 2022).

Beyond biochemical modulation, PGPB also regulates plant water homeostasis through effects on hydraulic conductivity. *Bacillus megaterium* B26 "enhanced salt-stress tolerance in maize through positive regulation of PIP-type aquaporin genes and improved root hydraulic conductance (Marulanda et al., 2010), and *Azospirillum brasilense* increased aquaporin gene transcription and improved growth in barley seedlings exposed to saline stress (Zawoznik et al., 2011)". The results altogether demonstrate PGPB activate several complementary mechanisms, including osmotic modulation, enhancement of antioxidant defence, and hydraulic regulation, which significantly enhance plant's resistance in saline soil.

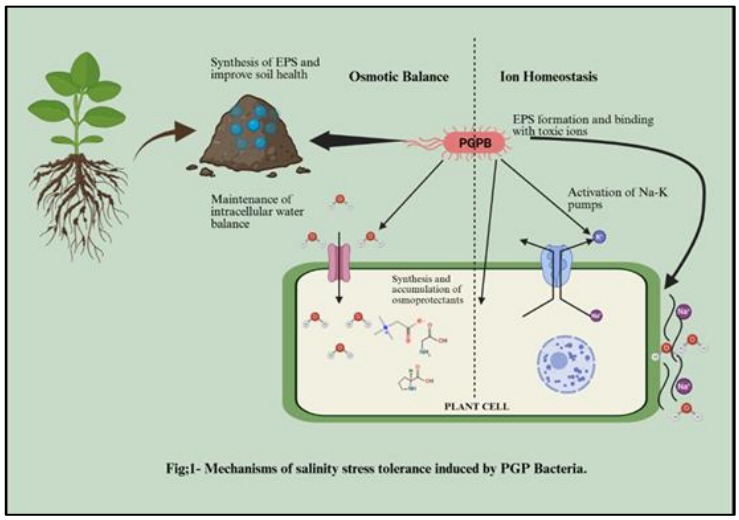


Figure 2

"Main mechanisms of salinity tolerance induced by plant growth-promoting bacteria" (PGPB): Complementary role in osmotic balance (EPS synthesis, accumulation of osmoprotectants, maintenance of water balance in cell) and ion homeostasis (EPS binding of toxic ions, activation of Na^+/K^+ pumps).

Figure source. Original figure prepared by the authors and synthesised from the mechanistic evidence discussed in Section 3.1-3.2 that was analysed in the primary studies cited (Ilangumaran & Smith, 2017).

Table 2
Biological processes mediated by Rep PGPB to maintain osmotic balance and control of ion homeostasis related to salinity tolerance

No.	Plant host	Bacterium	Effect	Mechanism	Citation
1	*Lactuca sativa* L.	*Pseudomonas mendocina (+ Glomus intraradices)*	Increased stable soil aggregation	EPS production	Kohler et al. (2006)
2	*Cicer arietinum* L.	*Halomonas variabilis + Planococcus rifietensis*	Increased growth and soil aggregation under salinity	Biofilm formation and EPS production	Qurashi & Sabri (2012)
3	*Medicago ciliaris* L.	*Sinorhizobium medicae*	Differential carbohydrate/hormonal changes between source-sink tissues	Nodulation and source-sink activity	Ben Salah et al. (2012)
4	*Glycine max* L.	*B. japonicum* 532C, *Rhizobium* sp. SL42, *Hydrogenophaga* sp. SL48	Improved shoot/root growth, N assimilation, K+/Na+ ratio	Nodulation and source-sink activity	Ilangumaran et al. (2021)
5	*Capsicum annuum* L.	*Azospirillum brasilense + Pantoea dispersa*	Higher dry weight and K+/Na+ ratio (40-120 mM NaCl)	Higher stomatal conductance/transpiration	Del Amor & Cuadra-Crespo (2012)
6	*Fragaria x ananassa*	*Bacillus licheniformis, B. subtilis, Bacillus* sp.	Enhanced growth, yield, fruit quality	Higher stomatal conductance/transpiration	Karlidag et al. (2013)
7	*Triticum aestivum* L.	*Bacillus aquimaris*	Increased biomass, weight, leaf nutrients	Osmoprotectant accumulation (proline, soluble sugar)	Upadhyay & Singh (2015)
8	*Zea mays* L.	*Azospirillum brasilense*	Increased survival, leaf/root biomass	Trehalose accumulation "water-deficit stress"	Rodríguez-Salazar et al. (2009)
9	*Zea mays* L.	*Bacillus spp. + Paenibacillus favisporus*	Increased biomass, water homeostasis, soil-aggregate stability	Osmoprotectant accumulation (proline, sugar)	Vardharajula et al. (2011)
10	*Zea mays* L.	*Rhizobium* sp. + *Pseudomonas* sp.	Enhanced development, biomass, nutrient uptake	Proline accumulation; ion/water homeostasis	Bano & Fatima (2009)
11	*Oryza sativa* L.	*Pseudomonas pseudoalcaligenes*	Higher plant weight and height	Osmoprotectant accumulation (glycine betaine-like compounds)	Jha et al. (2011)

		+ *Bacillus pumilus*			
12	*Triticum aestivum* L.	*B. megaterium* MPP7, *B. tequilensis* MPP8, *P. putida* MPP18	Reduced electrolytic leakage and oxidative damage	Osmoprotectant accumulation; SOS1/SOS4 transcriptional upregulation	Haroon et al. (2022)
13	*Pisum sativum* L.	*Acinetobacter, Enterobacter, Alcaligenes* spp.	Reduced oxidative damage	Osmoprotectant accumulation (proline, soluble sugar)	Sapre et al. (2022)
14	*Zea mays* L.	*Bacillus megaterium* B26	Higher root hydraulic conductance	Upregulation of PIP-type aquaporin genes	Marulanda et al. (2010)
15	*Hordeum vulgare* L.	*Azospirillum brasilense*	Increased biomass and height	Upregulation of PIP-type aquaporin genes	Zawoznik et al. (2011)
16	*Triticum aestivum* L.	*Aeromonas* sp. + *Bacillus* sp.	Increased growth, K+/Na+ ratio, soil aggregation	EPS production	Ashraf et al. (2004)
17	*Triticum aestivum* L.	*Bacillus subtilis* + *Marinobacter lipolyticus*	Increased growth, K+/Na+ ratio, selective nutrient uptake	EPS production	Talebi Atouei et al. (2019)
18	*Lactuca sativa* L.	*Pseudomonas mendocina*	Increased biomass and water content (water stress)	Phosphatase activity; proline accumulation	Kohler et al. (2008)
19	*Medicago sativa* L.	*Halomonas maura* + *Ensifer meliloti*	Increased plant biomass and leghemoglobin	Nodulation and EPS production	Martínez et al. (2015)
20	*Pistacia vera* L.	*Staphylococcus sciuri, Zobellella denitrificans, Arthrobacter endophyticus*	Increased productivity traits and K+/Na+ ratio	EPS production	Khalilpour et al. (2021)

This data was compiled by the authors from the studies in the primary data column identified in the last column (Citation) of the table above.

3.2. Homeostasis-Ion Homeostasis (The Regulation of Ions)

Salinity causes the accumulation of ions (Na+, Cl-, Ca2+, Mg2+, SO42-, and CO32-) and results in an ion toxicity stage when the plant is no longer able to exclude the ions. As one of the initial protective responses, plants sequester excess salts into vacuoles with no accumulation in other compartments, such as cytosol that would otherwise interfere with photosynthesis and respiration. High levels of Na^+ affect K^+-dependent processes because biochemical reactions that involve K^+ are affected by substituting K^+ with Na^+ which alters protein structure and synthesis. There is a clear relationship between productivity and ionic equilibrium, mostly studied in relation to salinity imposed by NaCl, but soil microorganisms play a role in maintaining ionic equilibrium and hence improve growth and salinity tolerance, particularly for other ions that cause salinity stress (Tester & Davenport, 2003).

Maintenance of high K^+/Na^+ ratio is one of the important PGPB mechanisms that involves "reducing the accumulation of Na^+/Cl^- in leaves, stimulation of ion exclusion at the root surface, or regulation of the expression of genes encoding ion transporters. High-affinity K^+ transporters (HKT) are" important in limiting excessive Na^+ accumulation in the shoot by exporting Na^+ to the roots. In Puccinellia tenuiflora, the halophyte grass, the salt tolerance was enhanced by the inoculation with Bacillus subtilis GB03, which promoted selective K^+ uptake over Na^+, inhibited the root and shoot growth and expression of the HKT1 and HKT2 genes (Niu et al., 2016). In the case of maize, inoculation with Kocuria rhizophila Y1 led to the increased expression of HKT1, NHX1, NHX2 and NHX3 genes, which resulted in higher salt tolerance and protection against salt (Li et al., 2020).

Sodium antiporters, which are encoded by Salt Overly Sensitive (SOS) genes are also important in salinity tolerance besides the HKT transporters. Wheat was stressed with salt and then inoculated with Bacillus megaterium, Bacillus tequilensis, and Pseudomonas putida, which led to an induction of expression of SOS1 and SOS4, which was associated with an improvement in the relative water content and an increase in the photosynthetic pigments (Haroon et al., 2022).

PGPB also help reduce the buildup of Na^+/Cl^- by controlling macro- and micronutrient exchange. The production of proteins associated with phosphatase activity can be stimulated by PGPB inoculation, and by microbial phosphate solubilisation and siderophore production, nutrient availability can be improved. Pseudomonas simiae AU under saline stress conditions promoted the expression of vegetative storage protein (VSP) which play an important role in the acid-phosphatase activity along with increase in weight, length and K^+/Na^+ ratio in soybean (Vaishnav et al., 2015) while under water stress condition, Pseudomonas mendocina colonized lettuce and resulted into increased acid-phosphatase activity and reduced oxidative stress (Kohler et al., 2008). Azotobacter chroococcum strains inoculated in maize increased the exclusion of Na ions and improved the uptake of K ions as well as the polyphenol/chlorophyll content, compared to plants not inoculated with A. chroococcum (Rojas-Tapias et al., 2012).

Production of exopolysaccharides (EPS) is another important microbial mechanism that can help mitigate the toxicity of ions by building up a protective physical barrier around the root system, which sequesters cations like Na^+ which are harder to take up by "the root system and reduces the movement of these ions to the aerial parts of the plant". The EPS-producing rhizobacteria have shown positive effects on wheat growth and changed the nutrient uptake in saline soils, with reduced uptake of Na^+ and increased uptake of K^+/Ca^{2+} (Ashraf et al., 2004; Talebi Atouei et al., 2019), and similar effects have been seen with soybean, alfalfa and pistachio (Martínez et al., 2015; Khalilpour et al., 2021).

4. Other Bioactive Molecules from Rhizobacteria which are Affecting Plant Health

There are several bacterial mechanisms of plant salt stress regulation that include the release of extracellular metabolites such as volatile organic compounds and low molecular weight organic substances. These compounds are molecules that are involved in the process of signalling between organisms, regulating plant processes, and creating beneficial physiological responses in plants under stressful conditions.

4.1. Volatile Organic Compounds (VOCs) Emission

The "Volatile Organic Compounds (VOCs) are low molecular weight, carbon-based chemicals with high vapour pressure and low boiling point which can be emitted by rhizosphere associated bacteria. Microbial volatiles have been reported to promote plant growth and protect against phytopathogens, and" growing evidence suggests their ability to alleviate salt stress.

Under 100 mM NaCl, exposure to the VOC mixture produced by Pseudomonas simiae resulted in decreased sodium concentrations in the root tissue and increased proline and chlorophyll content,

while associated changes in induced protein expression were observed (Vaishnav et al., 2015) in another study, the VOCs 4-nitroguaiacol and quinoline were specifically found to enhance soybean seed germination under the same salt concentration (Vaishnav et al., 2016). In Mentha x piperita VOCs produced by Bacillus amyloliquefaciens GB03, with acetoin as the major compound, offset the negative effects of salt stress over the entire range of NaCl tested (0–100 mM), and were correlated with a decrease in endogenous ABA levels, indicating a possible hormonal mechanism of action (Cappellari & Banchio, 2020).

4.2. Biosynthesis of Polyamines

Small aliphatic amines known as polyamines (PAs) have a potent antioxidant potential and "are essential for plant growth, development, and the response to abiotic stress". They also control gene expression, antioxidant enzyme activity, and ROS homeostasis. The three most common physiologically active forms found in plants are putrescine, spermidine, and spermine.

Comparatively few studies have examined polyamines produced directly by PGPB. Spermidine secreted by *Bacillus amyloliquefaciens* SQR9 mitigated oxidative damage, limited sodium toxicity, and suppressed ABA accumulation in *Zea mays*, an effect further validated using polyamine-deficient bacterial mutants (Chen et al., 2017). In tomato, *Bacillus megaterium* TG1-E1 elevated extracellular arginine a key polyamine precursor under hyperosmotic stress, suggesting that bacterial inoculation may indirectly enhance endogenous polyamine synthesis and contribute to improved stress resilience (Morcillo et al., 2021).

4.3. Production of Lipo-Chito-Oligosaccharides and Bacteriocins

"Bacteriocins are ribosomally synthesised antimicrobial peptides with bactericidal or bacteriostatic activity against closely related" microbial species, effective at very low concentrations and providing producing bacteria with a competitive advantage in the rhizosphere.

Lipo-chito-oligosaccharides (LCOs) are microbial signalling molecules that initiate and regulate symbiotic interactions with plants; the best-known group, "Nod factors, are released by rhizobacteria in response to root-exudate flavonoids" and are central to root-nodule initiation in legumes. Beyond symbiosis, nod factors also positively influence plant growth under abiotic stress. "Thuricin 17, a bacteriocin produced by *Bacillus thuringiensis* NEB17", combined with LCOs from *Bradyrhizobium japonicum* 532C, enhanced canola (*Brassica napus*) accumulation and root development under stress conditions (Schwinghamer et al., 2016). Proteomic analysis of the same Thuricin 17 + *B. japonicum* 532C LCO combination applied to soybean under 100 mM NaCl revealed substantial reprogramming of proteins associated with photosynthesis, primary metabolism, and stress defence, including PEP carboxylase, the large subunit of Rubisco, glutathione-S-transferase, and late embryogenesis abundant (LEA) proteins linked to dehydration tolerance (Subramanian et al., 2016). In total, these results suggest that the plant proteome can be reprogrammed by bacteriocins and LCOs, as well as improving its physiological tolerance to salinity stress.

Table 3

Representative compounds produced by PGPB were volatile organic compounds, polyamines, and bacteriocins/lipo-chito-oligosaccharides associated with salinity tolerance

No.	Plant host	Bacterium	Mechanism	Effect	Citation
1	*Glycine max* L.	*Pseudomonas simiae*	VOC production; phosphatase-activity changes	Higher weight/length, K+/Na+ ratio "100 mM NaCl"	Vaishnav et al. (2015)

2	*Glycine max* L.	*P. simiae (4-nitroguaiacol, quinoline)*	VOC production	Promoted seed germination “100 mM NaCl"	Vaishnav et al. (2016)
3	*Mentha x piperita* L.	*Bacillus amyloliquefaciens* GB03	VOC production (acetoin); reduced ABA	Higher chlorophyll and improved morphology	Cappellari & Banchio (2020)
4	*Zea mays* L.	*Bacillus amyloliquefaciens* SQR9	Polyamine (spermidine) production	Decreased oxidative/Na+ damage; ABA suppression	Chen et al. (2017)
5	*Solanum lycopersicum* L.	*Bacillus megaterium* TG1-E1	Arginine (polyamine-precursor) accumulation	Osmotic-stress resistance	Morcillo et al. (2021)
6	*Brassica napus* L.	*B. thuringiensis NEB17* + *B. japonicum* 532C	Bacteriocin (Thuricin 17) + LCO production	Enhanced biomass and root development under stress	Schwinghamer et al. (2016)
7	*Glycine max* L.	*B. thuringiensis NEB17* + *B. japonicum* 532C	Bacteriocin (Thuricin 17) + LCO production	Proteome reprogramming “under 100 mM NaCl”	Subramanian et al. (2016)

The source is the authors' compilation based on the primary studies mentioned in the last column (Citation) of the table.

5. Conclusion

Soil salinity is an important and global problem that adds multiple stresses to plants: “osmotic stress, ion toxicity, nutrient stress, and oxidative stress, and can also decrease the soil structure and fertility. In this context, the idea of using plant growth-promoting bacteria has” proven to be a promising strategy that is sustainable and economically viable to enhance plant resistance to salinity. There are several physiological and biochemical mechanisms that contribute to PGPB mediated salt-stress tolerance, e.g., modulation of phytohormone balance (IAA, ABA) along with inhibition of the ethylene production pathway by ACC deaminase, secretion of signalling molecules and bioactive metabolites (lipo-chito-oligosaccharides, polyamines, VOCs, EPSs), activation of ion-transport systems, and “accumulation of osmoprotectants (proline, trehalose, soluble sugars)”.

“Despite significant advances, the complexity of plant-microbe interactions” and the diversity of microbial functional traits remain insufficiently understood. The synergistic and context-dependent nature of PGPB mechanisms evident, for example, in strain- and host-dependent ABA modulation necessitates deeper investigation to unravel their coordinated roles under field conditions. Variability in microbial performance across crops and environmental settings further highlights the need for targeted screening and functional characterisation of halotolerant strains, and for validated multi-strain consortia and engineered microbiomes rather than single-strain inoculants alone.

In conclusion, harnessing the full potential of PGPB represents a transformative approach for sustainable agriculture in salt-affected soils. Future research should prioritise integrative multi-omics approaches, rational design of microbial consortia, CRISPR-enabled functional genomics of stress-

tolerance pathways, and long-duration, multi-location field-level validation to bridge the gap between laboratory findings and practical application. Such advances will be pivotal for developing climate-resilient cropping systems and ensuring long-term global food security.

Statement of credit authorship contribution

SRK: Writing–original draft, Literature survey, Formal analysis, data compilation, Software, Investigation**. SS:** Writing–review & editing, Supervision. **IA**: Writing–review & editing, Supervision, Investigation. **FAA**: Writing–review & editing, Supervision. **SK**: Literature survey, Software, Resources.

A statement of conflicting interests

The authors affirm that none of the work reported in this review could have been influenced by any known competing financial interests or personal relationships. **FAA** is a member of the journal's Editorial Board and was not involved in the editorial evaluation or publication decision concerning this manuscript.

Acknowledgements

The Integral Institute of Agricultural Science and Technology, Integral University, Lucknow, as well as the affiliated institutions of all co-authors, are acknowledged by the authors for providing institutional and infrastructure support during the production of this review.

Data availability

Not applicable

Funding

This research received no external funding from any funding agency in the public, commercial, or non-profit sectors.

References

Alhan, G., Sindhu, M., Kumar, A., Nagar, S., Sangwan, S., Singh, G., Prakash, R., & Mohanty, S. R. (2026). The molecular network in bacteria responsible for the mitigation of salinity stress. *World J. Microbiol. Biotechnol., 42*, 197. https://doi.org/10.1007/s11274-026-04932-y

Ali, S., Charles, T. C., & Glick, B. R. (2014). Amelioration of high salinity stress damage by plant growth-promoting bacterial endophytes that contain ACC deaminase. *Plant Physiol. Biochem., 80*, 160–167. https://doi.org/10.1016/j.plaphy.2014.04.003

Ansari, F. A., Jabeen, M., & Ahmad, I. (2021). *Pseudomonas azotoformans* FAP5, a novel biofilm-forming PGPR strain, alleviates drought stress in wheat plant. *Inter. J. Environ. Sci. Technol., 18*, 3855–3870. https://doi.org/10.1007/s13762-020-03045-9

Ansari, F. A., Ahmad, I., & Pichtel, J. (2023). Synergistic effects of biofilm-producing PGPR strains on wheat plant colonization, growth and soil resilience under drought stress. *Saudi J. Biol. Sci.*, *30*(6), 103664. https://doi.org/10.1016/j.sjbs.2023.103664

Ansari, F. A., Ahmad, I., & Pichtel, J. (2019). Growth stimulation and alleviation of salinity stress to wheat by the biofilm forming *Bacillus pumilus* strain FAB10. *Appl. Soil Ecol.*, 143, 45–54. https://doi.org/10.1016/j.apsoil.2019.05.023

Ansari, F. A., Ahmad, I., Pichtel, J., & Husain, F. M. (2024). Pantoea agglomerans FAP10: A novel biofilm-producing PGPR strain improves wheat growth and soil resilience under salinity stress. *Environ. Exp. Bot*., 222, 105759. https://doi.org/10.1016/j.envexpbot.2024.105759

Ashraf, M., Hasnain, S., Berge, O., & Mahmood, T. (2004). Inoculating wheat seedlings with exopolysaccharide-producing bacteria restricts sodium uptake and stimulates plant growth under salt stress. *Biol. Fertil. Soils, 40*, 157–162. https://doi.org/10.1007/s00374-004-0766-y

Bano, A., & Fatima, M. (2009). Salt tolerance in Zea mays (L.) following inoculation with *Rhizobium* and *Pseudomonas*. *Biol. Fertil. Soils, 45*, 405–413. https://doi.org/10.1007/s00374-008-0344-9

Barnawal, D., Bharti, N., Maji, D., Chanotiya, C. S., & Kalra, A. (2013). ACC deaminase-containing *Bacillus subtilis* reduces stress ethylene-induced damage and improves mycorrhizal colonization and rhizobial nodulation in *Trigonella foenum-graecum* under drought stress. *J. Plant Growth Regul., 32*, 809–822. https://doi.org/10.1007/s00344-013-9347-3

Basak, N., Rai, A. K., Sundha, P., Meena, R. L., Bedwal, S., Yadav, R. K., & Sharma, P. C. (2022). Assessing soil quality for rehabilitation of salt-affected agroecosystem: A comprehensive review. *Front. Environ. Sci., 10*, 935785. https://doi.org/10.3389/fenvs.2022.935785

Ben Salah, I., Jelali, N., Slatni, T., Gruber, M., Albacete, A., Martínez Andújar, C., Martinez, V., Pérez-Alfocea, F., & Abdelly, C. (2012). Involvement of source-sink relationship and hormonal control in the response of Medicago ciliaris–Sinorhizobium medicae symbiosis to salt stress. *Acta Biol. Hung., 63*(1), 97–112. https://doi.org/10.1556/ABiol.63.2012.1.8

Cappellari, L. del R., & Banchio, E. (2020). Microbial volatile organic compounds produced by *Bacillus amyloliquefaciens* GB03 ameliorate the effects of salt stress in Mentha piperita principally through acetoin emission. *J. Plant Growth Regul., 39*(2), 764–775. https://doi.org/10.1007/s00344-019-10020-3

Chakrovarty, A., Singh, A. K., & Pandey, A. K. (2026). Beneficial microbes in plant salinity stress responses: Integrating correlative evidence with mechanistic frameworks. *Physiol. Plant., 178*(3), e70930. https://doi.org/10.1111/ppl.70930

Chanson, A., Gould, I. J., Almas, A. R., Paz, A. M., Castanheira, N. L., Antunes, J. F., Barker, A., & Goddard, M. R. (2026). Supporting crop yields under climate change by engineering innate soil microbiomes. *Appl. Environ. Microbiol., 92*(8), e00437-26. https://doi.org/10.1128/aem.00437-26

Chen, L., Liu, Y., Wu, G., Zhang, N., Shen, Q., & Zhang, R. (2017). Beneficial *rhizobacterium Bacillus amyloliquefaciens* SQR9 induces plant salt tolerance through spermidine production. *Mol. Plant Microbe Interact., 30*(5), 423–432. https://doi.org/10.1094/MPMI-02-17-0027-R

Cohen, A. C., Travaglia, C. N., Bottini, R., & Piccoli, P. N. (2009). Participation of abscisic acid and gibberellins produced by endophytic *Azospirillum* in the alleviation of drought effects in maize. *Botany, 87*(5), 455–462. https://doi.org/10.1139/B09-023

de Andrade, L. A., Santos, C. H. B., Frezarin, E. T., Sales, L. R., & Rigobelo, E. C. (2023). Plant growth-promoting rhizobacteria for sustainable agricultural production. *Microorganisms, 11*(4), 1088. https://doi.org/10.3390/microorganisms11041088

Del Amor, F. M., & Cuadra-Crespo, P. (2012). Plant growth-promoting bacteria as a tool to improve salinity tolerance in sweet pepper. *Funct. Plant Biol., 39*(1), 82–90. https://doi.org/10.1071/FP11173

Derbew, Z., Abate, S., Ali, H., Tefera, S., & Assen, S. (2026). Review on impacts of soil salinity and sodicity on crop yield and management option. *Int. J. Nat. Resour. Ecol. Manag., 11*(1), 1–12. https://doi.org/10.11648/j.ijnrem.20261101.11

Dey, G., Banerjee, P., Sharma, R. K., Maity, J. P., Etesami, H., Shaw, A. K., Huang, Y.-H., Huang, H.-B., & Chen, C. Y. (2021). Management of phosphorus in salinity-stressed agriculture for sustainable crop production by salt-tolerant phosphate-solubilizing bacteria – a review. *Agronomy, 11*(8), 1552. https://doi.org/10.3390/agronomy11081552

Haroon, U., Khizar, M., Liaquat, F., Ali, M., Akbar, M., Tahir, K., Batool, S. S., Kamal, A., Chaudhary, H. J., & Munis, M. F. H. (2022). Halotolerant plant growth-promoting rhizobacteria induce salinity tolerance in wheat by enhancing the expression of SOS genes. *J. Plant Growth Regul., 41*, 2435–2448. https://doi.org/10.1007/s00344-021-10457-5

Hasanuzzaman, M., Raihan, M. R. H., Masud, A. A. C., Rahman, K., Nowroz, F., Rahman, M., Nahar, K., & Fujita, M. (2021). Regulation of reactive oxygen species and antioxidant defense in plants under salinity. *Int. J. Mol. Sci., 22*(17), 9326. https://doi.org/10.3390/ijms22179326

Hasanuzzaman, M., Zhou, M., & Shabala, S. (2023). How does stomatal density and residual transpiration contribute to osmotic stress tolerance? *Plants, 12*(3), 494. https://doi.org/10.3390/plants12030494

Hassani, A., Azapagic, A., & Shokri, N. (2021). Global predictions of primary soil salinization under changing climate in the 21st century. *Nat. Commun., 12*, 6663. https://doi.org/10.1038/s41467-021-26907-3

Ilangumaran, G., & Smith, D. L. (2017). Plant growth promoting rhizobacteria in amelioration of salinity stress: A systems biology perspective. *Front. Plant Sci., 8*, 1768. https://doi.org/10.3389/fpls.2017.01768

Ilangumaran, G., Schwinghamer, T. D., & Smith, D. L. (2021). Rhizobacteria from root nodules of an indigenous legume enhance salinity stress tolerance in soybean. *Front. Sustain. Food Syst., 4*, 617978. https://doi.org/10.3389/fsufs.2020.617978

Janni, M., Maestri, E., Gullì, M., Marmiroli, M., & Marmiroli, N. (2024). Plant responses to climate change, how global warming may impact on food security: A critical review. *Front. Plant Sci., 14*, 1297569. https://doi.org/10.3389/fpls.2023.1297569

Jha, Y., Subramanian, R. B., & Patel, S. (2011). Combination of endophytic and rhizospheric plant growth promoting rhizobacteria in Oryza sativa shows higher accumulation of osmoprotectant against saline stress. *Acta Physiol. Plant., 33*(3), 797–802. https://doi.org/10.1007/s11738-010-0604-9

Kang, S.-M., Khan, A. L., Waqas, M., You, Y.-H., Kim, J.-H., Kim, J.-G., Hamayun, M., & Lee, I.-J. (2014). Plant growth-promoting rhizobacteria reduce adverse effects of salinity and osmotic stress by regulating phytohormones and antioxidants in *Cucumis sativus*. *J. Plant Interact., 9*(1), 673–682. https://doi.org/10.1080/17429145.2014.894587

Karlidag, H., Yildirim, E., Turan, M., Pehluvan, M., & Donmez, F. (2013). Plant growth-promoting rhizobacteria mitigate deleterious effects of salt stress on strawberry plants (Fragaria × ananassa). *HortScience, 48*(5), 563–567. https://doi.org/10.21273/HORTSCI.48.5.563

Khalilpour, M., Mozafari, V., & Abbaszadeh-Dahaji, P. (2021). Tolerance to salinity and drought stresses in pistachio (Pistacia vera L.) seedlings inoculated with indigenous stress-tolerant PGPR isolates. *Sci. Hortic., 289*, 110440. https://doi.org/10.1016/j.scienta.2021.110440

Khan, M. A., Asaf, S., Khan, A. L., Adhikari, A., Jan, R., Ali, S., Imran, M., Kim, K.-M., & Lee, I.-J. (2019). Halotolerant rhizobacterial strains mitigate the adverse effects of NaCl stress in soybean seedlings. *Biomed Res. Int., 2019*, 9530963. https://doi.org/10.1155/2019/9530963

Kohler, J., Caravaca, F., Carrasco, L., & Roldán, A. (2006). Contribution of *Pseudomonas mendocina* and *Glomus intraradices* to aggregate stabilization and promotion of biological fertility in rhizosphere soil of lettuce plants under field conditions. *Soil Use Manag., 22*(3), 298–304. https://doi.org/10.1111/j.1475-2743.2006.00041.x

Kohler, J., Hernández, J. A., Caravaca, F., & Roldán, A. (2008). Plant-growth-promoting rhizobacteria and arbuscular mycorrhizal fungi modify alleviation biochemical mechanisms in water-stressed plants. *Funct. Plant Biol., 35*(2), 141–151. https://doi.org/10.1071/FP07218

Kopittke, P. M., McKenna, B. A., Sanchez, P. B., Gonzaga, N. R., Asio, V. B., Aguila, D. N. S., Gonzaga, A. B., Asio, L. G., Timbas, N. L., Colipano, M. C. L., Lina, S. B., Wang, P., Lombi, E., & Harper, S. M. (2026). The hidden costs of soil degradation: Threats to global food security and planetary health. *ACS Environ. Au, 6*(4), 539–552. https://doi.org/10.1021/acsenvironau.6c00058

Li, X., Sun, P., Zhang, Y., Jin, C., & Guan, C. (2020). A novel PGPR strain Kocuria rhizophila Y1 enhances salt stress tolerance in maize by regulating phytohormone levels, nutrient acquisition, redox potential, ion homeostasis, photosynthetic capacity and stress-responsive genes expression. *Environ. Exp. Bot., 174*, 104023. https://doi.org/10.1016/j.envexpbot.2020.104023

Liu, C., Jiang, X., & Yuan, Z. (2024). Plant responses and adaptations to salt stress: A review. *Horticulturae, 10*(11), 1221. https://doi.org/10.3390/horticulturae10111221

Liu, X., Lin, S., Li, C., Ren, S., Tang, Y., Tang, L., & Zhang, Z. (2026). Functional characteristics and distribution of microorganisms in saline and alkaline soils and their probiotic effects: A review. *Microb. Cell Fact., 25*(1), 39. https://doi.org/10.1186/s12934-026-02926-x

Manono, B. O. (2025). Effects of salinity on seed germination: Mechanisms, impacts, and mitigation strategies. *Seeds, 5*(1), 1. https://doi.org/10.3390/seeds5010001

Martínez, R., Espejo, A., Sierra, M., Ortiz-Bernad, I., Correa, D., Bedmar, E., López-Jurado, M., & Porres, J. M. (2015). Co-inoculation of *Halomonas maura* and *Ensifer meliloti* to improve alfalfa yield in saline soils. *Appl. Soil Ecol., 87*, 81–86. https://doi.org/10.1016/j.apsoil.2014.11.013

Marulanda, A., Azcón, R., Chaumont, F., Ruiz-Lozano, J. M., & Aroca, R. (2010). Regulation of plasma membrane aquaporins by inoculation with a Bacillus megaterium strain in maize (*Zea mays* L.) plants under unstressed and salt-stressed conditions. *Planta, 232*(2), 533–543. https://doi.org/10.1007/s00425-010-1196-8

Mayak, S., Tirosh, T., & Glick, B. R. (2004). Plant growth-promoting bacteria confer resistance in tomato plants to salt stress. *Plant Physiol. Biochem., 42*(6), 565–572. https://doi.org/10.1016/j.plaphy.2004.05.009

Melino, V., & Tester, M. (2023). Salt-tolerant crops: Time to deliver. *Annu. Rev. Plant Biol., 74*, 671–696. https://doi.org/10.1146/annurev-arplant-061422-104322

Mishra, P., Mishra, J., & Arora, N. K. (2021). Plant growth promoting bacteria for combating salinity stress in plants – recent developments and prospects: A review. *Microbiol. Res., 252*, 126861. https://doi.org/10.1016/j.micres.2021.126861

Morcillo, R. J. L., Vílchez, J. I., Zhang, S., Kaushal, R., He, D., Zi, H., Liu, R., Niehaus, K., Handa, A. K., & Zhang, H. (2021). Plant transcriptome reprograming and bacterial extracellular metabolites underlying tomato drought resistance triggered by a beneficial soil bacteria. *Metabolites, 11*(6), 369. https://doi.org/10.3390/metabo11060369

Negacz, K., Malek, Ž., de Vos, A., & Vellinga, P. (2022). Saline soils worldwide: Identifying the most promising areas for saline agriculture. *J. Arid Environ., 203*, 104775. https://doi.org/10.1016/j.jaridenv.2022.104775

Nguyen, T. T. M., Ha-Tran, D. M., & Huang, C.-C. (2025). Plant-growth-promoting rhizobacteria for mitigating salinity stress in rice farming: A review of the Vietnamese Mekong Delta. *Front. Plant Sci., 16*, 1635193. https://doi.org/10.3389/fpls.2025.1635193

Niu, S.-Q., Li, H.-R., Paré, P. W., Aziz, M., Wang, S.-M., Shi, H., Li, J., Han, Q.-Q., Guo, S.-Q., Li, J., Guo, Q., Ma, Q., & Zhang, J.-L. (2016). Induced growth promotion and higher salt tolerance in the halophyte grass *Puccinellia tenuiflora* by beneficial rhizobacteria. *Plant Soil, 407*, 217–230. https://doi.org/10.1007/s11104-015-2767-z

Orozco-Mosqueda, M. C., Duan, J., DiBernardo, M., Zetter, E., Campos-García, J., Glick, B. R., & Santoyo, G. (2019). The production of ACC deaminase and trehalose by the plant growth promoting bacterium Pseudomonas sp. UW4 synergistically protect tomato plants against salt stress. *Front. Microbiol., 10*, 1392. https://doi.org/10.3389/fmicb.2019.01392

Panwar, M., Tewari, R., Gulati, A., & Nayyar, H. (2016). Indigenous salt-tolerant rhizobacterium Pantoea dispersa (PSB3) reduces sodium uptake and mitigates the effects of salt stress on growth and yield of chickpea. *Acta Physiol. Plant., 38*, 278. https://doi.org/10.1007/s11738-016-2284-6

Qurashi, A. W., & Sabri, A. N. (2012). Bacterial exopolysaccharide and biofilm formation stimulate chickpea growth and soil aggregation under salt stress. *Braz. J. Microbiol., 43*(3), 1183–1191. https://doi.org/10.1590/S1517-83822012000300046

Remans, R., Croonenborghs, A., Torres Gutierrez, R., Michiels, J., & Vanderleyden, J. (2008). Physiological and genetic analysis of root responsiveness to auxin-producing plant growth-promoting bacteria in common bean (*Phaseolus vulgaris* L.). *Plant Soil, 302*, 149–161. https://doi.org/10.1007/s11104-007-9462-7

Rodríguez-Salazar, J., Suárez, R., Caballero-Mellado, J., & Iturriaga, G. (2009). Trehalose accumulation in *Azospirillum brasilense* improves drought tolerance and biomass in maize plants. *FEMS Microbiol. Lett., 296*(1), 52–59. https://doi.org/10.1111/j.1574-6968.2009.01614.x

Rojas-Tapias, D., Moreno-Galván, A., Pardo-Díaz, S., Obando, M., Rivera, D., & Bonilla, R. (2012). Effect of inoculation with plant growth-promoting bacteria (PGPB) on amelioration of saline stress in maize (*Zea mays*). *Appl. Soil Ecol., 61*, 264–272. https://doi.org/10.1016/j.apsoil.2012.01.006

Sadeghi, A., Karimi, E., Dahaji, P. A., Javid, M. G., Dalvand, Y., & Askari, H. (2012). Plant growth promoting activity of an auxin and siderophore producing isolate of Streptomyces under saline soil conditions. *World J. Microbiol. Biotechnol., 28*(4), 1503–1509. https://doi.org/10.1007/s11274-011-0952-7

Salomon, M. V., Bottini, R., de Souza Filho, G. A., Cohen, A. C., Moreno, D., Gil, M., & Piccoli, P. (2014). Bacteria isolated from roots and rhizosphere of Vitis vinifera retard water losses, induce abscisic acid accumulation and synthesis of defense-related terpenes in *in vitro* cultured grapevine. *Physiol. Plant., 151*(4), 359–374. https://doi.org/10.1111/ppl.12117

Sapre, S., Gontia-Mishra, I., & Tiwari, S. (2022). Plant growth-promoting rhizobacteria ameliorates salinity stress in pea (*Pisum sativum*). *J. Plant Growth Regul., 41*, 647–656. https://doi.org/10.1007/s00344-021-10329-y

Saravanakumar, D., & Samiyappan, R. (2007). ACC deaminase from *Pseudomonas fluorescens* mediated saline resistance in groundnut (*Arachis hypogea*) plants. *J. Appl. Microbiol., 102*(5), 1283–1292. https://doi.org/10.1111/j.1365-2672.2006.03179.x

Schwinghamer, T., Souleimanov, A., Dutilleul, P., & Smith, D. L. (2016). The response of canola cultivars to lipo-chitooligosaccharide (Nod Bj V [C18:1, MeFuc]) and thuricin 17. *Plant Growth Regul., 78*, 421–434. https://doi.org/10.1007/s10725-015-0104-4

Shahid, M., Ilyas, T., & Shafi, Z. (2026). Rhizobacterial exopolysaccharides in soil-plant systems: Molecular mechanisms, engineering approaches, and translational challenges. *J. Agric. Food Chem., 74*(23), 17694–17713. https://doi.org/10.1021/acs.jafc.6c02760

Shi, Y., Chu, H., He, R., Ma, W., Liang, Q., Li, Z., Gao, Y., & Luo, C. (2026). Harnessing rhizosphere microbes: The synergistic roles of PGPR and AMF in sustainable tomato production under stress. *Front. Microbiol., 17*, 1746930. https://doi.org/10.3389/fmicb.2026.1746930

Shokri, N., Hassani, A., & Sahimi, M. (2024). Multi-scale soil salinization dynamics from global to pore scale: A review. *Rev. Geophys., 62*(4), e2023RG000804. https://doi.org/10.1029/2023RG000804

Shukla, P. S., Agarwal, P. K., & Jha, B. (2012). Improved salinity tolerance of *Arachis hypogaea* (L.) by the interaction of halotolerant plant-growth-promoting rhizobacteria. *J. Plant Growth Regul., 31*, 195–206. https://doi.org/10.1007/s00344-011-9231-y

Siddikee, M. A., Glick, B. R., Chauhan, P. S., Yim, W. J., & Sa, T. (2011). Enhancement of growth and salt tolerance of red pepper seedlings (*Capsicum annuum* L.) by regulating stress ethylene synthesis with halotolerant bacteria containing 1-aminocyclopropane-1-carboxylic acid deaminase activity. *Plant Physiol. Biochem., 49*(4), 427–434. https://doi.org/10.1016/j.plaphy.2011.01.015

Singh, A. (2022). Soil salinity: A global threat to sustainable development. *Soil Use Manag., 38*, 39–67. https://doi.org/10.1111/sum.12772

Stavi, I., Thevs, N., & Priori, S. (2021). Soil salinity and sodicity in drylands: A review of causes, effects, monitoring, and restoration measures. *Front. Environ. Sci., 9*, 712831. https://doi.org/10.3389/fenvs.2021.712831

Subramanian, S., Ricci, E., Souleimanov, A., & Smith, D. L. (2016). A proteomic approach to lipo-chitooligosaccharide and thuricin 17 effects on soybean germination unstressed and salt stress. *PLoS ONE, 11*(8), e0160660. https://doi.org/10.1371/journal.pone.0160660

Talebi Atouei, M., Pourbabaee, A. A., & Shorafa, M. (2019). Alleviation of salinity stress on some growth parameters of wheat by exopolysaccharide-producing bacteria. *Iran. J. Sci. Technol. Trans. A Sci., 43*, 2725–2734. https://doi.org/10.1007/s40995-019-00753-x

Tester, M., & Davenport, R. (2003). Na+ tolerance and Na+ transport in higher plants. *Ann. Bot., 91*(5), 503–527. https://doi.org/10.1093/aob/mcg058

Upadhyay, S. K., & Singh, D. P. (2015). Effect of salt-tolerant plant growth-promoting rhizobacteria on wheat plants and soil health in a saline environment. *Plant Biol., 17*(1), 288–293. https://doi.org/10.1111/plb.12173

Vaishnav, A., Kumari, S., Jain, S., Varma, A., & Choudhary, D. K. (2015). Putative bacterial volatile-mediated growth in soybean (Glycine max L. Merrill) and expression of induced proteins under salt stress. *J. Appl. Microbiol., 119*(2), 539–551. https://doi.org/10.1111/jam.12866

Vaishnav, A., Kumari, S., Jain, S., Varma, A., Tuteja, N., & Choudhary, D. K. (2016). PGPR-mediated expression of salt tolerance gene in soybean through volatiles under sodium nitroprusside. *J. Basic Microbiol., 56*(11), 1274–1288. https://doi.org/10.1002/jobm.201600188

van Zelm, E., Zhang, Y., & Testerink, C. (2020). Salt tolerance mechanisms of plants. *Annu. Rev. Plant Biol., 71*, 403–433. https://doi.org/10.1146/annurev-arplant-050718-100005

Vardharajula, S., Zulfikar Ali, S., Grover, M., Reddy, G., & Bandi, V. (2011). Drought-tolerant plant growth promoting Bacillus spp.: Effect on growth, osmolytes, and antioxidant status of maize under drought stress. *J. Plant Interact., 6*(1), 1–14. https://doi.org/10.1080/17429145.2010.535178

Xing, Y., Liu, X., & Wang, X. (2026). Integrated soil salinisation management strategies in agriculture. *Mod. Agric., 4*(1), e70038. https://doi.org/10.1002/moda.70038

Yao, L., Wu, Z., Zheng, Y., Kaleem, I., & Li, C. (2010). Growth promotion and protection against salt stress by *Pseudomonas putida* Rs-198 on cotton. *Eur. J. Soil Biol., 46*(1), 49–54. https://doi.org/10.1016/j.ejsobi.2009.11.002

Zahir, Z. A., Akhtar, S. S., Ahmad, M., & Nadeem, S. M. (2012). Comparative effectiveness of *Enterobacter aerogenes* and *Pseudomonas fluorescens* for mitigating the depressing effect of brackish water on maize. *Int. J. Agric. Biol., 14*(3), 337–344.

Zawoznik, M. S., Ameneiros, M., Benavides, M. P., Vázquez, S., & Groppa, M. D. (2011). Response to saline stress and aquaporin expression in *Azospirillum*-inoculated barley seedlings. *Appl. Microbiol. Biotechnol., 90*(4), 1389–1397. https://doi.org/10.1007/s00253-011-3162-1

Zeng, W., Xiang, D., Li, X., Gao, Q., Chen, Y., Wang, K., Qian, Y., Wang, L., Li, J., Mi, Q., Huang, H., Xu, L., Zhao, M., Zhang, Y., & Xiang, H. (2024). Effects of combined inoculation of arbuscular mycorrhizal fungi and plant growth-promoting rhizosphere bacteria on seedling growth and rhizosphere microecology. *Front. Microbiol., 15*, 1475485. https://doi.org/10.3389/fmicb.2024.1475485

NATURE & SCIENCE
October 2026, Volume 8, Issue 5, pp. 61–69
DOI: https://doi.org/10.36719/2707-1146/68/61-69

Effects of Bread Waste Flour Utilization in Cattle Diets on Milk and Meat Productivity

Mahir Hajiyev[1], Yasin Gozalov[2], Zohrab Suleymanov[2], and Kanan Aliyev[3*]

Abstract. *Reducing feed costs and the cost of production is of great importance for increasing the economic efficiency of production in small, medium-sized, and large-scale farms. For this purpose, increasing attention is being paid to the use of by-products as alternative feed resources. Bread waste and bakery product residue flour is a promising feed component rich in carbohydrates, rapidly fermentable, and easily digestible. An experimental feeding trial was conducted through collaboration between the Scientific Research Institute of Animal Husbandry and Fisheries, ATS FOOD LLC, and the Agdash Feed Factory. The aim of the study was to evaluate the effect of incorporating bread waste flour (BWF) into feed mixtures on milk productivity and growth parameters of cattle. The study included 22 lactating cows in a 12-week feeding trial and 11 young cattle in a 50-day feeding trial. Feed mixtures containing 37.5% BWF for lactating cows and 34.0% BWF for young cattle were prepared. Daily milk yield and the main compositional characteristics of milk were evaluated in lactating cows, while changes in live body weight were assessed in young cattle. The results showed that the inclusion of bread waste flour in the feed ration improved milk yield and growth parameters. During the trial period, total milk production increased by 8–10 liters, while live body weight increased by 80–100 kg. The results indicate that the use of BWF as an alternative feed component in cattle feeding is appropriate.*

Keywords: *bread waste flour, milk productivity, milk fat percentage, live body weight, feed conversion efficiency*

Introduction

In cattle production, feed costs account for 60–70% of the total costs incurred in production (NRC, 2001; FAO, 2016). In recent years, the increase in the prices of conventional cereal-based feeds in foreign countries including Azerbaijan, has intensified the search for alternative feed sources. The use of alternative feed sources contributes to a reduction in the feed conversion ratio (Krause et al., 2013; Lee et al., 2000; Patra, 2012; Steele et al., 2012). Processed BWF is obtained from surplus bread and other bakery products and is considered one of the most promising energy-rich feed sources for use in animal nutrition.

[1]Azerbaijan Scientific Research Institute of Animal Husbandry and Fisheries, PhD in Agricultural Sciences, Goygol, Azerbaijan
[2]Azerbaijan Scientific Research Institute of Animal Husbandry and Fisheries, Goygol, Azerbaijan
[3]Agdash Feed Factory, Agdash, Azerbaijan
[*]Corresponding author. E-mail: kananaliyev2212@gmail.com
Received: 6 May 2026; Accepted: 14 September 2026; Published online: 25 October 2026
© The Author(s) 2026. This is an open access article distributed under the terms of the Creative Commons Attribution-NonCommercial 4.0 International License (CC BY-NC 4.0).

It is characterized by a high content of rapidly fermentable starch, moderate moisture content after processing, and a high digestible energy value, which makes it a potential partial substitute for corn and barley in animal diets (Van Soest, 1994; Hristov et al., 2013; Janssen, 2010). Globally, overproduction, expiration of shelf life, and inefficient consumption result in the generation of large quantities of bread waste every day, and its utilization in animal nutrition contributes to both economic efficiency and environmental sustainability (Gustavsson et al., 2011; FAO, 2016).

It has been demonstrated through conducted research studies that flour obtained from bread and other by-product wastes can replace 10–30% of cereal feeds in the diets of lactating cows without negatively affecting productivity (Kaltenegger et al., 2020). The increase in daily milk yield in cows, improvement in energy balance, and reduction in feed conversion are explained by the improvement of fermentation processes in the rumen of the animals (Kolver & Muller, 1998). The rapid degradation of starch obtained from bread waste stimulates the formation of volatile fatty acids (VFA), particularly propionate. Propionate, in turn, acts as one of the main precursors for glucose synthesis in the liver and the formation of milk lactose (Russell & Rychlik, 2001).

The use of BWF is strongly dependent on the level of its inclusion in the diet and the balancing of the overall diet. Thus, the excessive inclusion of rapidly fermentable carbohydrates may disrupt the balance of microorganisms in the rumen, lead to a decrease in pH, and increase the risk of subacute ruminal acidosis (SARA). This, in turn, negatively affects overall productivity (Plaizier et al., 2008; Allen, 1997; Zebeli et al., 2008). Therefore, careful formulation of the diet is essential to maintain stable digestion in animals.

In beef cattle production, the inclusion of activated bread waste products used as a partial substitute for the animals' energy requirements. This improves the growth performance of animals and the efficient utilization of feed (Fox & Tylutki, 1998; Owens et al., 1997). Increasing the energy balance in the diet creates conditions for the normal development of the microflora in the rumen and leads to an increase in protein synthesis (Bampidis & Robinson, 2006; Fregulia et al., 2021).

BWF is mainly used in the diet in an activated form together with other feed components, such as protein feeds and mineral supplements. Such a combination helps meet the organism's requirements for nitrogenous compounds, stabilizes fermentation, and increases the efficiency of nutrient utilization (Tedeschi et al., 2004; Van Soest, 1994; FAO, 2016; Gustavsson et al., 2011). Despite all its advantages, when using BWF, variations in its composition, moisture content, and storage conditions should be taken into consideration (AOAC International, 2019).

Materials and Methods

Experimental Trial and Selected Animals

The experimental trial was conducted to evaluate the effect of BWF on milk and meat productivity indicators. The experimental trial was carried out at the semi-intensive livestock farm of the Auxiliary Experimental Farm of the Scientific Research Institute of Animal Husbandry and Fisheries. A total of 22 clinically healthy dairy animals and 11 young animals were selected for the experiment.

Dairy Production Group. Holstein Friesian, Simmental, Jersey, Swiss, and Aberdeen Angus breed animals were selected.
Beef Production Group. In this group, Holstein Friesian, Simmental, Jersey, and Swiss breed animals were selected.

The experimental trial was conducted over a period of 12 weeks by adding 37.5% bread waste flour to the daily diet of lactating cows and over a period of 50 days by adding 34% to the daily diet of young animals. The control animals were raised under farm conditions.

Processing Regime
Bread waste flour was prepared from white and black bread waste. In the first stage of the processing procedure, bread residues with a moisture content of 38–44% were dried to a moisture content of 10% by keeping them in baking ovens at 60 °C for 20 minutes and then ground into flour with a particle size of 0.4 μm. This flour was incorporated into concentrate feed mixtures as a partial substitute for traditional energy sources such as corn and barley. Throughout the experimental period, the animals were continuously provided with clean drinking water.

Measurement of Milk Production
The total daily milk yield was recorded, and milk samples were analyzed in the laboratory of the Scientific Research Institute of Animal Husbandry and Fisheries using a Lactoscan device to determine the quantities of the main compositional parameters.

Growth Performance Indicators
In the beef cattle group, live body weight measurements were recorded at the beginning of the experiment and subsequently every 25 days until the end of the 50-day feeding period. Feed conversion was calculated.

Chemical Analysis Methods
The chemical composition of the feed was determined using spectral analysis method with a Perten DA 7250 NIR instrument.

Table 1
Composition of the prepared BWF, %

Sample	Moisture, %	Protein, %	Fat, %	Sugar, %	Starch, %	Ash, %
White bread	8.4	8.7	0.9	5.5	65.4	2.1
Black bread	8.2	11.4	0.5	4.8	64.1	2.2

White and black bread flour were mixed at a 50/50 ratio, and “Milk 2 Feed” was prepared for lactating cows, while “Super Fattening Trial Feed” was prepared for young animals. The “Milk 2 Feed” was prepared using 25% high-protein feed additive (protein 40%, ME-2700 kcal/kg), 37.5% bread waste flour, 12.5% wheat bran, and 25% corn (Table 2).

Table 2
Chemical composition of “Milk 2 Feed”

Parameters of the prepared feed	DM, %	ME (Mcal/kg)	CPr (g)	DPr (g)	Bypass Pr (g)	Ccell (g)	ADF (g)	NDF (g)	Cfat (g)	Crude Ash (g)	TDN, %	NEL (Mcal/kg)	NEL (MJ/kg)
Milk 2 Feed	0.90	2.81	190	130	53	37	43.9	114	28.8	44.3	73.2	1.77	7.40

Note. DM – dry matter; ME – metabolizable energy; CPr – crude protein; DPr – digestible protein; Bypass Pr – bypass protein; Ccell – crude cellulose; ADF – acid detergent fiber; Cfat – crude fat; TDN – total digestible nutrients; NEL – net energy for lactation (Mcal/kg or MJ/kg).

An experimental study was conducted over a period of 12 weeks on 22 lactating cows of different breeds, raised at the Auxiliary Experimental Farm of the Scientific Research Institute of Animal

Husbandry and Fisheries, located in Firuzabad settlement, Goygol District, using the prepared 19% protein “Milk 2 Feed” (Table 3).

Table 3
Breed composition of the selected lactating cows

Days in milk	Breed composition				
	Holstein Friesian	Simmental	Jersey	Swiss	Aberdeen Angus
5–150	3	1	2	2	0
151–305	4	0	0	0	1
305+	7	1	0	1	0
Total number of cows	14	2	2	3	1

Note. The average number of days in milk was 298 days.

During the feeding trial, a 7-day adaptation period was applied to lactating cows to allow the animals to adapt to the experimental diet (Table 4).

Table 4
Daily diet for the animals

Feed	At 1–3 days, kg	At 4–6 days, kg	At 1–12 weeks, kg
Barley straw	3	3	3
Dried alfalfa hay	9	9	9
Milk 2 Feed	6	9	12
Total	18	21	24

Results and Discussion

Milk Production Indicators under the Inclusion of BWF in the Daily Diet of Lactating Cows

The inclusion of BWF in the diet of lactating cows affected daily milk yield.

Table 5
Comparative indicators of milk production

Groups	Productivity indicators				
	Number of animals	Total milk, L	Average milk yield per animal, L	Milk fat, %	Milk density
			At 1–7 days		
Experimental	21	337.26	16.06	3.30	29.12
Control	21	273.21	13.01	3.65	28.89
			At 1–5 weeks		
Experimental	20	386.20	19.31	3.39	29.31
Control	22	299.20	13.60	3.66	29.12
			At 5–8 weeks		
Experimental	18	389	21.61	3.99	28.68
Control	21	267.12	12.72	3.99	28.69
			At 8–10 weeks		
Experimental	19	450	23.68	3.48	28.67
Control	21	277.2	13.2	3.71	28.85
			At 10–12 weeks		
Experimental	21	442	21.05	3.63	28.85
Control	21	276.99	13.19	3.89	28.78

As shown in the table, total milk production increased by 23.44–62.34%, while the average milk yield per animal increased by 23.44–79.39%. These results are consistent with the findings of previous studies. The inclusion of moderate levels of rapidly fermentable carbohydrate sources in the diet increases propionate production and milk lactose synthesis, which in turn increases milk yield (Broderick, 2003) (Fig. 1).

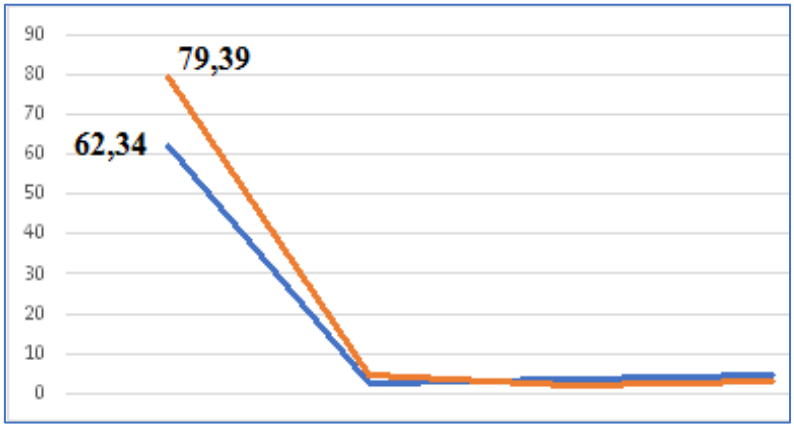


Figure 1
Diagram of the increase in total milk production and average milk yield per animal

Live Body Weight Gain Indicators under the Inclusion of BWF in the Daily Diet of Young Animals

To study the effect of the use of bread waste flour on live body weight gain in young animals, BWF was included in the daily diet at a level of 34%. For this purpose, Holstein Friesian, Simmental, Jersey, and Swiss breed animals were selected, and "Super Fattening Trial Feed" was prepared. The live body weight indicators of the young animals were recorded at the beginning of the experiment and subsequently every 25 days until the end of the 50-day feeding period (Table 6).

Table 6
Breed composition of selected young animals

Breed	Age, days	Sex	Live body weight at the beginning of the experiment, kg
Swiss	390	Female	212
Holstein Friesian	421	Female	260
Holstein Friesian	481	Male	291
Holstein Friesian	428	Female	283
Holstein Friesian	437	Female	241
Holstein Friesian	406	Male	317
Crossbred	507	Male	310
Aberdeen Angus	248	Female	196
Crossbred	468	Female	345
Crossbred	283	Male	246
Simmental	284	Female	207

When preparing the "Super Fattening Trial Feed", 15% high-protein feed additive (protein 31.4%, ME-2119.5 kcal/kg), 34.0% bread waste flour, 35.0% wheat bran, and 16.0% wheat were used. The feed mixture was prepared at Agdash Feed Factory, located in Laki settlement, Agdash District (Table 7).

Table 7
Chemical parameters of "Super Fattening Feed"

Parameters of the prepared feed	DM, %	ME (Mcal/kg)	CPr (g)	DPr (g)	Bypass Pr (g)	Ccell (g)	ADF (g)	NDF (g)	Cfat (g)	Crude Ash (g)	TDN, %	NEL (Mcal/kg)	NEL (MJ/kg)
Super Fattening Feed	0.90	2.68	156.55	105.91	41.38	60.82	73.14	204.51	31.96	44.72	70.30	1.69	7.06

Note. The protein content of "Super Fattening Feed" is 15.6%.

During the feeding trial, a 3-day adaptation period was applied to young animals to allow them to adapt to the experimental diet (Table 8).

Table 8
Daily diet for the animals

Feed	At 1–3 days, kg	At 4–22 days, kg	At 23–50 days, kg
Alfalfa	0	2	3
Straw	2	2	2
Natural grass	2	0	0
Super Fattening Feed	3	5.4	7.2
Total	7	9.4	12.2

The inclusion of BWF in the daily diet of young animals resulted in an increase in live body weight (Table 9; Figure 2).

Table 9
Live body weight gain of young animals

Breed	Sex	Live body weight at the beginning of the experiment, kg	Live body weight at the end of the experiment, kg	Difference in live body weight, kg
Swiss	Female	212	300	88
Holstein Friesian	Female	260	321	61
Holstein Friesian	Male	291	380	89
Holstein Friesian	Female	283	345	62
Holstein Friesian	Female	241	325	84
Holstein Friesian	Male	317	397	80
Crossbred	Male	310	413	103
Aberdeen Angus	Female	196	272	76
Crossbred	Female	345	414	69
Crossbred	Male	246	316	70
Simmental	Female	207	254	47

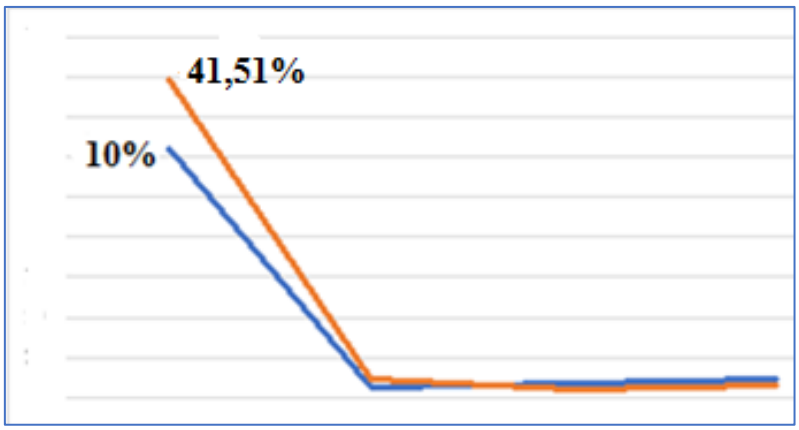


Figure 2
Live weight gain diagram

As shown in the table, the highest live weight gain was observed in the Swiss breed (41.51%), while the lowest increase was observed in crossbred animals (20.0%). The studies revealed that, under farm conditions, the live weight of young animals increased by 8–10% during the 50-day rearing period. In comparison, up to 31.5% greater live weight was obtained in the experimental group. The degree of consistency with international practices was demonstrated in the studies conducted (Fox & Tylutki, 1998; Owens et al., 1997).

Analysis of the Results

Reasons for the Increase in Milk Productivity of the Animals
1. Increase in the Energy Value of the Diet
BWF is rich in highly digestible starch and rapidly fermentable carbohydrates. This increases the energy density of the overall diet and provides animals with energy for higher milk synthesis.
2. Increase in Propionate Production
The rapid fermentation of BWF in the rumen leads to an increase in volatile fatty acids, particularly propionate. Propionate is a major source for glucose synthesis in the liver and enhances the formation of milk lactose. Lactose, in turn, directly regulates milk volume.
3. Enhancement of Milk Lactose Synthesis
Increased glucose availability enhances lactose synthesis in the mammary glands. Since lactose regulates the osmotic composition of milk, it leads to an increase in milk volume.
4. Improvement in Feed Utilization Efficiency
BWF acts as a partial substitute for cereal feeds in the diet, thereby improving feed conversion. As a result, greater milk production is achieved from the same amount of feed.
5. Optimization of Rumen Fermentation
The inclusion of BWF at an appropriate level stimulates microbial activity and makes the fermentation processes more efficient. This leads to improved absorption of nutrients.
6. Stabilization of Energy Balance
The presence of an additional rapidly available energy source in the diet reduces negative energy balance in animals, thereby contributing to a sustained increase in milk yield.

Reasons for the Increase in Live Weight of the Animals
1. Provision of High Energy Density
BWF is rich in starch and rapidly digestible carbohydrates. This increases the overall energy value of the diet and provides the calories required for daily weight gain in animals.
2. Increase in Propionate Production and Glucose Synthesis

BWF is rapidly fermented in the rumen, resulting in increased propionate production. Propionate is a major source for glucose synthesis in the liver, and this energy is directed toward growth and tissue formation.

3. Improvement in Protein and Energy Balance

When BWF is used together with other feed components (barley, corn, etc.), the energy-to-protein ratio is optimized. This accelerates muscle tissue formation and supports the increase of lean body mass.

4. Improvement in Feed Utilization Efficiency

When BWF is included in the diet, feed is utilized more efficiently, the feed conversion ratio improves, and greater live weight gain is achieved with the same amount of feed.

5. Activation of Rumen Microflora

Moderately fermentable carbohydrates stimulate microbial activity. This accelerates the breakdown of fiber and other nutrients and increases nutrient absorption.

6. Improvement in Nitrogen Utilization Efficiency

When BWF is used together with other protein sources, microbial protein synthesis is enhanced. This contributes to muscle tissue growth and promotes an increase in live weight.

7. Stabilization of Energy Balance and Reduction of Stress

Adequate energy supply reduces negative energy balance in animals, minimizes metabolic stress, and results in more stable growth dynamics.

Comparative Analysis of the Results

1. When 37.5% bread waste flour was added to the daily diet of lactating cows, total milk production increased by 23.44–62.34%, while the average milk yield per animal increased by 23.44–79.39%.

2. When 34% bread waste flour was added to the daily diet of young animals, the highest live weight gain was observed in the Swiss breed (41.51%), while the lowest increase was observed in crossbred animals (20.0%). The studies revealed that, under farm conditions, the live weight of young animals increased by 8–10% during the 50-day rearing period. In comparison, up to 31.5% greater live weight was obtained in the experimental group.

Conflict of Interest

The authors declare that they have no conflict of interest regarding this article.

References

Allen, M. S. (1997). Relationship between fermentation acid production in the rumen and the requirement for physically effective fiber. *Journal of Dairy Science*, *80*(7), 1447–1462. https://doi.org/10.3168/jds.S0022-0302(97)76074-0

AOAC International. (2019). *Official methods of analysis of AOAC International* (21st ed.).

Bampidis, V. A., & Robinson, P. H. (2006). Citrus by-products as ruminant feeds: A review. *Animal Feed Science and Technology*, *128*(3–4), 175–217. https://doi.org/10.1016/j.anifeedsci.2005.12.002

Broderick, G. A. (2003). Effects of Varying Dietary Protein and Energy Levels on the Production of Lactating Dairy Cows. *Journal of Dairy Science, 86*(4), 1370–1381. https://doi.org/10.3168/jds.S0022-0302(03)73721-7

FAO. (2016). *FAO's work on climate change: Livestock and climate change*. https://openknowledge.fao.org/handle/20.500.14283/i6345en

Fregulia, P., Neves, A. L. A., Dias, R. J. P., & Campos, M. M. (2021). A review of rumen parameters in bovines with divergent feed efficiencies: What do these parameters tell us about improving animal productivity and sustainability? *Livestock Science, 254*, 104761. https://doi.org/10.1016/j.livsci.2021.104761

Fox, D. G., & Tylutki, T. P. (1998). Accounting for the effects of environment on the nutrient requirements of dairy cattle. *Journal of Dairy Science, 81*(11), 3085–3095.

https://doi.org/10.3168/jds.S0022-0302(98)75873-4

Gustavsson, J., Cederberg, C., Sonesson, U., van Otterdijk, R., & Meybeck, A. (2011). *Global food losses and food waste: Extent, causes and prevention*. Food and Agriculture Organization of the United Nations.

Hristov, A. N., Oh, J., Firkins, J. L., Dijkstra, J., Kebreab, E., Waghorn, G., Makkar, H. P. S., Adesogan, A. T., Yang, W., Lee, C., Gerber, P. J., Henderson, B., & Tricarico, J. M. (2013). Mitigation of methane and nitrous oxide emissions from animal operations: I. A review of enteric methane mitigation options. *Journal of Animal Science, 91*(11), 5045–5069. https://doi.org/10.2527/jas.2013-6583

Janssen, P. H. (2010). Influence of hydrogen on rumen methane formation and fermentation balances through microbial growth kinetics and fermentation thermodynamics. *Animal Feed Science and Technology, 160*(1–2), 1–22. https://doi.org/10.1016/j.anifeedsci.2010.07.002

Kaltenegger, A., Humer, E., Stauder, A., & Zebeli, Q. (2020). Feeding of bakery by-products in the replacement of grains enhanced milk performance, modulated blood metabolic profile, and lowered the risk of rumen acidosis in dairy cows. *Journal of Dairy Science, 103*(11), 10122–10135. https://doi.org/10.3168/jds.2020-18425

Kolver, E. S., & Muller, L. D. (1998). Performance and nutrient intake of high producing Holstein cows consuming pasture or a total mixed ration. *Journal of Dairy Science, 81*(5), 1403–1411. https://doi.org/10.3168/jds.S0022-0302(98)75704-2

Krause, D. O., Nagaraja, T. G., Wright, A.-D. G., & Callaway, T. R. (2013). Board-invited review: Rumen microbiology: Leading the way in microbial ecology. *Journal of Animal Science, 91*(1), 331–341. https://doi.org/10.2527/jas.2012-5567

Lee, S. S., Ha, J. K., & Cheng, K.-J. (2000). Influence of an anaerobic fungal culture administration on in vivo ruminal fermentation and nutrient digestion. *Animal Feed Science and Technology, 88*(3–4), 201–217. https://doi.org/10.1016/S0377-8401(00)00216-9

NRC. (2001). *Nutrient Requirements of Dairy Cattle* (7th ed.). National Academy Press.

Owens, F. N., Secrist, D. S., Hill, W. J., & Gill, D. R. (1997). The effect of grain source and grain processing on performance of feedlot cattle: A review. *Journal of Animal Science, 75*(3), 868–879. https://doi.org/10.2527/1997.753868x

Patra, A. K. (2012). Enteric methane mitigation technologies for ruminant livestock: a synthesis of current research and future directions. *Environmental Monitoring and Assessment*, *184*(4), 1929–1952. https://doi.org/10.1007/s10661-011-2090-y

Plaizier, J. C., Krause, D. O., Gozho, G. N., & McBride, B. W. (2008). Subacute ruminal acidosis in dairy cows: The physiological causes, incidence and consequences. *The Veterinary Journal, 176*(1), 21–31. https://doi.org/10.1016/j.tvjl.2007.12.016

Russell, J. B., & Rychlik, J. L. (2001). Factors That Alter Rumen Microbial Ecology. *Science*, *292*(5519), 1119–1122. https://doi.org/10.1126/science.1058830

Steele, M. A., Dionissopoulos, L., AlZahal, O., Doelman, J., & McBride, B. W. (2012). Rumen epithelial adaptation to ruminal acidosis in lactating cattle involves the coordinated expression of insulin-like growth factor-binding proteins and a cholesterolgenic enzyme. *Journal of Dairy Science, 95*(1), 318–327. https://doi.org/10.3168/jds.2011-4465

Tedeschi, L. O., Fox, D. G., & Guiroy, P. J. (2004). A decision support system to improve individual cattle management. 1. A mechanistic, dynamic model for animal growth. *Agricultural Systems, 79*, 171–204. https://doi.org/10.1016/S0308-521X(03)00070-2

Van Soest, P. J. (1994). *Nutritional Ecology of the Ruminant*. Cornell University Press.

Zebeli, Q., Dijkstra, J., Tafaj, M., Steingass, H., Ametaj, B. N., & Drochner, W. (2008). Modeling the adequacy of dietary fiber in dairy cows based on the responses of ruminal pH and milk fat production to composition of the diet. *Journal of Dairy Science, 91*(5), 2046–2066. https://doi.org/10.3168/jds.2007-0572

NATURE & SCIENCE
October 2026, Volume 8, Issue 5, pp. 70–77
DOI: https://doi.org/10.36719/2707-1146/68/70-77

Ecochemical Assessment of Synthetic Pesticide Residues in a Tomato Sample Grown in Azerbaijan: Analysis of Plant Extract-Based Biopesticides as a Promising Alternative

Nigar Hashimova[1*] and Sevinj Hajiyeva[1]

Abstract. *Synthetic pesticides are widely used in modern agriculture to increase productivity and protect crops from pests, pathogens, and weeds, but their intensive and long-term application may result in pesticide residues in agricultural products and potential risks to human health and the environment. This study aimed to determine pesticide residues in a tomato sample grown in Azerbaijan using the QuEChERS–LC–MS/MS method, assess the analytical result from food-safety and ecochemical perspectives, and examine plant-extract-based biopesticides as potential alternatives to synthetic pesticides. The analytical procedure included sample preparation, citrate-buffered QuEChERS extraction, dispersive solid-phase clean-up, and LC–MS/MS determination using a Shimadzu LCMS-8045 Triple Quadrupole system with a Raptor Biphenyl column. Buprofezin was detected in the tomato sample at a concentration of 0.12 mg/kg. This value was compared with the applicable maximum residue level (MRL) for the intended European market, and the result was classified as non-compliant according to the source data. The findings demonstrate the importance of regular pesticide-residue monitoring and risk-based assessment of agricultural products. The literature review further indicates that plant-extract-based biopesticides may contribute to more sustainable crop-protection strategies, although their efficacy, stability, toxicological and ecotoxicological properties require case-specific evaluation.*

Keywords: *pesticide residues, tomato, ecochemistry, QuEChERS, LC–MS/MS, food safety, biopesticides*

Introduction

Synthetic pesticides are widely used to increase agricultural productivity and protect crops from pests, diseases, and weeds (Rani et al., 2021; Tudi et al., 2021). Although these substances play an important role in reducing crop losses, their intensive and long-term application may result in residues in soil, water, and agricultural products, biodiversity loss, and potential risks to human health (Rani et al., 2021; Tudi et al., 2021; Carvalho, 2017). The entry of pesticide residues into the food chain may pose potential risks to human health and ecosystems (Nicolopoulou-Stamati et al., 2016; Kim et al., 2017; Carvalho, 2017). Therefore, monitoring pesticide residues in agricultural products using modern analytical methods is considered one of the key directions of food safety and environmental protection (European Food Safety Authority et al., 2023; Alder et al., 2006).

[1]Department of Ecological Chemistry, Baku State University, PhD Candidate, Baku, Azerbaijan
[1]Department of Ecological Chemistry, Baku State University, Doctor of Chemical Sciences, Baku, Azerbaijan
[*]Corresponding author. E-mail: n.hashimova.89@gmail.com
Received: 13 May 2026; Accepted: 17 September 2026; Published online: 25 October 2026
© The Author(s) 2026. This is an open access article distributed under the terms of the Creative Commons Attribution-NonCommercial 4.0 International License (CC BY-NC 4.0).

Vegetables play an important role in human nutrition; therefore, their assessment with respect to pesticide residues is of particular importance (Carvalho, 2017). The establishment of maximum residue levels (Maximum Residue Levels – MRLs) and their regular monitoring are key elements of international food safety approaches to the assessment of pesticide residues in food products (EFSA et al., 2023; European Parliament and Council, 2005).

The QuEChERS extraction method and liquid chromatography–tandem mass spectrometry (LC–MS/MS) are widely used analytical approaches for the determination of pesticide residues across multiple active substances (Alder et al., 2006; Lehotay et al., 2010; Wilkowska & Biziuk, 2011). The high selectivity and sensitivity of these methods provide suitable opportunities for monitoring pesticide residues in various food matrices (Alder et al., 2006). In recent years, interest in biopesticides based on plant extracts has increased with the aim of reducing the potential environmental impacts of synthetic pesticides (Isman, 2020; Damalas & Koutroubas, 2018). Because these preparations are based on naturally derived active substances, they are considered promising alternatives to synthetic pesticides. Nevertheless, their efficacy, biodegradation, and effects on non-target organisms should be evaluated separately depending on the properties of the active components and the conditions of application (Isman, 2020; Pavela & Benelli, 2016; Isman & Grieneisen, 2014).

Research Objective

The objective of this study was to determine synthetic pesticide residues in a tomato sample grown in Azerbaijan using the QuEChERS–LC–MS/MS method, to assess the obtained result from food safety and ecochemical perspectives, and to substantiate, based on the scientific literature, the prospects for applying biopesticides based on plant extracts as potential alternatives to synthetic pesticides.

Scientific Novelty

The scientific novelty of this study lies in linking the analytical determination of synthetic pesticide residues in tomatoes grown in Azerbaijan using the QuEChERS–LC–MS/MS method with ecochemical assessment, and in analyzing, based on the scientific literature, biopesticides based on plant extracts as potential alternatives to synthetic pesticides. The general conceptual framework of the study is presented in Figure 1.

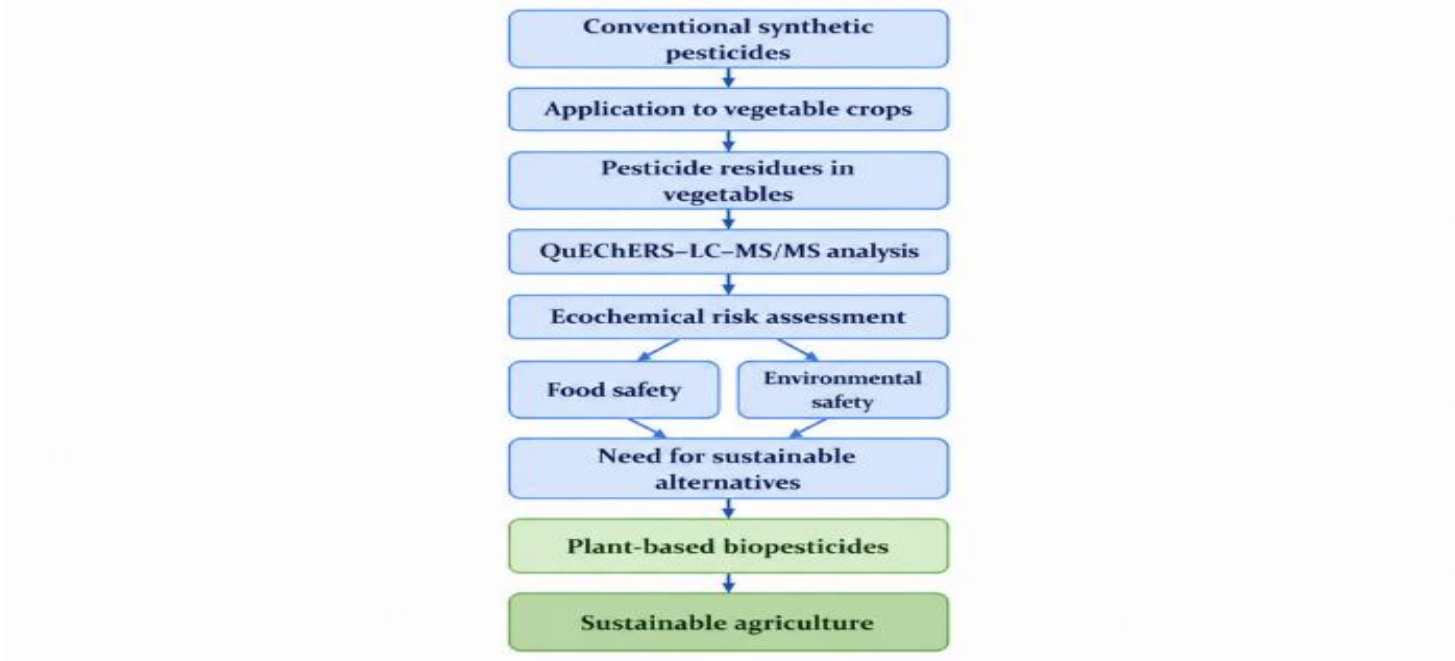


Figure 1
General conceptual framework of the study

Materials and Methods

General Study Design

The study was conducted to determine synthetic pesticide residues in a tomato sample grown in Azerbaijan and to assess them from an ecochemical perspective. The analytical process consisted of sample collection, sample preparation, extraction using the QuEChERS method, dispersive solid-phase extraction (d-SPE) clean-up, analysis using an LC–MS/MS system, and evaluation of the results against the relevant regulatory requirements.

The analytical methodology was applied in accordance with the European standard EN 15662:2015 and relevant quality control and method validation requirements for the analytical determination of pesticide residues (European Committee for Standardization, 2015; OECD, 2017). The general workflow of the analytical procedure is presented in Figure 2.

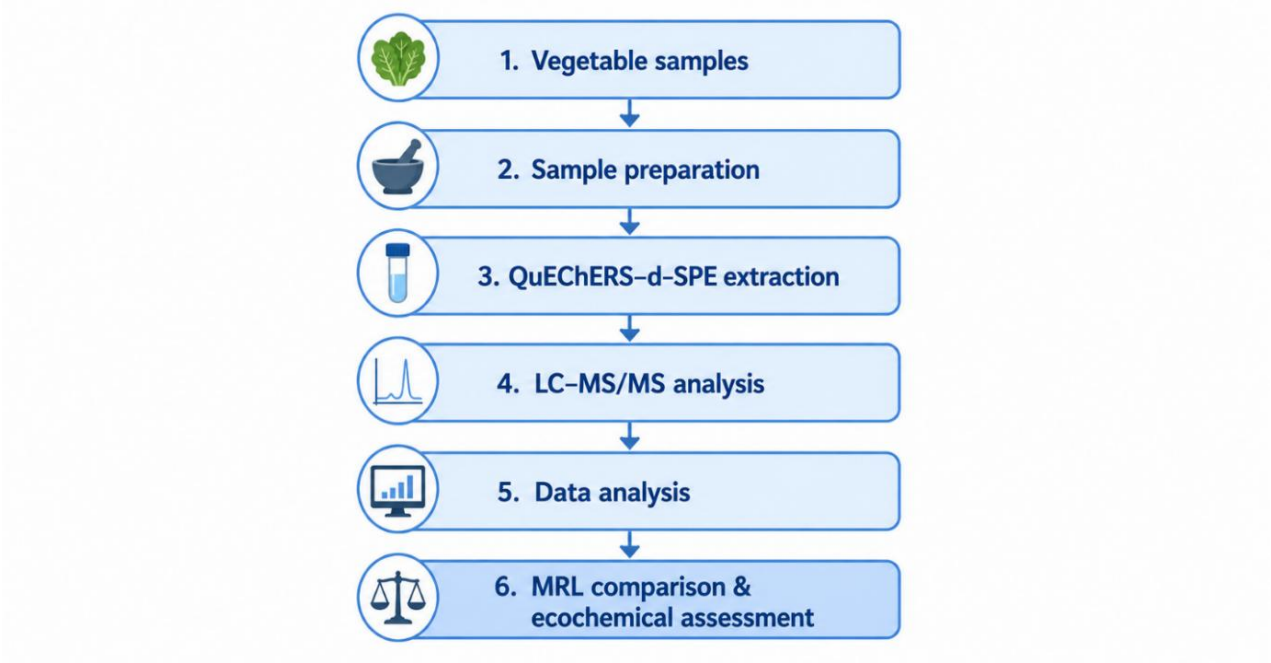


Figure 2

General workflow of the analytical procedure used in the study

Study Objects

Tomato (*Solanum lycopersicum* L.) samples grown in Azerbaijan were selected as the study objects. After being delivered to the laboratory, the samples were homogenized and stored under refrigerated conditions until analysis.

Equipment and Reagents Used

A Shimadzu LCMS-8045 Triple Quadrupole LC–MS/MS system, Raptor Biphenyl analytical column, refrigerated centrifuge, vortex mixer, analytical balance, and homogenizer were used for the analysis of pesticide residues (Table 1).

Table 1

Main laboratory equipment

Equipment	Specification
LC–MS/MS system	Shimadzu LCMS-8045 Triple Quadrupole
Analytical column	Raptor Biphenyl (100 × 3.0 mm, 2.7 µm)
Centrifuge	Refrigerated centrifuge

Vortex mixer	Laboratory vortex
Analytical balance	± 0.0001 g
Homogenizer	Laboratory blender

Only solvents and analytical reagents of a purity grade suitable for LC–MS analysis were used during the analysis. The main reagents used are presented in Table 2.

Table 2
Chemicals and reagents

Reagent	Purpose
Acetonitrile	Extraction solvent
Methanol	Mobile phase
Formic acid	Mobile phase modifier
Ammonium formate	Buffer
Magnesium sulfate ($MgSO_4$)	Water removal
Sodium chloride (NaCl)	Phase separation
Trisodium citrate	Buffering salt
Disodium hydrogen citrate	Buffering salt
PSA sorbent	Matrix clean-up
C18 sorbent	Removal of lipids
Ultrapure water	Mobile phase preparation

Sample Preparation
A 10.0 ± 0.1 g portion of the homogenized sample was placed in a 50 mL polypropylene centrifuge tube, and 10 mL of acetonitrile of a purity grade suitable for LC–MS/MS analysis was added. The sample was homogenized until a uniform mixture was obtained; for low-moisture matrices, ultrapure water was added to improve extraction efficiency.

QuEChERS Extraction
Extraction was performed using the citrate-buffered QuEChERS method in accordance with EN 15662:2015 (Lehotay et al., 2010; Wilkowska & Biziuk, 2011; CEN, 2015; Anastassiades et al., 2003). Magnesium sulfate, sodium chloride, trisodium citrate dihydrate, and disodium hydrogen citrate sesquihydrate were added to the extraction mixture. After intensive vortex mixing, the mixture was centrifuged, and the upper acetonitrile phase was transferred to kits containing PSA, $MgSO_4$, and C18 sorbents for dispersive solid-phase extraction (d-SPE) clean-up. The purified extract was centrifuged again and prepared for LC–MS/MS analysis.

QuEChERS Extraction Procedure
10 g sample → 10 mL Acetonitrile → Extraction salts → Vortex → Centrifugation → Organic phase → PSA + $MgSO_4$ + C18 → Vortex → Centrifugation → LC vial for analysis→ LC–MS/MS

LC–MS/MS Analysis
Identification and quantitative determination of pesticide residues were performed using a Shimadzu LCMS-8045 Triple Quadrupole LC–MS/MS system. Chromatographic separation was carried out on a Raptor Biphenyl column in gradient elution mode. Detection was performed using multiple reaction monitoring (MRM) in ESI (+) and ESI (−) ionization modes.

Analytes were identified based on retention time, precursor ion, product ion, and MRM transitions (Alder et al., 2006). The main operating parameters of the LC–MS/MS system are presented in Table 3.

Table 3
LC–MS/MS operating conditions

Parameter	Value
Instrument	Shimadzu LCMS-8045
Column	Raptor Biphenyl
Flow rate	0.45 mL/min
Column temperature	50 °C
Injection volume	5 µL
Ionization	ESI (+/−)
Acquisition mode	MRM

Regulatory Assessment of Results

The analytical results were processed using the instrument software. The detected buprofezin residue level was assessed based on the relevant regulatory requirements, taking into account the intended export destination of the product. For products intended for export to the European market, the maximum residue level (MRL) established in the European Union was used as the reference (Nicolopoulou-Stamati et al., 2016).

The detected buprofezin concentration was compared with the maximum residue level (MRL) specified in the relevant regulatory document, and the result was assessed in terms of food safety, regulatory compliance, and ecochemical risks (Nicolopoulou-Stamati et al., 2016; Kim et al., 2017). The result is presented in Table 3.

Results and Discussion

Analytical Assessment of Conventional Pesticide Residues

The analyzed tomato sample was assessed using the EN 15662:2015 method. Buprofezin was detected in the tomato sample. The detected buprofezin residue concentration was evaluated by comparison with the maximum residue level (MRL) established in accordance with the relevant regulatory requirement (European Parliament and Council, 2005). The representative LC–MS/MS chromatogram obtained for buprofezin in the tomato sample is presented in Figure 3.

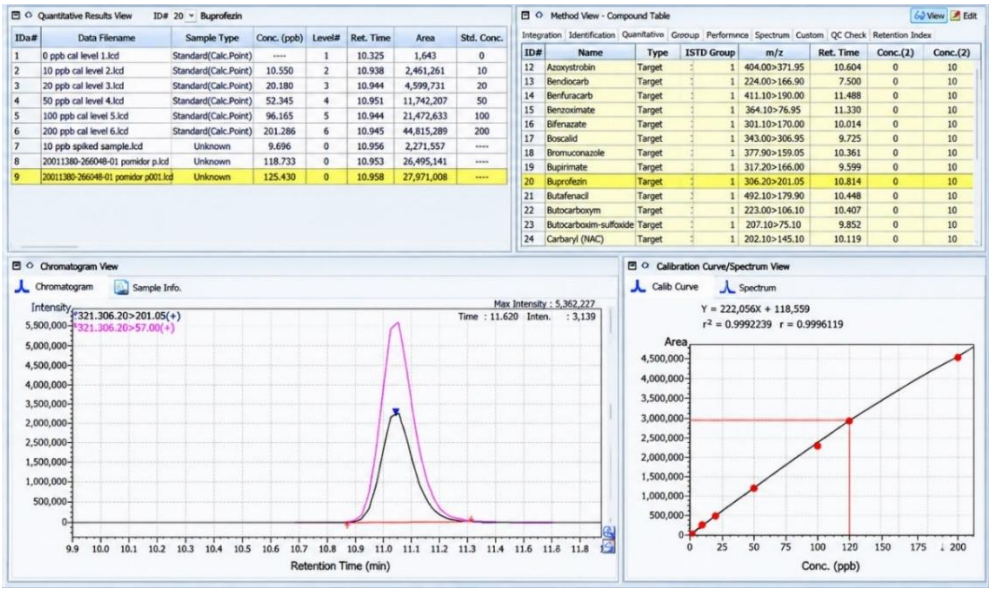


Figure 3
Representative LC–MS/MS chromatogram of buprofezin in the tomato sample

The determination of buprofezin residues in the tomato sample demonstrates the importance of regular monitoring of pesticide residues in agricultural products and the implementation of risk-based control measures (Carvalho, 2017; EFSA et al., 2023).

Table 4
Experimental pesticide residue results

Sample	Detected pesticide	Concentration (mg/kg)	Applicable MRL (mg/kg)	MRL source	Compliance
Tomato	Buprofezin	0.12	0.01	EU Pesticides Database	Non-compliant

Ecochemical Risks of Conventional Pesticides
The environmental impact of synthetic pesticides depends on their physicochemical properties and environmental fate (Tudi et al., 2021; Carvalho, 2017). After application, active substances may enter soil and water environments and undergo sorption, degradation, leaching, and other processes. These processes determine pesticide persistence, mobility, and the likelihood of exposure of non-target organisms (Tudi et al., 2021; Alengebawy et al., 2021).

Assessment from the Perspective of Food Safety and Human Health
Because vegetables are an important component of the daily diet, the determination of pesticide residues in them is of particular importance for food safety (Carvalho, 2017; EFSA et al., 2023). Risk assessment should be based not only on the detection of pesticide residues but also on their concentrations and compliance with existing maximum residue levels (MRLs) (EFSA et al., 2023; European Parliament and Council, 2005).
Modern analytical monitoring

systems enable early detection of pesticide residues, assessment of compliance with regulatory requirements, and protection of consumer health (EFSA et al., 2023).

Plant-Extract Biopesticides – a Safer Alternative
The potential environmental impacts of synthetic pesticide use have increased interest in biopesticides based on plant extracts (Isman, 2020; Damalas & Koutroubas, 2018). Scientific studies have demonstrated the biological activity of extracts and essential oils obtained from plants such as neem (*Azadirachta indica*), garlic (*Allium sativum*), thyme (*Thymus vulgaris*), rosemary (*Salvia rosmarinus*), clove (*Syzygium aromaticum*), and cinnamon (*Cinnamomum verum*) against various pests and plant pathogens (Isman, 2020; Pavela & Benelli, 2016).

The promising characteristics of plant-extract-based biopesticides are associated with their basis in naturally derived bioactive substances, their diverse modes of action, and, in some cases, their lower persistence in the environment (Isman, 2020; Pavela & Benelli, 2016; Regnault-Roger et al., 2012). However, the efficacy and ecotoxicological properties of these preparations may vary depending on the composition of the active components, formulation characteristics, and conditions of application (Pavela & Benelli, 2016; Isman & Grieneisen, 2014). Their relatively short duration of action, low stability, and the need for repeated application in some cases are among the factors that should be considered in practical use (Pavela & Benelli, 2016; Isman & Grieneisen, 2014; Regnault-Roger et al., 2012).

In this regard, rather than completely replacing synthetic pesticides, optimizing their use and gradually integrating plant-derived biopesticides into integrated plant protection systems is

considered a more realistic approach (Isman, 2020; Damalas & Koutroubas, 2018; European Commission, 2020). The application of plant-based preparations as alternatives to synthetic pesticides requires a comprehensive assessment of their efficacy, toxicological and ecotoxicological properties, residue behavior, and applicability under local agroecological conditions (Damalas & Koutroubas, 2018; Pavela & Benelli, 2016; Isman & Grieneisen, 2014).

Prospects for Application in Azerbaijan's Agriculture

Expanding the monitoring of pesticide residues using modern analytical methods, implementing risk-based control programs, and studying biopesticides based on plant extracts are considered promising directions for the development of sustainable agriculture in Azerbaijan (Damalas & Koutroubas, 2018; European Commission, 2020). Studying local plant resources as sources of biopesticides may contribute to reducing potential environmental impacts and improving the food safety system.

Conclusion

This study examined the applicability of the QuEChERS–LC–MS/MS method for determining synthetic pesticide residues in tomatoes grown in Azerbaijan and the ecochemical assessment of the obtained results. Modern analytical approaches enable the determination of pesticide residues and comparison of the obtained results with relevant regulatory requirements.

Scientific literature analysis indicates that biopesticides based on plant extracts can be considered among the promising alternatives for optimizing the use of synthetic pesticides and developing more sustainable plant protection approaches. However, their efficacy, safety, ecotoxicological properties, and applicability under local agroecological conditions should be evaluated separately.

Thus, regular monitoring of pesticide residues, application of risk-based assessment approaches, and scientifically based research on plant-derived biopesticides may support the development of sustainable and safe plant protection systems in Azerbaijan.

Conflict of Interest

The authors declare that they have no conflict of interest regarding this article.

References

Alder, L., Greulich, K., Kempe, G., & Vieth, B. (2006). Residue analysis of 500 high priority pesticides: Better by GC–MS or LC–MS/MS? *Mass Spectrometry Reviews, 25*(6), 838–865. https://doi.org/10.1002/mas.20091

Alengebawy, A., Abdelkhalek, S. T., Qureshi, S. R., & Wang, M.-Q. (2021). Heavy metals and pesticides toxicity in agricultural soil and plants: Ecological risks and human health implications. *Toxics, 9*(3), 42. https://doi.org/10.3390/toxics9030042

Anastassiades, M., Lehotay, S. J., Štajnbaher, D., & Schenck, F. J. (2003). Fast and easy multiresidue method employing acetonitrile extraction/partitioning and "dispersive solid-phase extraction" for the determination of pesticide residues in produce. *Journal of AOAC International, 86*(2), 412–431. https://doi.org/10.1093/jaoac/86.2.412

Carvalho, F. P. (2017). Pesticides, environment, and food safety. *Food and Energy Security, 6*(2), 48–60. https://doi.org/10.1002/fes3.108

Damalas, C. A., & Koutroubas, S. D. (2018). Current status and recent developments in biopesticide use. *Agriculture, 8*(1), 13. https://doi.org/10.3390/agriculture8010013

European Food Safety Authority (EFSA), Carrasco Cabrera, L., Di Piazza, G., Dujardin, B., & Medina Pastor, P. (2023). The 2021 European Union report on pesticide residues in food. *EFSA Journal, 21*(4), 7939. https://doi.org/10.2903/j.efsa.2023.7939

European Commission. (2020). *Farm to fork strategy for a fair, healthy and environmentally-friendly food system*. EUR-Lex. https://eur-lex.europa.eu/EN/legal-content/summary/farm-to-fork-strategy-for-a-fair-healthy-and-environmentally-friendly-food-system.html

European Committee for Standardization (CEN). (2015). *EN 15662:2015. Foods of plant origin—Multimethod for the determination of pesticide residues using GC- and LC-based analysis following acetonitrile extraction/partitioning and clean-up by dispersive SPE* (QuEChERS method).

European Parliament and Council. (2005). Regulation (EC) No 396/2005 of 23 February 2005 on maximum residue levels of pesticides in or on food and feed of plant and animal origin and amending Council Directive 91/414/EEC. *Official Journal of the European Union, L 70*, 1–16.

Isman, M. B. (2020). Botanical insecticides in the twenty-first century—Fulfilling their promise? *Annual Review of Entomology, 65*, 233–249. https://doi.org/10.1146/annurev-ento-011019-025010

Isman, M. B., & Grieneisen, M. L. (2014). Botanical insecticide research: Many publications, limited useful data. *Trends in Plant Science, 19*(3), 140–145. https://doi.org/10.1016/j.tplants.2013.11.005

Kim, K.-H., Kabir, E., & Jahan, S. A. (2017). Exposure to pesticides and the associated human health effects. *Science of the Total Environment, 575*, 525–535. https://doi.org/10.1016/j.scitotenv.2016.09.009

Lehotay, S. J., Son, K. A., Kwon, H., Koesukwiwat, U., Fu, W., Maštovská, K., Hoh, E., & Leepipatpiboon, N. (2010). Comparison of QuEChERS sample preparation methods for the analysis of pesticide residues in fruits and vegetables. *Journal of Chromatography A, 1217*(16), 2548–2560. https://doi.org/10.1016/j.chroma.2010.01.044

Nicolopoulou-Stamati, P., Maipas, S., Kotampasi, C., Stamatis, P., & Hens, L. (2016). Chemical pesticides and human health: The urgent need for a new concept in agriculture. *Frontiers in Public Health, 4*, 148. https://doi.org/10.3389/fpubh.2016.00148

OECD. (2017). *Guidance document on pesticide residue analytical methods* (Series on Pesticides and Biocides). OECD Publishing. https://doi.org/10.1787/5900bd46-en

Pavela, R., & Benelli, G. (2016). Essential oils as ecofriendly biopesticides? Challenges and constraints. *Trends in Plant Science, 21*(12), 1000–1007. https://doi.org/10.1016/j.tplants.2016.10.005

Rani, L., Thapa, K., Kanojia, N., Sharma, N., Singh, S., Grewal, A. S., Srivastav, A. L., & Kaushal, J. (2021). An extensive review on the consequences of chemical pesticides on human health and environment. *Journal of Cleaner Production, 283*, 124657. https://doi.org/10.1016/j.jclepro.2020.124657

Regnault-Roger, C., Vincent, C., & Arnason, J. T. (2012). Essential oils in insect control: Low-risk products in a high-stakes world. *Annual Review of Entomology, 57*, 405–424. https://doi.org/10.1146/annurev-ento-120710-100554

Tudi, M., Ruan, H. D., Wang, L., Lyu, J., Sadler, R., Connell, D., Chu, C., & Phung, D. T. (2021). Agriculture development, pesticide application and its impact on the environment. *International Journal of Environmental Research and Public Health, 18*(3), 1112. https://doi.org/10.3390/ijerph18031112

Wilkowska, A., & Biziuk, M. (2011). Determination of pesticide residues in food matrices using the QuEChERS methodology. *Food Chemistry, 125*(3), 803–812. https://doi.org/10.1016/j.foodchem.2010.09.094

NATURE & SCIENCE
October 2026, Volume 8, Issue 5, pp. 78–88
DOI: https://doi.org/10.36719/2707-1146/68/78-88

Contamination Level Determines Whether Soil-Applied Zinc Oxide Nanoparticles Limit Cadmium Uptake in Maize

Miebaka Emmanuel Ikiriko[1*], Isaac Glory Chimamanda[1], and Idiami Victoria Ogie[2]

Abstract. *Cadmium (Cd) persists in agricultural soils and maize, a staple cereal, takes it up readily. Zinc oxide nanoparticles (ZnO NPs) are widely proposed as a remedy, yet most supporting evidence comes from foliar sprays or from soils with little Cd. We grew maize (Zea mays* L.*) in a strongly acidic loamy sand amended with Cd at 150, 250 and 350 mg kg^{-1} and treated it with soil-applied ZnO NPs at 100, 150 and 200 mg kg^{-1}, in a screen-house factorial experiment with an untreated control. Cd reduced growth in proportion to dose; plants at the highest rate were 42% shorter than those at the lowest. No ZnO NP rate restored growth to control levels, and 100 mg kg^{-1} gave taller plants and longer roots than 150 or 200 mg kg^{-1}. The effect of ZnO NPs on tissue Cd depended on contamination. At 150 mg kg^{-1} Cd, raising ZnO NPs from 100 to 200 mg kg^{-1} lowered shoot Cd by 51%. At 250 and 350 mg kg^{-1} Cd, higher ZnO NP rates were instead associated with higher root and shoot Cd. The translocation factor stayed below 1 in every treatment and was lowest at 200 mg kg^{-1} ZnO NPs. Soil-applied ZnO NPs cannot be relied on as a general control on Cd uptake by maize. Where they lowered shoot Cd, at the lowest contamination level tested, they did so at a cost to growth.*

Keywords: *cadmium, zinc oxide nanoparticles, maize, translocation factor, soil contamination, nanoremediation*

Introduction

Cadmium (Cd) is a Group 1 human carcinogen (IARC, 2012) with no known function in plants. It reaches people mainly through crops grown on polluted soil. A recent global synthesis of 796,084 soil samples estimated that 14–17% of the world's cropland is affected by toxic metal pollution, and that 0.9–1.4 billion people live in regions of elevated risk (Hou et al., 2025); Cd is one of the seven metals it covers. How much of the Cd in a soil reaches a crop depends on soil chemistry. Cd mobility is governed by pH, organic matter and competition from other cations, and acidic soils release more of it to roots (Kubier et al., 2019).

Maize is a staple cereal across sub-Saharan Africa, which makes its Cd content a matter of food safety. The root is the first organ to meet Cd. Cd slows root elongation and alters root anatomy (Lux et al., 2011), and it changes the uptake of other metals (Wang et al., 2007). Cd also resembles zinc (Zn) chemically, and the two elements compete for uptake, which is why Zn supply has long been considered a way of limiting Cd entry (Rizwan et al., 2019b).

[1]Department of Crop and Soil Science, Faculty of Agriculture, University of Port Harcourt, Choba, Rivers State, Nigeria
[2]Department of Soil Science, Faculty of Agriculture, Ignatius Ajuru University of Education, Port Harcourt, Nigeria
[*]Corresponding Author. E-mail: miebaka.ikiriko@uniport.edu.ng
Received: 13 April 2026; Accepted: 9 September 2026; Published online: 25 October 2026
© The Author(s) 2026. This is an open access article distributed under the terms of the Creative Commons Attribution-NonCommercial 4.0 International License (CC BY-NC 4.0).

The root can, in addition, hold Cd back from the shoot: high Cd in the rhizosphere accelerates the maturation of apoplastic barriers in the root (Lux et al., 2011). Zinc oxide nanoparticles (ZnO NPs) have attracted interest as a vehicle for that Zn. In wheat, ZnO NPs applied through soil or as a foliar spray lowered grain Cd by 16–78% and 30–77%, respectively, and improved growth (Hussain et al., 2018). In maize, foliar ZnO NPs have been reported to reduce Cd accumulation, alone or combined with biochar (Rizwan et al., 2019a; Zha et al., 2022), and to lessen Cd-induced oxidative and metabolic damage in seedlings (Hussain et al., 2024).

The evidence is, however, conditional. A review by Rizwan et al. (2019b), concluded that the effect of Zn on Cd accumulation is inconsistent and depends on the concentrations of both metals, the exposure period, the species and the growth conditions. In rice, Zn and Cd were antagonistic in roots and shoots, yet higher Zn activity increased the transfer of Cd from root to shoot, and the net effect depended on genotype (Cai et al., 2019). Soil-applied ZnO NPs raised rice growth under Cd stress but, at high doses, also raised the bioavailable Cd in the rhizosphere (Zhang et al., 2019).

The maize studies cited above used foliar sprays at 25–100 mg L^{-1} or, in one case, seedlings in nutrient solution at 0.6 mM Cd (Hussain et al., 2024), and the soil-based rice work used Cd at 1.0–5.0 mg kg^{-1} (Zhang et al., 2019). We found no study that tested soil-applied ZnO NPs in maize across a wide gradient of soil Cd.

This gap has practical consequences. Neither the nanoparticle rate that best serves maize nor the Cd level beyond which the treatment stops working has been established. Advisers working on land polluted by mining, industrial effluent or waste need to know whether a nanoparticle amendment deserves a recommendation, at what rate, and for what degree of pollution. Applying it without that knowledge risks paying for a treatment that, under some conditions, may increase Cd in the crop. A dose–response test across contamination levels, in a soil of the kind on which maize is commonly grown in the humid tropics, is therefore needed.

We framed the study around three processes that operate when ZnO NPs enter an acidic soil carrying Cd (Fig. 1). First, the nanoparticles dissolve and release Zn^{2+}. Second, Zn^{2+} competes with Cd^{2+} for uptake sites at the root surface, which lowers Cd entry (Rizwan et al., 2019b; Cai et al., 2019). Third, Zn^{2+} may displace Cd from soil exchange sites and raise the amount available to roots, since competition between cations is a recognised route of Cd release (Kubier et al., 2019; Zhang et al., 2019), and excess Zn or nanoparticles may damage roots directly (Lin & Xing, 2007).

The first process favours lower tissue Cd; the second and third work against it. Their balance should depend on how much Cd the soil carries and how much ZnO is added, and root retention then determines how much of the absorbed Cd reaches the shoot (Lux et al., 2011). Tissue Cd and its partitioning, expressed as the bioconcentration factor (BCF) and translocation factor (TF), are therefore the response variables that show which process dominates, and growth shows the cost to the plant. The framework does not assume that ZnO NPs protect maize. It treats protection as one possible outcome.

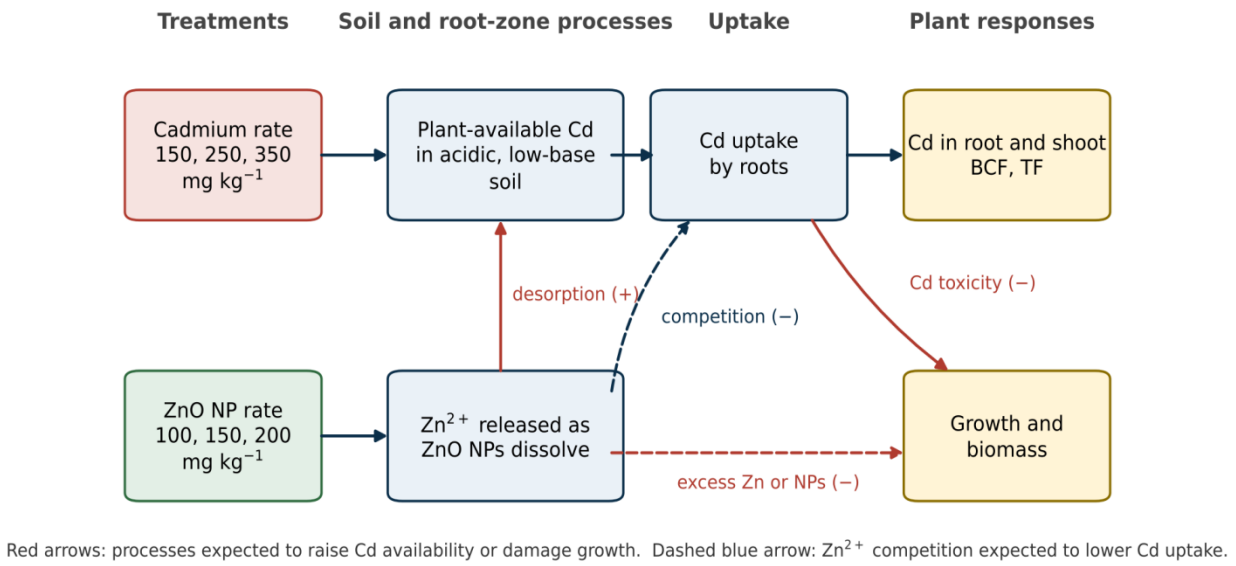


Figure 1

Conceptual framework. ZnO NPs release Zn^{2+}, which may lower Cd uptake by competition at the root surface, raise Cd availability by displacing Cd from exchange sites, or harm growth directly at high rates. Tissue Cd, BCF and TF show which process dominates; growth shows the cost to the plant.

The main objective of this study was to determine how soil-applied ZnO NPs at three rates affect Cd uptake by maize grown at three levels of Cd contamination. The specific objectives were to (i) determine the effect of ZnO NP rate on the growth and biomass of maize exposed to different levels of Cd; (ii) evaluate the influence of ZnO NPs on Cd accumulation in the roots and shoots across the Cd gradient; and (iii) calculate the BCF and TF of Cd in maize under each combination of ZnO NP and Cd.

Materials and Methods

Site and Soil

The experiment was carried out in the screen house of the Department of Crop and Soil Science, Faculty of Agriculture, University of Port Harcourt, Choba, Rivers State, Nigeria (about 4°53′–4°54′ N, 6°54′–6°55′ E), in the humid tropical rainforest zone. Surface soil (0–30 cm) was taken from an uncultivated part of the Faculty's Teaching and Research Farm, bulked, cleaned of debris, air-dried for seven days and sieved (2 mm). A subsample was analysed before treatment in triplicate. Particle size was determined by the hydrometer method (Bouyoucos, 1962); pH in a 1:1 soil–water suspension; electrical conductivity in a 1:2 suspension; organic carbon by dichromate wet oxidation (Walkley & Black, 1934); total nitrogen by macro-Kjeldahl digestion (Bremner & Mulvaney, 1982); available phosphorus by Bray P-1 extraction (Bray & Kurtz, 1945) with molybdenum-blue colorimetry (Murphy & Riley, 1962); exchangeable bases in 1 N neutral ammonium acetate, with potassium read by flame photometry and calcium and magnesium by atomic absorption spectrophotometry (AAS); and background Cd after aqua regia digestion, by AAS at 228.8 nm.

Treatments and Design

Cd was added as analytical-grade $CdCl_2 \cdot 2.5H_2O$ at 150, 250 and 350 mg Cd kg^{-1} soil. ZnO NPs (average particle size 10–30 nm, purity 99.8%, according to the manufacturer; SkySpring Nanomaterials, Houston, USA) were added at 100, 150 and 200 mg kg^{-1}. The nine Cd × ZnO NP combinations, plus an untreated control, were arranged in a completely randomised design with four replicate pots each (40 pots analysed here). Ten kilograms of soil were placed in each perforated 10-

litre bag, with a bowl beneath to collect leachate, which was returned to the same bag so that no Cd, Zn or nutrients were lost. The Cd salt was dissolved in 100 mL of distilled water, sprinkled over the soil and mixed in. Pots were brought to field capacity and left to equilibrate for two weeks. ZnO NPs were then dispersed in 20 mL of deionised water, sonicated for 30 minutes, mixed into the soil, and the pots were left for three days before sowing. Cd-only and ZnO-only pots included in the original plan were not part of the analysis reported here.

Crop Management and Measurements

Three seeds of maize variety Oba Super 6 were sown per pot at 3 cm depth and thinned to two plants two weeks after sowing. Pots were watered to near field capacity and weeded by hand. Plant height, leaf number (fully opened green leaves) and stem girth (Vernier caliper, 5 cm above the soil) were recorded at 2, 4, 6 and 8 weeks after planting. Plants were harvested at 8 weeks. Shoot length, root length, and fresh shoot and root weights were recorded, and tissues were dried at 70 °C to constant weight (about 72 h) for dry weights. Dried tissue was ground (0.5 mm), digested in a 4:1 mixture of concentrated HNO_3 and $HClO_4$, and Cd was read by AAS at 228.8 nm against standards prepared from a certified 1,000 mg L^{-1} stock, with reagent blanks and a drift check every ten samples. The bioconcentration factor was calculated as root Cd divided by soil Cd, and the translocation factor as shoot Cd divided by root Cd (Yoon et al., 2006).

Statistical Analysis

Data were subjected to two-way analysis of variance for a factorial experiment in a completely randomised design, testing the main effects of Cd rate and ZnO NP rate and their interaction, with the contrast between control and treated plants also evaluated. Growth data were analysed separately for each sampling date. Means were separated by Duncan's multiple range test at $P \leq 0.05$. Pearson correlation was used to relate tissue Cd to growth and biomass traits ($n = 40$). Analyses were run in SAS version 9.4.

Results and Discussion

Soil Conditions Favour Cd Mobility

The experimental soil was a loamy sand (81.0% sand, 12.8% silt, 6.2% clay) and strongly acidic (pH 5.21). Organic matter was high for the texture (104.0 g kg^{-1}), but exchangeable bases were low (2.09 cmol kg^{-1}) and the background Cd concentration was 0.07 mg kg^{-1} (Table 1). With so little clay, the capacity of this soil to hold added Cd rests largely on its organic matter, and at pH near 5 a considerable share of added Cd is expected to remain available to roots (Kubier et al., 2019). The scarcity of base cations has a second consequence. Zn released from the nanoparticles would meet little competition from calcium, magnesium and potassium and could therefore act directly on Cd at exchange sites and at the root surface.

Table 1

Properties of the experimental soil before treatment (means of three determinations)

Property	Value
pH (H_2O)	5.21
Sand / silt / clay (%)	81.0 / 12.8 / 6.2
Textural class	Loamy sand
Total organic carbon (g kg^{-1})	61.8
Organic matter (g kg^{-1})	104.0
Total nitrogen (g kg^{-1})	6.8
Available phosphorus (mg kg^{-1})	14.20
Exchangeable Ca, Mg, K, Na (cmol kg^{-1})	1.60, 0.34, 0.06, 0.09

Property	Value
Total exchangeable bases (cmol kg^{-1})	2.09
Cadmium, background (mg kg^{-1})	0.07

Values are those reported in the dissertation (Isaac, 2026).

Cadmium Suppresses Growth in Proportion to Dose

Cd rate was the dominant influence on growth. By 8 weeks after planting (WAP), mean plant height fell from 36.33 cm at 150 mg kg^{-1} Cd to 25.42 cm at 250 mg kg^{-1} and 21.08 cm at 350 mg kg^{-1}, a loss of 42.0% across the range, and the three rates differed significantly at every sampling date. Leaf number (10.25 versus 6.50), shoot fresh weight (17.33 versus 10.33 g), root dry weight (3.70 versus 2.26 g) and root length (16.25 versus 9.92 cm) followed the same direction, with reductions of 37–40% between the lowest and highest rate (Table 2). Stem girth was the least responsive trait. Cd affected it at 2 and 8 WAP only, and the difference at 8 WAP was confined to the highest rate (1.92 cm, against 2.60 and 2.38 cm at the two lower rates).

Compared with the untreated control, no treatment combination came close. From 4 WAP onwards the control was taller and carried more leaves than every Cd-treated combination. At 8 WAP the best combination (150 mg kg^{-1} Cd with 100 mg kg^{-1} ZnO NPs) was still 25.8% shorter than the control, carried about half as many leaves (12.50 against 23.50) and produced 29.3% less shoot fresh weight. The worst combination (350 mg kg^{-1} Cd with 200 mg kg^{-1} ZnO NPs) reached one-third of control height and 71% less shoot fresh weight (Table 2; Fig. 2).

Table 2

Growth and biomass of maize at 8 weeks after planting (WAP), by treatment combination

Treatment (mg kg^{-1})	Plant height (cm)	Leaves (no.)	Stem girth (cm)	Shoot fresh wt (g)	Root length (cm)	Root dry wt (g)
Control	60.00±3.74^{a}	23.50±3.00^{a}	5.83±0.45^{a}	33.25±11.35^{a}	26.50±4.04^{a}	6.58±2.36^{a}
Cd 150 + ZnO 100	44.50±6.56^{b}	12.50±4.04^{b}	2.80±0.70^{b}	23.50±7.90^{b}	20.00±4.08^{b}	4.68±2.30^{b}
Cd 150 + ZnO 150	31.75±3.86^{c}	10.25±4.99^{bc}	2.40±0.36^{bc}	14.75±2.22^{c}	14.75±1.26^{c}	3.58±0.95^{bc}
Cd 150 + ZnO 200	32.75±1.50^{c}	8.00±1.41^{cd}	2.60±0.36^{bc}	13.75±3.20^{c}	14.00±1.63^{cd}	2.85±0.73^{bc}
Cd 250 + ZnO 100	28.25±3.86^{cd}	7.25±1.50^{cd}	2.43±0.72^{bc}	13.25±3.10^{c}	12.25±1.89^{cde}	3.05±0.90^{bc}
Cd 250 + ZnO 150	24.00±4.32^{de}	6.50±1.29^{cd}	2.28±0.43^{bc}	12.25±1.26^{c}	11.25±2.63^{cde}	3.08±0.72^{bc}
Cd 250 + ZnO 200	24.00±4.62^{de}	5.75±0.96^{d}	2.43±0.26^{bc}	12.00±2.31^{c}	11.50±1.91^{cde}	2.63±0.35^{c}
Cd 350 + ZnO 100	22.25±5.06^{de}	7.00±1.41^{cd}	2.05±0.26^{bc}	11.25±2.63^{c}	10.25±2.06^{de}	2.23±0.86^{c}
Cd 350 + ZnO 150	21.00±1.15^{e}	6.75±0.96^{cd}	1.83±0.65^{c}	10.25±0.50^{c}	10.00±0.82^{e}	2.20±0.26^{c}
Cd 350 + ZnO 200	20.00±2.45^{e}	5.75±0.96^{d}	1.88±0.53^{c}	9.50±1.00^{c}	9.50±1.73^{e}	2.35±0.35^{c}

Values are means ± SD of four replicate pots. Means in a column sharing a letter do not differ at $P \leq 0.05$ (Duncan's multiple range test). Treatments are Cd rate + ZnO NP rate in mg kg^{-1}.

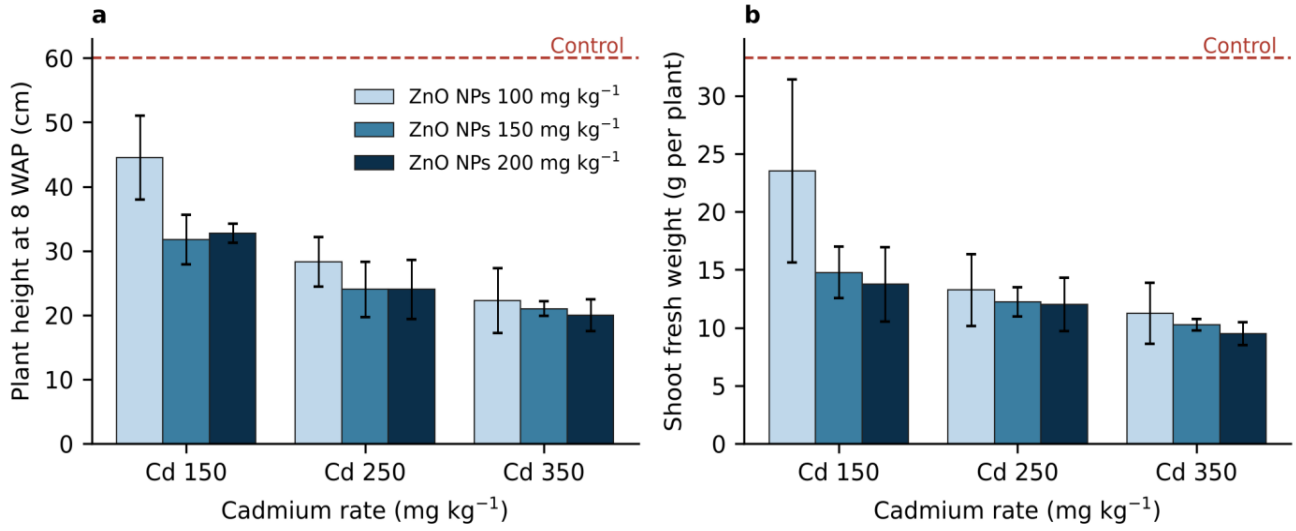


Figure 2

Growth of maize at 8 WAP under three Cd rates and three ZnO NP rates. ***a****, Plant height.* ***b****, Shoot fresh weight. Bars show means and error bars show SD (four replicate pots); the dashed line marks the untreated control mean. ZnO NP rate is given in mg* kg^{-1}.

These results agree with the established view that Cd restricts maize growth in step with the amount present in the root zone. The root is the first organ to meet Cd, and Cd slows root elongation and alters root anatomy (Lux et al., 2011). A shorter, damaged root system would supply the shoot with less water and fewer nutrients, which is a plausible route to the reduced height and leaf production we observed, although we did not measure water or nutrient status.

Nanoparticle Rate did not Restore Growth, and the Lowest Rate did Best

If ZnO NPs protected maize from Cd, growth should have risen with the nanoparticle rate. It did not. Among ZnO-treated plants, 100 mg kg^{-1} produced the tallest plants at 2, 6 and 8 WAP (31.67 cm at 8 WAP) and the longest roots (14.17 cm), whereas 150 and 200 mg kg^{-1} did not differ from each other (25.58 cm in both cases for height; 12.00 and 11.67 cm for root length). The nanoparticle rate had no significant effect on leaf number, stem girth or any fresh or dry weight, although leaf number fell steadily from 8.92 to 7.83 to 6.50 as the rate rose. The Cd × ZnO interaction for height was significant only at 2 WAP, when the two lowest-Cd combinations with 100 and 200 mg kg^{-1} ZnO NPs were tallest. It had vanished by 4 WAP, which suggests that any early benefit was overtaken by the cumulative effect of Cd.

This pattern differs from published reports in which ZnO NPs improved the growth of Cd-stressed plants (Hussain et al., 2018; Hussain et al., 2024; Rizwan et al., 2019a; Zhang et al., 2019). The contrast needs careful reading. Those studies compared ZnO-treated plants with plants exposed to Cd alone, and the maize studies applied the nanoparticles to leaves at 25–100 mg L^{-1}, so the root zone never received a large dose. We mixed the whole dose into the soil, and we did not analyse Cd-only pots. Our data therefore cannot show whether ZnO NPs improved growth relative to no nanoparticles. They show something narrower: no rate restored growth to control levels, and rates above 100 mg kg^{-1} were associated with poorer height and root length than the lowest rate.

A direct toxic effect of the nanoparticles is one explanation. Lin and Xing (2007) found that ZnO NPs at 2,000 mg L^{-1} almost stopped root elongation in several species, maize among them, although the exposure was in suspension and the concentrations are not comparable with ours in soil. In an acidic soil, dissolution of ZnO would release Zn^{2+} quickly, and the two higher rates may have supplied more Zn than the plants could tolerate. We did not measure Zn in soil or tissue, so this explanation remains untested.

The Effect on Tissue Cd Depends on Contamination Level

Cd concentrations in roots, shoots and soil rose significantly with Cd rate ($P < 0.01$ in each case). Root Cd increased from 16.72 mg kg^{-1} at 150 mg kg^{-1} Cd to 37.43 mg kg^{-1} at 350 mg kg^{-1}, a factor of 2.2, and shoot Cd rose from 9.42 to 18.86 mg kg^{-1}. This is the expected dose response, as reported for Cd accumulation in maize by Wang et al. (2007). Concentrations followed the order soil > root > shoot in every treatment.

The nanoparticle effect was not uniform, and the significant Cd × ZnO interaction ($P < 0.01$) shows that it depended on Cd rate (Table 3; Fig. 3). At 150 mg kg^{-1} Cd, root Cd fell from 20.90 to 16.41 to 12.86 mg kg^{-1}, and shoot Cd from 12.69 to 9.34 to 6.24 mg kg^{-1}, as the ZnO NP rate increased from 100 to 150 to 200 mg kg^{-1}. The shoot value at 200 mg kg^{-1} was 50.8% lower than at 100 mg kg^{-1} and was the lowest recorded in the experiment, statistically similar to the control. The result matches the reductions in wheat tissues described by Hussain et al. (2018) and the Zn–Cd antagonism reported for rice by Cai et al. (2019), who attributed lower Cd to competition between the two metals and to dilution through greater biomass.

Table 3

Cadmium concentrations (mg kg^{-1}), bioconcentration factor (BCF) and translocation factor (TF), by treatment combination

Treatment (mg kg^{-1})	Root Cd	Shoot Cd	Soil Cd	BCF	TF
Control	15.96±2.57^{e}	7.63±1.27^{fg}	31.80±5.06^{e}	0.502±0.002	0.479±0.030^{cd}
Cd 150 + ZnO 100	20.90±1.76^{d}	12.69±2.08^{cd}	41.80±2.80^{d}	0.500±0.010	0.607±0.080^{ab}
Cd 150 + ZnO 150	16.41±3.04^{e}	9.34±2.27^{ef}	32.18±5.85^{e}	0.511±0.045	0.566±0.051^{bc}
Cd 150 + ZnO 200	12.86±2.14^{e}	6.24±0.80^{g}	25.69±3.36^{e}	0.499±0.030	0.489±0.048^{cd}
Cd 250 + ZnO 100	15.42±2.41^{e}	10.37±2.75^{def}	30.91±4.58^{e}	0.499±0.011	0.664±0.086^{a}
Cd 250 + ZnO 150	20.62±1.97^{d}	11.66±1.70^{de}	41.72±4.20^{d}	0.494±0.007	0.565±0.058^{bc}
Cd 250 + ZnO 200	28.16±1.57^{c}	15.38±2.25^{bc}	56.43±3.32^{c}	0.499±0.005	0.544±0.053^{bc}
Cd 350 + ZnO 100	21.26±2.37^{d}	10.91±1.24^{de}	42.19±5.16^{d}	0.505±0.008	0.514±0.043^{cd}
Cd 350 + ZnO 150	54.65±2.35^{a}	29.09±1.13^{a}	106.65±5.24^{a}	0.513±0.024	0.533±0.028^{bcd}
Cd 350 + ZnO 200	36.38±4.27^{b}	16.59±2.60^{b}	72.19±8.66^{b}	0.504±0.007	0.455±0.032^{d}

Values are means ± SD of four replicate pots. Means in a column sharing a letter do not differ at $P \leq 0.05$ (Duncan's multiple range test); BCF did not differ among treatments. Cd × ZnO interaction: $P < 0.01$ for root, shoot and soil Cd. Root and shoot Cd on a dry-weight basis.

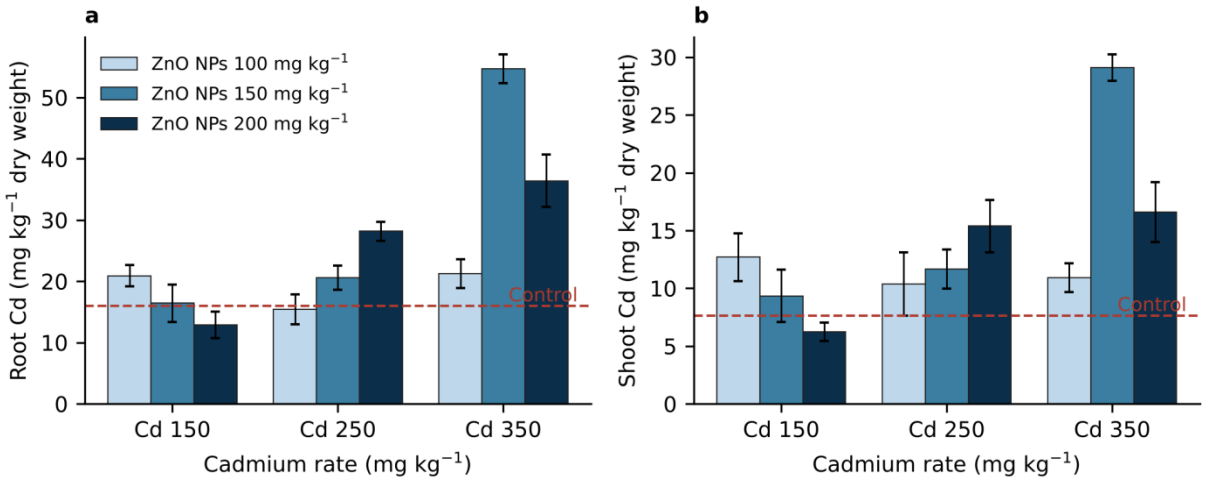


Figure 3

*Cadmium concentration in maize tissue at 8 WAP. **a**, Root Cd. **b**, Shoot Cd. Bars show means and error bars show SD (four replicate pots); the dashed line marks the untreated control mean. The Cd × ZnO NP interaction was significant ($P < 0.01$). Note that the control was not Cd-free in the measurements (see text).*

At the higher Cd rates, the response reversed. At 250 mg kg^{-1} Cd, root Cd rose from 15.42 to 28.16 mg kg^{-1} (+82.6%) and shoot Cd from 10.37 to 15.38 mg kg^{-1} (+48.3%) as ZnO NPs went from 100 to 200 mg kg^{-1}. At 350 mg kg^{-1} Cd, the 150 mg kg^{-1} nanoparticle rate produced the highest concentrations of the whole study, 54.65 mg kg^{-1} in roots and 29.09 mg kg^{-1} in shoots, which were 157% and 167% above the values at 100 mg kg^{-1}. These results do not support a general protective role for soil-applied ZnO NPs. They fit the conclusion of Rizwan et al. (2019b) that the outcome of Zn supply under Cd stress is inconsistent and conditional, and they parallel the finding of Zhang et al. (2019) that high ZnO NP doses raised bioavailable Cd in the rhizosphere of rice and, in a lightly contaminated soil, raised rice Cd above the Chinese limit of 0.2 mg kg^{-1}.

We think the following account is the most economical, and we offer it as a hypothesis. Where Cd is relatively scarce, competition between Zn^{2+} and Cd^{2+} at the root surface dominates, and more Zn means less Cd entering the plant. Where Cd is abundant, Zn^{2+} released from the nanoparticles may displace Cd from the exchange sites of a soil that has few base cations and little clay, moving Cd into solution faster than the plant's uptake machinery is blocked. Kubier et al. (2019) list competition-induced desorption as one route by which Cd is mobilised in soils. Soil pH, available Cd and available Zn were not measured after the nanoparticles were added, so the mechanism awaits direct testing.

Cd is Retained in Roots, and the Highest ZnO Rate Retains More

The bioconcentration factor (BCF; root Cd divided by soil Cd) was essentially constant, between 0.494 and 0.513 in all treatments, and did not respond to Cd rate, nanoparticle rate or their interaction. The translocation factor (TF; shoot Cd divided by root Cd) was below 1 everywhere, from 0.455 to 0.664, so roots held more of the absorbed Cd than shoots did. Under the criteria of Yoon et al. (2006), who defined BCF as the ratio of root to soil concentration and TF as the ratio of shoot to root concentration, maize in this experiment qualifies neither for phytoextraction nor for phytostabilisation, both of which, on those criteria, require a BCF above 1. The retention of Cd in roots is consistent with the barrier function of the root endodermis and exodermis, which restricts movement of Cd towards the xylem (Lux et al., 2011).

The TF was significantly lower at 200 mg kg^{-1} ZnO NPs (0.496) than at 100 mg kg^{-1} (0.595) or 150 mg kg^{-1} (0.555), and it was lowest at the 200 mg kg^{-1} rate within each Cd level. It was also lower at

the highest Cd rate (0.501) than at the two lower rates (0.554 and 0.591). Taken at face value, a large Zn supply reduced the share of absorbed Cd that reached the shoot, even in pots where total tissue Cd was higher. That is the one nanoparticle effect observed at every Cd rate, and for food safety it is the most useful. It runs against Cai et al. (2019), who found in rice that high Zn activity increased Cd transfer from root to shoot, so the effect appears to depend on species, genotype or Zn status, as those authors suggest. The direction of the TF response also needs caution in its own right: the differences were modest (0.455 to 0.664) and the TF of the control did not differ significantly from most treated combinations.

Plant Cd Tracks Growth Loss, but Only Moderately

Across the control and the nine treatment combinations (n = 40 pots), all growth and biomass traits were strongly and positively correlated with one another (r = 0.692 to 0.966), which indicates that the treatments affected the plants as a whole and not single traits. Shoot Cd correlated negatively and significantly with all eight growth and biomass traits, the strongest with plant height (r = −0.469), stem girth (r = −0.460) and root length (r = −0.428). Root Cd was significantly and negatively correlated with seven of the eight traits; its correlation with shoot dry weight (r = −0.297) was not significant. Root, shoot and soil Cd were closely related (r = 0.966 to 0.997), whereas BCF and TF were unrelated to any growth trait (r from −0.268 to 0.209).

These coefficients confirm that more Cd in the plant went with less growth. They are also moderate. An r of −0.47 means that tissue Cd accounts for about 22% of the variation in plant height. The remainder reflects the dose of Cd in the pot, the nanoparticle rate and plant-to-plant variation, and the absence of any link between TF and growth shows that how Cd was divided between root and shoot mattered little to growth over eight weeks.

Conclusion and Recommendation

Conclusion

In a strongly acidic, coarse-textured soil, Cd reduced the growth and biomass of maize in proportion to the rate applied, and soil-applied ZnO NPs did not restore growth to the level of the control at any rate tested. The lowest nanoparticle rate (100 mg kg^{-1}) supported taller plants and longer roots than 150 or 200 mg kg^{-1}.

The effect of ZnO NPs on tissue Cd depended on the level of contamination. Only at 150 mg kg^{-1} Cd did raising the nanoparticle rate lower root and shoot Cd, and at 200 mg kg^{-1} it halved shoot Cd relative to 100 mg kg^{-1}. At 250 and 350 mg kg^{-1} Cd, higher nanoparticle rates did not lower Cd uptake and in several cases raised it. Soil-applied ZnO NPs are therefore not a dependable means of limiting Cd uptake by maize across the range of contamination studied. Maize retained most absorbed Cd in its roots (TF below 1 throughout), and the 200 mg kg^{-1} rate lowered the translocation factor at every Cd level. At the lowest Cd level, the rate that gave the least shoot Cd was not the rate that gave the best growth.

Recommendations

1. Soils suspected of Cd contamination, such as those that have received industrial effluent or waste, should be tested before maize is grown on them. Cd reduced growth and accumulated in shoots at every contamination level examined here.
2. Where ZnO NPs are applied to acidic sandy soil contaminated with Cd, the rate should not exceed 100 mg kg^{-1} if the aim is to support growth, because 150 and 200 mg kg^{-1} gave shorter plants with shorter roots.

3. Where contamination is at the lowest level tested (150 mg kg^{-1} Cd) and the priority is a lower shoot Cd, ZnO NPs at 200 mg kg^{-1} may be considered, since this rate halved shoot Cd relative to 100 mg kg^{-1}. The user should expect a growth penalty (plants about 26% shorter at 8 WAP than at 100 mg kg^{-1}) and should confirm grain Cd before any produce is used for food or feed.
4. ZnO NPs should not be relied on as the only remediation measure for soils at or above 250 mg kg^{-1} Cd, because they did not lower, and in places raised, Cd uptake at these levels. Such soils should not be used to grow maize for food or feed until they have been remediated.
5. Future trials should include Cd-only and ZnO-only controls, measure soil pH and available Cd and Zn after nanoparticle application, test Cd rates closer to those found on farmland, and report grain Cd. These additions address the main gaps identified in this study.

Conflict of Interest

The authors declare that they have no conflict of interest regarding this article.

References

Bouyoucos, G. J. (1962). Hydrometer method improved for making particle size analyses of soils. *Agronomy Journal, 54*(5), 464–465. https://doi.org/10.2134/agronj1962.00021962005400050028x

Bray, R. H., & Kurtz, L. T. (1945). Determination of total, organic, and available forms of phosphorus in soils. *Soil Science, 59*(1), 39–45. https://doi.org/10.1097/00010694-194501000-00006

Bremner, J. M., & Mulvaney, C. S. (1982). Nitrogen—Total. In A. L. Page, R. H. Miller, & D. R. Keeney (Eds.), *Methods of soil analysis: Part 2. Chemical and microbiological properties* (2nd ed., pp. 595–624). American Society of Agronomy; Soil Science Society of America. https://doi.org/10.2134/agronmonogr9.2.2ed.c31

Cai, Y., Xu, W., Wang, M., Chen, W., Li, X., Li, Y., & Cai, Y. (2019). Mechanisms and uncertainties of Zn supply on regulating rice Cd uptake. *Environmental Pollution, 253*, 959–965. https://doi.org/10.1016/j.envpol.2019.07.077

Hou, D., Jia, X., Wang, L., McGrath, S. P., Zhu, Y.-G., Hu, Q., Zhao, F.-J., Bank, M. S., O'Connor, D., & Nriagu, J. (2025). Global soil pollution by toxic metals threatens agriculture and human health. *Science, 388*(6744), 316–321. https://doi.org/10.1126/science.adr5214

Hussain, A., Ali, S., Rizwan, M., Zia ur Rehman, M., Javed, M. R., Imran, M., Chatha, S. A. S., & Nazir, R. (2018). Zinc oxide nanoparticles alter the wheat physiological response and reduce the cadmium uptake by plants. *Environmental Pollution, 242*(Part B), 1518–1526. https://doi.org/10.1016/j.envpol.2018.08.036

Hussain, M., Kaousar, R., Haq, S. I. U., Shan, C., Wang, G., Rafique, N., Shizhou, W., & Lan, Y. (2024). Zinc-oxide nanoparticles ameliorated the phytotoxic hazards of cadmium toxicity in maize plants by regulating primary metabolites and antioxidants activity. *Frontiers in Plant Science, 15*, Article 1346427. https://doi.org/10.3389/fpls.2024.1346427

International Agency for Research on Cancer. (2012). *Arsenic, metals, fibres, and dusts* (IARC Monographs on the Evaluation of Carcinogenic Risks to Humans, Vol. 100C). World Health Organization.

Isaac, G. C. (2026). *Effect of zinc oxide nanoparticles on cadmium uptake by maize plants (Zea mays* L.*) under different levels of cadmium contamination* [Bachelor's dissertation, University of Port Harcourt].

Kubier, A., Wilkin, R. T., & Pichler, T. (2019). Cadmium in soils and groundwater: A review. *Applied Geochemistry, 108*, Article 104388. https://doi.org/10.1016/j.apgeochem.2019.104388

Lin, D., & Xing, B. (2007). Phytotoxicity of nanoparticles: Inhibition of seed germination and root growth. *Environmental Pollution, 150*(2), 243–250. https://doi.org/10.1016/j.envpol.2007.01.016

Lux, A., Martinka, M., Vaculík, M., & White, P. J. (2011). Root responses to cadmium in the rhizosphere: A review. *Journal of Experimental Botany, 62*(1), 21–37. https://doi.org/10.1093/jxb/erq281

Murphy, J., & Riley, J. P. (1962). A modified single solution method for the determination of phosphate in natural waters. *Analytica Chimica Acta, 27*, 31–36. https://doi.org/10.1016/S0003-2670(00)88444-5

Rizwan, M., Ali, S., Zia ur Rehman, M., Adrees, M., Arshad, M., Qayyum, M. F., Ali, L., Hussain, A., Chatha, S. A. S., & Imran, M. (2019a). Alleviation of cadmium accumulation in maize (*Zea mays* L.) by foliar spray of zinc oxide nanoparticles and biochar to contaminated soil. *Environmental Pollution, 248*, 358–367. https://doi.org/10.1016/j.envpol.2019.02.031

Rizwan, M., Ali, S., Zia ur Rehman, M., & Maqbool, A. (2019b). A critical review on the effects of zinc at toxic levels of cadmium in plants. *Environmental Science and Pollution Research, 26*(7), 6279–6289. https://doi.org/10.1007/s11356-019-04174-6

Walkley, A., & Black, I. A. (1934). An examination of the Degtjareff method for determining soil organic matter, and a proposed modification of the chromic acid titration method. *Soil Science, 37*(1), 29–38. https://doi.org/10.1097/00010694-193401000-00003

Wang, M., Zou, J., Duan, X., Jiang, W., & Liu, D. (2007). Cadmium accumulation and its effects on metal uptake in maize (*Zea mays* L.). *Bioresource Technology, 98*(1), 82–88. https://doi.org/10.1016/j.biortech.2005.11.028

Yoon, J., Cao, X., Zhou, Q., & Ma, L. Q. (2006). Accumulation of Pb, Cu, and Zn in native plants growing on a contaminated Florida site. *Science of the Total Environment, 368*(2–3), 456–464. https://doi.org/10.1016/j.scitotenv.2006.01.016

Zha, Y., Zhao, B., & Niu, T. (2022). Bamboo biochar and zinc oxide nanoparticles improved the growth of maize (*Zea mays* L.) and decreased cadmium uptake in Cd-contaminated soil. *Agriculture, 12*(9), Article 1507. https://doi.org/10.3390/agriculture12091507

Zhang, W., Long, J., Li, J., Zhang, M., Xiao, G., Ye, X., Chang, W., & Zeng, H. (2019). Impact of ZnO nanoparticles on Cd toxicity and bioaccumulation in rice (*Oryza sativa* L.). *Environmental Science and Pollution Research, 26*(22), 23119–23128. https://doi.org/10.1007/s11356-019-05551-x

NATURE & SCIENCE
October 2026, Volume 8, Issue 5, pp. 89–96
DOI: https://doi.org/10.36719/2707-1146/68/89-96

Integrated Biophysical Assessment of the Effect of Zinc Oxide Nanoparticles on the Photosynthetic Apparatus of Spinach (*Spinacia oleracea* L.)

Ramig Mammadzada[1*], Ismat Ahmadov[2], Farayat Ahmadova[3], Ziyaddin Mammadov[3], and Yashar Feyziyev[4]

Abstract. *Zinc oxide nanoparticles have been reported as the most common nanostructured materials in agricultural areas and, recently, researchers found that the concentration of zinc oxide nanoparticles in the soils and air is growing, causing concerns in society regarding their possible effects on plant photosynthesis. This study used an integrated biophysical approach that incorporated three different techniques to assess the short-term effect of zinc oxide nanoparticles on the photobiochemical apparatus of spinach (Spinacia oleracea L.): (i) delayed luminescence measurements of isolated thylakoid membranes to determine Photosystem II charge recombination, (ii) Clark-type oxygen electrode measurements for the determination of photosynthetic oxygen evolution from isolated chloroplasts, and (iii) UV-Vis spectrophotometric analysis of acetone-extracted chlorophyll pigments exposed to red, blue, and white LED light for photostability assessment. Zinc oxide nanoparticles treated samples displayed a gradual decrease in the levels of delayed luminescence over 60 min of dark incubation, while control samples remained quite unchanged, implying disturbed charge recombination in P_{680}^{+}/Q_A^{-} pair of PSII (reaction center). It was observed that photosynthetic oxygen production gradually declined in both the control and the treated chloroplast samples, yet the initially high rates were retained in the latter. UV-Vis spectrophotometric analysis of the extracted chlorophyll pigments showed a faster decrease in the main chlorophyll absorption peaks at 437 nm (Soret) and 668 nm (Qy) in ZnO-treated samples, an effect that was most evident under white light.*

Keywords: *environmental nanotoxicology, ZnO nanoparticles, Photosystem II, thylakoid membranes, electron transport, photobleaching, chlorophyll degradation*

[1]Institute of Molecular Biology, Ministry of Science and Education of the Republic of Azerbaijan, MS in Biology, Baku, Azerbaijan
[2]Baku State University, PhD in Biology, Baku, Azerbaijan
[3]Baku State University, DS in Biology, Baku, Azerbaijan
[4]Institute of Molecular Biology, Ministry of Science and Education of the Republic of Azerbaijan, DS in Biology, Baku, Azerbaijan
[*]Corresponding author. E-mail: ramigmammadzada7@gmail.com
Received: 21 April 2026; Accepted: 14 September 2026; Published online: 25 October 2026
© The Author(s) 2026. This is an open access article distributed under the terms of the Creative Commons Attribution-NonCommercial 4.0 International License (CC BY-NC 4.0).

Introduction

Well known that nanoparticles due to smaller sizes interact strongly with biological systems, they have found broad use in agriculture (Mgadi et al., 2024), plant physiology (Singh et al., 2024), biotechnology processes (Vinukonda et al., 2025), medical practices (Haleem et al., 2023), diagnostics, drug delivery (Paluszkiewicz et al., 2021) and therapeutic applications (Yetisgin et al., 2020). Agriculture is the leading segment among industries trying out this potential: using tiny particles for delivery of agrochemicals only in the needed area and at the right time, minimizing losses caused by leaching, drift, hydrolysis, photolysis, and microbial degradation of conventional pesticides and fertilizers, while nanosensors and slow-release nanofertilizers help reduce pollution by better input management (Jainendra et al., 2024). This increased use of engineered nanomaterials has turned zinc oxide nanoparticles (ZnO NPs) into a top-produced, nanostructured material thanks to their catalytic, antimicrobial, and UV-absorbing properties for the agriculture, cosmetics, and consumer goods sectors.

Nevertheless, these very qualities that make ZnO NPs highly useful for farmers have also been the reasons for environmental and human health concerns when they were released. For instance, exposure to high concentrations of ZnO nanoparticles has been reported to significantly suppress seedlings emergence and root development in ryegrass and a subsequent study on the same species found that ZnO NP exposure reduced biomass and caused severe root damage, with root cells becoming highly vacuolated or collapsed, while most nanoparticles remained adhered to the root surface and translocation of free zinc ions to shoots stayed minimal (Rehman et al., 2023). Beyond the root system, ZnO NPs have also been reported to reduce photosynthetic efficiency by disturbing electron transport, altering membrane integrity, and inducing oxidative stress (Chen et al., 2024).

Despite this evidence, most existing studies characterize ZnO NP phytotoxicity at a single organizational level whole-plant biomass, root morphology, or bulk photosynthetic efficiency without resolving which step of the photosynthetic process is primarily affected, or whether ZnO NPs act mainly at the level of Photosystem II (PSII) reaction-center photochemistry, the downstream electron-transport and water-splitting machinery, or the chlorophyll pigment pool itself (Dang et al., 2024). Addressing this gap requires techniques that can isolate and probe each step individually, since PSII, embedded in the thylakoid membrane, depends on a finely tuned sequence of light-driven charge separations, electron transfers, and water-splitting reactions that make it one of the most sensitive targets of nanoparticle-induced stress (Wang et al., 2016).

Three complementary biophysical techniques can meet this need. Delayed luminescence (DL) arises from the recombination of charges separated during PSII photochemistry, providing a sensitive, non-destructive readout of PSII reaction-center function. Oxygen evolution, measured polarographically with a Clark-type electrode, gives a direct measure of PSII's water-splitting and electron-transport capacity, especially with an artificial acceptor such as DCBQ. The absorption spectrum of extracted chlorophyll, with its Soret band near 430–440 nm and Qy band near 660–670 nm, reflects pigment integrity, and its light-dependent decay indexes photo-oxidative degradation.

The present study therefore combines these three approaches to determine how short-term ZnO NP exposure affects the photosynthetic apparatus of spinach (*Spinacia oleracea* L.) at three organizational levels isolated thylakoid membranes, intact chloroplasts, and the free pigment pool under different light qualities asking whether ZnO NPs primarily disturb PSII photochemistry, the electron-transport chain, the pigment pool, or all three simultaneously, and whether this depends on light exposure.

Materials and Methods

Plant Material and ZnO Nanoparticle Suspension

Fresh leaves of spinach *(Spinacia oleracea L.)* were used as the source of thylakoid membranes, chloroplasts, and pigment extracts in all three experiments. Zinc oxide nanoparticles (99.8% purity, 10–30 nm particle size, SkySpring Nanomaterials, Inc.) were used throughout. In each experiment, a ZnO stock suspension was freshly prepared by dispersing 10 mg of ZnO powder in 100 mL of distilled water, followed by ultrasonic sonication (15–20 min) to ensure homogeneous dispersion of the particles before further dilution into the respective assay mixtures.

Oxygen Evolution of Isolated Chloroplasts

Photosynthetic oxygen evolution was measured polarographically using a Clark-type oxygen electrode. 2,6-dichloro-p-benzoquinone (DCBQ) was used as an artificial electron acceptor to assess the efficiency of electron transport independently of downstream (Calvin cycle) limitations. The ZnO-treated reaction mixture consisted of 7.0 mL HEPES buffer (pH 7.0), 70 µL of chloroplast suspension, and 700 µL of the ZnO nanoparticle suspension (100 µg/mL stock), giving a total volume of approximately 7.77 mL and a final ZnO concentration of approximately 9 µg/mL. The control mixture consisted of 5 mL HEPES buffer (pH 7.0) and 50 µL of chloroplast suspension, with no ZnO added. Both mixtures were kept in the dark on ice throughout the incubation period to minimize uncontrolled photochemical or thermal degradation.

At each time point, a 1 mL aliquot was withdrawn from the incubation mixture. Before each measurement, 5 µL of DCBQ was pipetted into the sample; the oxygen evolution was measured by a Clark electrode approximately 20 seconds after this step. The control group was exposed to four time points of measurements (0, 30, 60, and 90 min), while the ZnO-treated group was subjected to six of them (0, 15, 30, 45, 60, and 90 min). Time series obtained from the electrode response were digitized and converted with respect to the time elapsed to analyze the pattern of oxygen production over time.

Delayed Luminescence of Isolated Thylakoid Membranes

Isolated spinach thylakoid membranes were used as the biological material. Two reaction mixtures were prepared in MES buffer (25 mM, pH 6.5): a control mixture consisting of 10 mL buffer containing only the thylakoid membranes, and a treatment mixture consisting of 9 mL buffer plus 1 mL of the ZnO nanoparticle suspension. Two corresponding stock samples were prepared in parallel one containing 30 µL of thylakoid suspension alone (control stock) and one containing 30 µL of thylakoid suspension plus 3 µL of the ZnO suspension. The latter corresponded to a final ZnO concentration of 9.09 mg/L in the treatment sample.

For each measurement, 4 µL of the appropriate stock was placed quartz cuvette and combined with 2 mL of buffer. The sample was kept in the dark for approximately 3 minutes to allow thermal relaxation and to minimize photooxidative processes before recording. Delayed luminescence was then excited with a high-intensity light pulse (1100 units, ~2s) and recorded with a chart-recorder DL apparatus. Measurements were performed at 0, 30, and 60 minutes of incubation for both the control and the ZnO-treated samples, all under dark, ice-cold conditions to minimize spontaneous photooxidative degradation during the incubation period.

Chlorophyll Pigment Extraction and Light-Dependent UV-Vis Absorption Spectroscopy

A ZnO nanoparticle suspension was prepared by dispersing 10 mg of ZnO powder in 100 mL of distilled water and homogenizing the mixture for 15 minutes in an ultrasonic sonicator. The photosynthetic pigment extract was obtained by homogenizing 1 g of fresh spinach leaves in 100 mL of 95% acetone. Homogenization was carried out by mixing it thoroughly and then it was centrifuged at 15, 000 rpm for five minutes keeping the sample at 4 ºC. After that, only the supernatant was used for carrying out the experiments.

To prepare the ZnO-treated samples, 7 mL of the ZnO suspension was added to 35 mL of pigment extract to obtain a homogeneous mixture; control samples consisted solely of the pigment extract. For spectrophotometric analysis, 1 mL aliquots of both the control and ZnO-treated samples were mixed with 2 mL of 95% acetone. Absorption spectra were recorded on a Shimadzu UV-1280 UV-Visible spectrophotometer over the wavelength range of 350–750 nm.

Samples were incubated under white, red, and blue LED light sources at an intensity of 50 µmol $m^{-2}s^{-1}$, and UV-Vis absorption spectra were recorded at successive incubation intervals for both control and ZnO-treated extracts under each of the three light qualities. This design allowed the rate of light-driven chlorophyll pigment degradation to be compared between untreated extracts and extracts exposed to ZnO nanoparticles, separately for red, blue, and white illumination.

Results

ZnO Nanoparticles Accelerate Light-Dependent Bleaching of Extracted Chlorophyll

It is well known that light plays a powerful modulator role in the synthesis of nanoparticles, significantly influencing their morphological and functional properties (Rasulzadeh & Ramazanli, 2025). The absorption spectra of the acetone-extracted pigment fraction showed the two characteristic chlorophyll bands expected for this extraction method: a blue-region (Soret) band near 430–440 nm and a red-region (Q_y) band near 660–670 nm, the latter serving as the principal diagnostic peak for chlorophyll a integrity. Under all three light qualities tested (red, blue, and white LED, 50 µmol m^{-2} s^{-1}), both the control and the ZnO-treated pigment extracts showed a progressive decline in the height of these bands with increasing illumination time, consistent with light-driven bleaching of chlorophyll during incubation. However, the rate of this decline was consistently greater in the ZnO-treated extracts.

Table 1

Chlorophyll Q_y absorption peak (~668 nm) of control and ZnO-treated pigment extracts under red, blue, and white light illumination (0, 30, and 60 min of incubation)

Light group / Time, min.	Red, control	Red, ZnO	Blue, control	Blue, ZnO	White, control	White, ZnO
0 min	0.920	0.869	0.962	0.945	0.633	0.492
30 min	0.717	0.471	0.701	0.535	0.479	0.281
60 min	0.492	0.299	0.532	0.415	0.348	0.187
Decline at 60 min	46.5%	65.6%	44.7%	56.1%	45.0%	62.0%

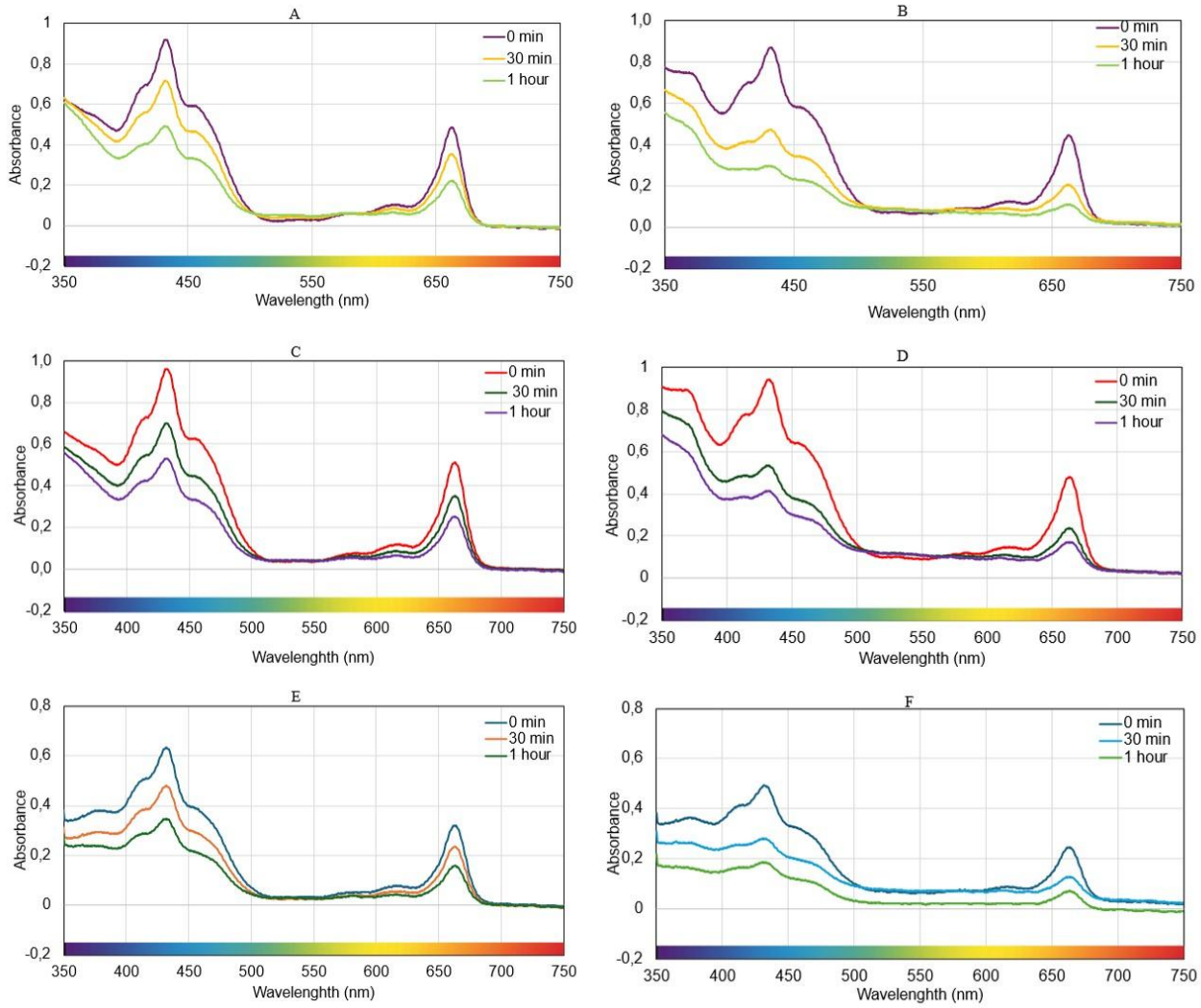


Figure 1

Absorption spectra (350–750 nm) of acetone-extracted chlorophyll, exposed to red, blue, and white LED illumination (50 µmol m^{-2} s^{-1}), for control extracts (A, C, E) and ZnO-treated extracts (B, D, F), recorded at 0 min, 30 min, and 1 hour

Under red light, the Q_y peak of the control extract declined 46.5% over 60 minutes, while the ZnO-treated extract fell from declined 65.6% over the same period despite starting from a similar initial value, the ZnO-treated sample lost pigment absorbance markedly faster. A similar pattern was observed under blue light, where the control declined by 44.7% and the ZnO-treated extract by 56.1%, and under white light, where the control declined by 45.0% and the ZnO-treated extract by 62.0%. The corresponding Soret-band absorbance (~437 nm) followed the same trend in all three light conditions, confirming that the effect was not restricted to a single spectral feature but reflected an overall loss of intact chlorophyll in the extract. White-light illumination produced the most pronounced overall effect (Ramazanli, 2024): the ZnO-treated extract already showed a lower Qy absorbance than the control at the beginning (0.492 vs. 0.633), before any additional incubation time had elapsed, suggesting that under broad-spectrum white light the interaction between ZnO nanoparticles and chlorophyll begins essentially immediately upon mixing, rather than developing gradually as observed under monochromatic red or blue light. By 60 minutes of white-light exposure, the ZnO-treated extract retained only about 30% of the control's initial Qy absorbance, compared with roughly 55% retention in the control itself.

Oxygen Evolution Declines Gradually in Both Control and Zno-Treated Chloroplasts

Photosynthetic oxygen evolution, decreased over time in both the control and the ZnO-treated thylokoid preparations, but the two groups differed in their starting values and in the shape of the decline.

In the control group the amount of oxygen evolved over time was set as 100% at the beginning and then slowly decreased to 90.3% (after 60 and 90 min) that is a relative decrease of 9.7% compared with the period during the experiment. Similarly, in the ZnO-treated group, the oxygen production was considered as 100% at time zero, there was no change in the first 15 min but decreased later to 89.2% at 60 and 90 min, a relative decrease of 10.8% compared to the starting point.

Notably, the ZnO-treated samples maintained a higher absolute oxygen-evolution signal than the control at every measured time point. However, because the two groups started from different baseline activities, the absolute comparison cannot, by itself, be used to conclude that ZnO nanoparticles stimulated PSII activity; it more plausibly reflects batch-to-batch variability in thylokoid preparation combined with a genuine, but proportionally similar, time-dependent decline shared by both groups. The comparable relative rates of decline (9.7% vs. 10.8%) suggest that, at the ZnO concentration used here (approximately 9 µg/mL), electron transport through PSII was not severely disrupted, and that both groups predominantly reflect the natural loss of thylokoid activity with incubation time for example, gradual destabilization of the isolated thylokoid preparation, weakening of membrane integrity, or natural deactivation of enzyme systems outside the thylakoid rather than an acute ZnO-induced inhibition of electron transport. The absence of an additional, faster decline specific to the ZnO group also suggests that the nanoparticle concentration used was not high enough to induce severe oxidative stress in the chloroplast preparation under these short-term, dark, ice-cold conditions (Hsu et al., 2023).

Delayed Luminescence Diminishes Continually in ZnO-Treated Thylakoids

Thylakoid membranes of control plants gave almost the same delayed luminescence signal from 0 to 60 min dark incubation except that intensity even got a little higher (~7%). Such constant DL is an indication that isolation procedure, buffer system (MES) and incubation conditions (dark cold on ice) little change the functionality of the photosystem for the course of the experiment. Hence, any variations found in the group of ZnO can not be explained by deterioration of the thylakoid preparation only. On the other hand, thylakoid membranes exposed to ZnO nanoparticles had consistently lower levels of delayed luminescence (DL) at every time point than the controls, with the DL gradually declining during the incubation period.

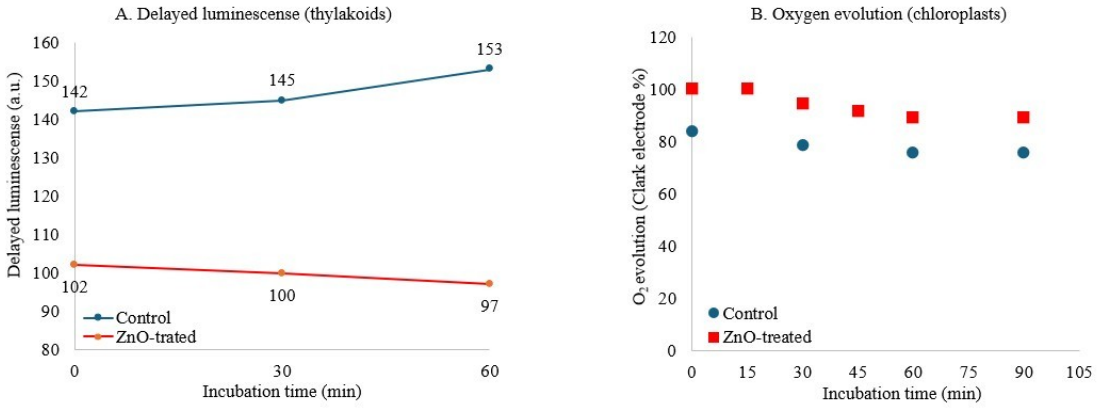


Figure 2

(A) Delayed luminescence of control and ZnO-treated spinach thylakoid membranes over 60 min of dark incubation. (B) Photosynthetic oxygen evolution of control and ZnO-treated isolated chloroplasts, measured with a Clark-type electrode

Relative to the control at the same time point, ZnO-treated samples showed a 28% lower DL amplitude at 0 min, a 31% lower amplitude at 30 min, and a 37% lower amplitude at 60 min a widening gap that indicates a progressive, rather than instantaneous, perturbation of PSII charge recombination by the nanoparticles. Because the experiment was conducted entirely in the dark and on ice, extensive light-driven reactive oxygen species (ROS) generation is unlikely to explain this decline; the pattern is more consistent with a direct physicochemical interaction between ZnO nanoparticles and the thylakoid membrane that develops over the incubation period.

Discussion

The three complementary assays revealed distinct mechanisms of ZnO nanoparticle–photosystem interaction. Delayed luminescence demonstrated gradual, dark-developing impairment of PSII charge recombination, indicating direct physicochemical interactions between nanoparticles and thylakoid membranes rather than light-driven reactive oxygen species (ROS) production. Similarly, these results are consistent with studies that had already explained the ZnO-induced suppression of the photosynthetic efficiency by electron transport and alterations of membrane integrity. But, when it comes to oxygen evolution the control and ZnO samples had similar decrease in relative rates (9.7% vs. 10.8%), indicating the electron transport capacity had not been severely affected by that concentration of ZnO.

This difference could very well explain why some methods can find the electron transport perturbation before it becomes obvious, such as through changes in bulk of the electron transport capacity. Chlorophyll absorption spectroscopy revealed a third mechanism: accelerated photo-oxidative bleaching under illumination. Zinc oxide nanoparticles have a well-documented photocatalytic activity that allows them to generate a significant amount of ROS under different light wavelengths, white. red, blue, and especially white light, thereby triggering the degradation of pigment molecules in unprotected form. The response of photosynthetic membranes to illumination was a major factor and far greater than under the dark condition, which indicates that the light availability is one of the crucial features for the plant toxicity due to ZnO nanoparticles. DL and photooxidation of water methods used different biological samples and buffer systems, so they did not allow for a fair quantitative comparison on this basis. Also, the assay for pigments made use of cell-free extracts hence it was not influenced by intact membrane protection effects or photoprotective mechanisms that are operational in planta.

Conclusion

This study demonstrates that ZnO nanoparticles perturb spinach photosynthesis through at least two distinguishable mechanisms: (1) light-independent impairment of PSII charge recombination, and (2) light-dependent acceleration of chlorophyll photo-oxidation. Delayed luminescence proved most sensitive for detecting subtle reaction-center perturbations, while oxygen-evolution measurements confirmed that bulk electron transport remains relatively intact at tested concentrations. These results show that delayed luminescence and pigment absorption spectroscopy are two powerful methods in complementing each other and allowing for non-invasive assessments of nanoparticle-photosystem interactions in plant systems. The results underline the necessity of including both dark and light conditions in the study of nanomaterial-related plant toxicity.

Declaration of Competing Interests

The authors declare that they have no known competing financial interests or personal relationships that could have appeared to influence the work reported in this paper.

References

Chen, H., Song, Y., Wang, Y., Wang, H., Ding, Z., & Fan, K. (2024). ZnO nanoparticles: Improving photosynthesis, shoot development, and phyllosphere microbiome composition in tea plants. *Journal of Nanobiotechnology, 22*(1), 389. https://doi.org/10.1186/s12951-024-02667-2

Dang, K., Wang, Y., Tian, H., Bai, J., Cheng, X., Guo, L., Zhang, Q., Geng, Y., & Shao, X. (2024). Impact of ZnO NPs on photosynthesis in rice leaves plants grown in saline-sodic soil. *Scientific Reports, 14*, 16233. https://doi.org/10.1038/s41598-024-66935-9

Haleem, A., Javaid, M., Singh, R. P., Rab, S., & Suman, R. (2023). Applications of nanotechnology in medical field: A brief review. *Global Health Journal, 7*(2), 70–77. https://doi.org/10.1016/j.glohj.2023.02.008

Hsu, C.-Y., Rheima, A. M., Kadhim, M. M., Ahmed, N. N., Mohammed, S. H., Abbas, F. H., Abed, Z. T., Mahdi, Z. M., Abbas, Z. S., Hachim, S. K., Ali, F. K., Mahmoud, Z. H., & Kianfar, E. (2023). An overview of nanoparticles in drug delivery: Properties and applications. *South African Journal of Chemical Engineering, 46*, 233–270. https://doi.org/10.1016/j.sajce.2023.08.009

Jainendra, P., Singh, D. K., Singh, P. R., Kumari, N., Jaiswal, J., Gupta, A., & Sinha, R. P. (2024). Application of nanoparticles in agriculture: Nano-based fertilizers, pesticides, herbicides, and nanobiosensors. In *Nanomaterial-plant interactions: Molecular impacts of nanoparticles on plants and algae* (pp. 305–331). Academic Press. https://doi.org/10.1016/B978-0-323-95721-2.00012-9

Mgadi, K., Ndaba, B., Roopnarain, A., Rama, H., & Adeleke, R. (2024). Nanoparticle applications in agriculture: Overview and response of plant-associated microorganisms. *Frontiers in Microbiology, 15*, 1354440. https://doi.org/10.3389/fmicb.2024.1354440

Paluszkiewicz, P., Martuszewski, A., Zareba, N., Wala, K., Banasik, M., & Kepinska, M. (2021). The application of nanoparticles in diagnosis and treatment of kidney diseases. *International Journal of Molecular Sciences, 23*(1), 131. https://doi.org/10.3390/ijms23010131

Rasulzadeh, F., & Ramazanli, V. (2025). Effect of white light on the biosynthesis of nanoparticles. *Nature & Science, 7*(5), 12–17. https://doi.org/10.36719/2707-1146/56/12-17

Rehman, F. ur, Paker, N. P., Khan, M., Zainab, N., Ali, N., Munis, M. F. H., Iftikhar, M., & Chaudhary, H. J. (2023). Assessment of application of ZnO nanoparticles on physiological profile, root architecture and antioxidant potential of *Solanum lycopersicum*. *Biocatalysis and Agricultural Biotechnology, 53*, 102874. https://doi.org/10.1016/j.bcab.2023.102874

Singh, D., Sharma, A., Verma, S. K., Pandey, H., & Pandey, M. (2024). Impact of nanoparticles on plant physiology, nutrition, and toxicity: A short review. *Next Nanotechnology, 6*, 100081. https://doi.org/10.1016/j.nxnano.2024.100081

Ramazanli, V. (2024). The effect of light on the synthesis of silver nanoparticles in biological systems. *Nature & Science, 6*(11), 34–40. https://doi.org/10.36719/2707-1146/50/34-40

Vinukonda, A., Bolledla, N., Jadi, R. K., Chinthala, R., & Devadasu, V. R. (2025). Synthesis of nanoparticles using advanced techniques. *Next Nanotechnology, 8*, 100169. https://doi.org/10.1016/j.nxnano.2025.100169

Wang, X., Yang, X., Chen, S., Li, Q., Wang, W., Hou, C., Gao, X., Wang, L., & Wang, S. (2016). Zinc oxide nanoparticles affect biomass accumulation and photosynthesis in *Arabidopsis*. *Frontiers in Plant Science, 6*, 1243. https://doi.org/10.3389/fpls.2015.01243

Yetisgin, A. A., Cetinel, S., Zuvin, M., Kosar, A., & Kutlu, O. (2020). Therapeutic nanoparticles and their targeted delivery applications. *Molecules, 25*(9), 2193. https://doi.org/10.3390/molecules25092193

NATURE & SCIENCE
October 2026, Volume 8, Issue 5, pp. 97–103
DOI: https://doi.org/10.36719/2707-1146/68/97-103

Ontogenetic Structure of a Cenopopulation of *Astragalus Cicer* L. in the Northeastern Lesser Caucasus

Sevil Babayeva[1], Gunay Nasibova[2*], and Shalala Huseynova[2]

Abstract. *The ontogenetic structure of Astragalus cicer* L. *(Fabaceae* Lindl.*) was studied in one natural cenopopulation in the northeastern Lesser Caucasus, near Asrik Jirdakhan village in the Tovuz district of Azerbaijan. Field observations were carried out in 2025 on a stony-gravelly slope at approximately 750–850 m above sea level. Thirty individuals were classified into six ontogenetic states on the basis of morphological characteristics and the development of vegetative and generative organs. The recorded numbers were juvenile, three (10.00%); immature, five (16.67%); virginal, six (20.00%); generative, twelve (40.00%); subsenile, three (10.00%); and senile, one (3.33%). The generative stage formed the maximum of the individual-stage ontogenetic spectrum. When grouped into broader developmental periods, pregenerative individuals accounted for 46.67%, generative individuals for 40.00%, and postgenerative individuals for 13.33%. The numerical ratio of pregenerative to generative individuals was 1.17. These findings provide a preliminary quantitative characterization of the studied cenopopulation. Because the observations concern a single site and survey year, repeated field studies are needed to assess population renewal and longer-term changes in ontogenetic composition.*

Keywords: *Astragalus cicer, cenopopulation, ontogenetic spectrum, Fabaceae, Lesser Caucasus*

Introduction

Studying the natural populations of plant species is of great importance for determining their distribution characteristics, developmental stages and current condition. One of the main characteristics of populations is their ontogenetic structure (Gatsuk et al., 1980; Barton et al., 2024). Ontogenetic structure reflects the proportions of individuals at different developmental stages within a population and helps assess the species' potential for renewal under natural conditions (Alahuhta et al., 2021; Gascoigne et al., 2023).

The genus *Astragalus* L., belonging to the family *Fabaceae*, is distinguished by its numerous species and adaptation to diverse ecological conditions. Representatives of this genus occur in various botanical-geographical regions of Azerbaijan and contribute to the formation of natural vegetation. Investigating the morphological, ecological and phytocoenological characteristics of Astragalus species is important for studying the condition of their natural populations (Asgarov, 2016; Gurbanov, 2024; Nasibova, 2025; Govaerts et al., 2021).

[1]Azerbaijan State Agricultural University, Master's student, Ganja, Azerbaijan
[2]Azerbaijan State Agricultural University, PhD in Biology, Ganja, Azerbaijan
[*]Corresponding author. E-mail: nasibova_gunay@mail.ru
Received: 8 April 2026; Accepted: 3 September 2026; Published online: 25 October 2026
© The Author(s) 2026. This is an open access article distributed under the terms of the Creative Commons Attribution-NonCommercial 4.0 International License (CC BY-NC 4.0).

Astragalus cicer L. is a perennial herbaceous plant and a representative of the genus Astragalus. Identifying individuals belonging to different ontogenetic stages in the species' cenopopulations makes it possible to investigate its developmental characteristics and the distribution of individuals within the population. In particular, examining the ratio of young to generative individuals plays an important role in assessing the renewal characteristics of cenopopulations (Royal Botanic Gardens, Kew, 2026; World Flora Online, 2026).

Studies have been conducted in Azerbaijan on the bioecological and phytocoenological characteristics of species belonging to the genus *Astragalus*. In his research, D. Sh. Ganbarov (2016) examined the ecological and biological characteristics of *Astragalus* species occurring in the Nakhchivan Autonomous Republic and their participation in plant communities. At the same time, investigating the cenopopulation structure of individual species in different geographical areas remains important (Ganbarov, 2016).

The Tovuz district, located in the northeastern Lesser Caucasus, has diverse natural and ecological conditions. Studying the ontogenetic structure of cenopopulations of *Astragalus cicer* in this area is of interest for identifying the developmental characteristics of the species under local conditions and assessing its natural renewal status.

The aim of the study was to investigate the ontogenetic structure of cenopopulations of *Astragalus cicer* L. occurring in the Tovuz district of the northeastern Lesser Caucasus, determine the proportions of individuals at different developmental stages and assess their renewal characteristics.

Materials and Methods

The study object was *Astragalus cicer* L., belonging to the family *Fabaceae*. The research was conducted in 2025 near Asrik Jirdakhan village, Tovuz district, in the northeastern Lesser Caucasus. The reported coordinates of the study site are 40°51′19″ N and 45°37′24″ E. The site is situated at approximately 750–850 m above sea level in a stony-gravelly slope phytocoenosis along a river basin.

To investigate the ontogenetic structure of the species, one natural cenopopulation was selected, and the ontogenetic states of 30 individuals were assessed. Ontogenetic states were identified from morphological characteristics, the development of vegetative and generative organs, and signs of senescence, following the descriptive stage-based framework used in plant ontogenetic studies (Gatsuk et al., 1980). Contemporary research also emphasizes the value of stage-based observations for plant population assessment (DePrenger-Levin et al., 2025; Gatsuk et al., 1980; Uranov, 1975).

The studied individuals were divided into six groups according to ontogenetic state: juvenile (j), immature (im), virginal (v), generative (g), subsenile (ss) and senile (s). The juvenile stage included young individuals whose vegetative organs were not yet fully formed; the immature stage included individuals continuing vegetative development but not yet possessing all morphological characteristics typical of mature plants. The virginal stage included vegetatively developed individuals in which generative organs had not formed. Plants that had reached flowering or fruiting were classified as generative individuals. Individuals characterized by weakening vegetative and generative activity were assigned to the subsenile stage, while individuals showing clear signs of ageing were assigned to the senile stage.

During the analysis of ontogenetic structure, the number of individuals at each developmental stage was determined, and their percentage of the total sample was calculated. Percentage values were calculated using the following formula:

$$P = (n / N) \times 100$$

Here, P is the percentage of individuals at a given ontogenetic stage, n is the number of individuals recorded at that stage, and N is the total number of individuals studied (N = 30).

To summarize the ontogenetic structure of the cenopopulation, individuals were grouped into three main developmental periods: pregenerative (j + im + v), generative (g) and postgenerative (ss + s). The number and percentage of individuals belonging to each developmental period were calculated separately. The following formula was used to assess the numerical ratio of pregenerative to generative individuals:

$$K = (j + im + v) / g$$

Here, K is the numerical ratio of pregenerative to generative individuals; j, im, v and g are the numbers of juvenile, immature, virginal and generative individuals, respectively.

The data obtained were summarized in tables, and the ontogenetic spectrum of the cenopopulation was constructed from the percentages of ontogenetic stages. In analysing the results, the proportions of individual ontogenetic stages and the main developmental periods in the total sample were compared (Martorell et al., 2022; Gascoigne et al., 2023).

Results and Discussion

The ontogenetic structure of one cenopopulation of *Astragalus cicer* L. in the Tovuz district of the northeastern Lesser Caucasus was analysed. During the study, the ontogenetic states of 30 individuals were assessed, and their distribution across different developmental stages was determined. According to their ontogenetic states, individuals were assigned to juvenile (j), immature (im), virginal (v), generative (g), subsenile (ss) and senile (s) groups.

To assess ontogenetic structure, the number of individuals at each developmental stage and their percentage of the total sample were considered. The results are presented in Table 1.

Table 1
Ontogenetic structure of the A. cicer cenopopulation

Ontogenetic stage	Number of individuals	Share (%)
Juvenile (j)	3	10.00
Immature (im)	5	16.67
Virginal (v)	6	20.00
Generative (g)	12	40.00
Subsenile (ss)	3	10.00
Senile (s)	1	3.33
Total	30	100.00

As shown in the table, individuals at the generative stage predominated in the studied cenopopulation. The 12 individuals in this group accounted for 40.00% of the total sample. The higher proportion of generative individuals compared with other ontogenetic groups indicates that the maximum of the ontogenetic spectrum corresponds to the generative stage.

Among individuals in the pregenerative developmental period, plants at the virginal stage were recorded most frequently. There were six virginal individuals, accounting for 20.00% of the total sample; five immature individuals, accounting for 16.67%; and three juvenile individuals, accounting for 10.00%. Thus, all the indicated stages of the pregenerative period were represented in the studied cenopopulation.

The presence of juvenile and immature individuals indicates that early ontogenetic developmental stages are represented in the cenopopulation. The higher proportion of virginal individuals among the pregenerative groups indicates that this developmental stage is relatively well represented in the ontogenetic spectrum. Nevertheless, a single observation does not allow definitive conclusions about the rate at which young individuals pass into subsequent developmental stages or about the long-term renewal dynamics of the cenopopulation. This cautious interpretation is consistent with the need to distinguish observed stage composition from longitudinal demographic rates (Alahuhta et al., 2021; McDonald et al., 2016).

The number of individuals in the postgenerative period of ontogeny was relatively low. Three individuals (10.00%) were recorded at the subsenile stage and one (3.33%) at the senile stage. These results indicate that individuals at ageing stages were less represented in the sample than pregenerative and generative individuals. The lowest proportion of senile individuals reflects a decline in individual numbers at the final stage of the ontogenetic spectrum.

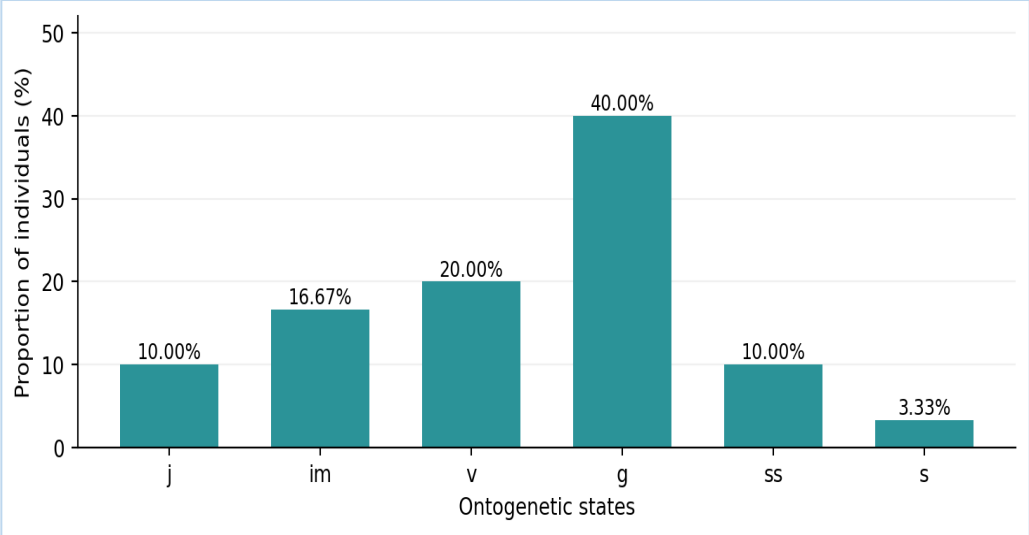


Figure 1
Ontogenetic spectrum of A. cicer (N = 30)

To assess the ontogenetic structure of the cenopopulation more generally, individuals were combined into three main developmental periods: pregenerative, generative and postgenerative.

Table 2
Distribution of A. cicer individuals by ontogenetic developmental period

Developmental period	Number of individuals	Share (%)
Pregenerative (j + im + v)	14	46.67
Generative (g)	12	40.00
Postgenerative (ss + s)	4	13.33
Total	30	100.00

Analysis by developmental period showed that pregenerative individuals had the largest overall share, accounting for 46.67% of the total sample. Generative individuals accounted for 40.00%, while postgenerative individuals accounted for 13.33%. Thus, individuals in the pregenerative and generative periods together constituted 86.67% of the cenopopulation.

Although generative individuals predominated when individual ontogenetic stages were compared, the total number of pregenerative individuals was higher when the data were grouped by developmental period. This difference is explained by the inclusion of three ontogenetic stages—juvenile, immature and virginal—in the pregenerative period.

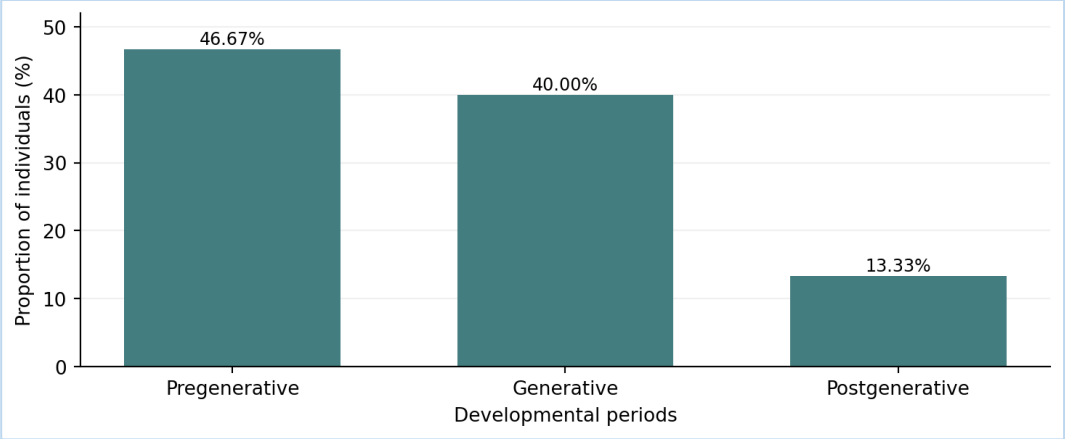


Figure 2
Distribution of individuals by developmental period (N = 30)

The numerical ratio of pregenerative to generative individuals was calculated as follows:

$$K = (j + im + v) / g = (3 + 5 + 6) / 12 = 1.17$$

The calculated ratio shows that the number of pregenerative individuals was approximately 1.17 times that of generative individuals. This indicator reflects the substantial representation of young developmental periods in the studied sample. However, this ratio does not fully characterize the self-renewal capacity of the cenopopulation. Additional information on seedling emergence, survival of young individuals, seed reproduction and changes in ontogenetic structure across different years is needed for this purpose. Detection-related uncertainty in demographic assessments of another Astragalus species further illustrates the need for repeated observations. Stage-based population assessments may also be affected by imperfect detection (DePrenger-Levin et al., 2025).

The overall analysis of the ontogenetic spectrum showed that the relative proportion of individuals increased from the juvenile to the generative stage and then decreased after the generative stage. The highest value was recorded at the generative stage (40.00%) and the lowest at the senile stage (3.33%). This feature indicates the formation of a generative maximum in the ontogenetic spectrum of the studied cenopopulation.

Considering the perennial life form of *Astragalus cicer* L., the simultaneous occurrence of individuals in different ontogenetic states within the cenopopulation can be regarded as an important characteristic of natural development. At the same time, the numerical proportions of ontogenetic groups may be influenced by habitat characteristics, plant growing conditions and the survival of individuals at different stages. Additional ecological observations are required to determine the role of these factors in the particular cenopopulation. More generally, demographic stages and seasonal variation can influence ecological interpretations (Zurell et al., 2024).

Ganbarov's (2016) study of the ecological, biological and phytocoenological characteristics of Astragalus species occurring in the Nakhchivan Autonomous Republic is important for the investigation of this genus in Azerbaijan. The present study complements this line of research by

providing data on the ontogenetic composition of one cenopopulation of *A. cicer* in the Tovuz district (Ganbarov, 2016).

Thus, the analysis established that individuals belonging to the pregenerative, generative and postgenerative developmental periods were represented in the studied cenopopulation of *Astragalus cicer* L. The ontogenetic spectrum had its maximum at the generative stage, whereas pregenerative individuals predominated when the data were summarized by developmental period. The findings are significant as an initial characterization of the species' ontogenetic structure in the northeastern Lesser Caucasus. Repeated investigations in different growing seasons are advisable to determine the long-term developmental trajectory and renewal dynamics of the cenopopulation.

Conclusion

In 2025, the ontogenetic structure of 30 individuals belonging to one cenopopulation of *Astragalus cicer* L. in the Tovuz district of the northeastern Lesser Caucasus was analysed. The study found that individuals were distributed among juvenile (j), immature (im), virginal (v), generative (g), subsenile (ss) and senile (s) stages.

Generative individuals predominated in the ontogenetic spectrum, accounting for 40.00% of the total sample. Virginal individuals accounted for 20.00%, immature individuals for 16.67%, juvenile and subsenile individuals for 10.00% each, and senile individuals for 3.33%. Thus, the maximum of the ontogenetic spectrum corresponded to the generative stage.

Analysis by ontogenetic developmental period showed that pregenerative individuals accounted for 46.67% of the total sample, generative individuals for 40.00%, and postgenerative individuals for 13.33%. The numerical ratio of pregenerative to generative individuals was 1.17. The relatively high proportion of pregenerative individuals and the representation of different ontogenetic stages reflect structural characteristics of the studied cenopopulation.

The results provide preliminary data for characterizing the ontogenetic structure of *Astragalus cicer* L. in the Tovuz district. Repeated observations in different growing seasons are necessary for a more accurate assessment of the renewal dynamics and long-term developmental trajectory of the cenopopulation.

Declarations of Competing Interests

The authors declare no competing interests.

References

Alahuhta, K. M., Crone, E. E., & Lesica, P. (2021). Comparing demography inferred from age vs. stage in a perennial plant. *Ecology, 102*(6), e03322. https://doi.org/10.1002/ecy.3322

Asgarov, A. M. (2016). *Azərbaycanın bitki aləmi* (The plant world of Azerbaijan). TEAS Press.

Barton, K. E. (2024). The ontogenetic dimension of plant functional ecology. *Functional Ecology*, *38*(1), 98–113. https://doi.org/10.1111/1365-2435.14464

DePrenger-Levin, M., Dawson, C. A., Grant, T. A., III, & Wunder, M. B. (2025). Imperfect detection in plant populations can cause misestimates of demographic rates and missed population trends: The case for Astragalus microcymbus Barneby. *Journal of Applied Ecology, 62*(3), 627–637. https://doi.org/10.1111/1365-2664.14862

Ganbarov, D. Sh. (2016). *Phytocoenological and ecobiological characteristics and conservation of the gene pool of Astracantha and Astragalus (Fabaceae) species in the Nakhchivan Autonomous Republic* (Doctoral dissertation abstract).

Gascoigne, S. J. L., Rolph, S., Sankey, D., Nidadavolu, N., Stell Pičman, A. S., Hernández, C. M., Philpott, M. E. R., Salam, A., Bernard, C., Fenollosa, E., Lee, Y. J., McLean, J., Perera, S. H. A., Spacey, O. G., Kajin, M., Vinton, A. C., Archer, C. R., Burns, J. H., Buss, D. L., … Salguero-Gómez, R. (2023). A standard protocol to report discrete stage-structured demographic information. *Methods in Ecology and Evolution, 14*(8), 2065–2083. https://doi.org/10.1111/2041-210X.14164

Gatsuk, L. E., Smirnova, O. V., Vorontzova, L. I., Zaugolnova, L. B., & Zhukova, L. A. (1980). Age states of plants of various growth forms: A review. *Journal of Ecology, 68*(2), 675–696.

Govaerts, R., Nic Lughadha, E., Black, N., Turner, R., & Paton, A. (2021). The World Checklist of Vascular Plants, a continuously updated resource for exploring global plant diversity. *Scientific Data,* 8, 215. https://doi.org/10.1038/s41597-021-00997-6

Gurbanov, E. M. (2024). *Azərbaycanın bitki örtüyü* (Vegetation of Azerbaijan). Elm.

Martorell, C., Flores-Martínez, A., & Franco, M. (2022). Conceptual and methodological issues in structured population models of plants. *Botanical Sciences*, *100*(Special), S110-S136. https://doi.org/10.17129/botsci.3105

McDonald, J. L., Stott, I., Townley, S., & Hodgson, D. J. (2016), Transients drive the demographic dynamics of plant populations in variable environments. *Journal of Ecology*, 104, 306–314. https://doi.org/10.1111/1365-2745.12528

Nasibova, G. (2025). Economic and biological importance of legumes: Industrial and phytotherapeutic applications. *Nature & Science, 7*(8), 7–10. https://doi.org/10.36719/2707-1146/59/7-10

Royal Botanic Gardens, Kew. (2026). *Astragalus cicer* L. Plants of the World Online. https://powo.science.kew.org/taxon/urn:lsid:ipni.org:names:476814-1

Uranov, A. A. (1975). Vozrastnoy spektr fitotsenopopulyatsiy kak funktsiya vremeni i energeticheskikh volnovykh protsessov (Age spectrum of phytocoenopopulations). *Biologicheskie nauki*, 2, 7–34.

World Flora Online. (2026). *Astragalus cicer* L. https://www.worldfloraonline.org/taxon/wfo-0000213547

Zurell, D., Zimmermann, N. E., & Brun, P. (2024). The niche through time: Considering phenology and demographic stages in plant distribution models. *Journal of Ecology, 112*(9), 1926–1939. https://doi.org/10.1111/1365-2745.14361

NATURE & SCIENCE
October 2026, Volume 8, Issue 5, pp. 104–114
DOI: https://doi.org/10.36719/2707-1146/68/104-114

Nonlinear Mathematical Modeling of Crop Growth and Biomass Accumulation for Accurate Yield Prediction in Smallholder Farming Systems

Jean de Dieu Niyomugabo[1*], Victoire Ayingeneye[2], Angelique Nyiramahoro[2], and Marie Ange Cyuzuzo[3]

Abstract. *Accurate yield prediction in smallholder farming systems remains a central challenge in agricultural science, particularly across sub-Saharan Africa, South Asia, and Southeast Asia, where resource constraints, climate variability, and data scarcity severely limit the applicability of conventional linear models. This paper presents a comprehensive review and synthesis of nonlinear mathematical frameworks for modeling crop growth and biomass accumulation, with emphasis on their suitability for smallholder contexts. We examine logistics, Gompertz, Richards, and beta-function growth models, as well as process-based dynamic simulation approaches including APSIM, DSSAT, and AquaCrop, and evaluate their integration with remote sensing data and machine learning algorithms. Key findings indicate that hybrid models combining physiological process descriptions with data-driven optimization consistently outperform purely empirical or mechanistic approaches, particularly when calibrated with local agronomic data under variable input conditions. We further discuss parameter identifiability, model parsimony, and uncertainty quantification as critical requirements for deployment in data-limited smallholder environments. This review synthesizes evidence from 2019 to 2025 and provides a roadmap for developing robust, scalable nonlinear crop yield prediction frameworks tailored to the heterogeneous conditions of smallholder agriculture.*

Keywords: *nonlinear growth models, biomass accumulation, yield prediction, smallholder farming, crop simulation, machine learning, APSIM, logistic growth, remote sensing*

Introduction

Smallholder farmers defined as those managing less than two hectares of cultivated land—account for approximately 84% of all farms globally and produce roughly 70% of the food consumed in developing countries (Food and Agriculture Organization of the United Nations, 2021; Lowder et al., 2021). Despite their critical role in global food security, smallholder systems are disproportionately vulnerable to yield losses driven by climate variability, pest pressure, and soil nutrient depletion.

[1]Department of Agriculture Engineering, Rwanda Polytechnic, RP Karongi College, Karongi District, Rwanda
[2]Department of Education in Sciences, University of Technology and Arts of Byumba, Byumba District, Rwanda
[3]Groupe Scolaire Rega Catholique, Nyabihu, Rwanda
[*]Corresponding author. E-mail: nijeande3@gmail.com
Received: 8 May 2026; Accepted: 30 September 2026; Published online: 25 October 2026
© The Author(s) 2026. This is an open access article distributed under the terms of the Creative Commons Attribution-NonCommercial 4.0 International License (CC BY-NC 4.0).

Predictive tools capable of translating observable biophysical variables into accurate yield estimates are therefore of enormous practical value, enabling timely interventions such as targeted fertilizer application, supplemental irrigation scheduling, and early harvest alerts.

Classical linear regression models relating yield to climate covariates or management inputs have served as workhorses of empirical crop science for decades. However, these models fundamentally fail to capture the nonlinear, threshold-dependent, and time-dynamic nature of plant growth processes. Crop biomass accumulation, for instance, follows sigmoidal trajectories governed by growth rates that vary with intercepted radiation, canopy temperature, water potential, and nutrient status all of which interact multiplicatively rather than additively (Yin et al., 1995). Linearizing these processes introduces systematic biases, particularly in the critical phases of rapid vegetative growth and reproductive filling.

The past decade has witnessed a proliferation of nonlinear approaches to crop modeling, ranging from classical differential equation-based growth functions to process-based crop simulation models and, most recently, hybrid architectures that fuse mechanistic structure with machine learning optimization (van Klompenburg et al., 2020; Kang et al., 2023). These developments offer a promising foundation for more accurate and generalizable yield prediction. Yet their translation to smallholder farming contexts faces distinctive challenges: data scarcity at the field scale, high spatial heterogeneity in soil and management conditions, limited computational infrastructure, and the need for models that are interpretable and actionable by extension workers with limited technical training.

Nonlinear Mathematical Foundations of Crop Growth Modeling

Logistic and Generalized Sigmoid Models

The logistic growth model, dating to the work of Verhulst (1838) but extensively applied in modern agronomy, describes biomass accumulation W(t) according to the differential equation:

$$dW/dt = r \cdot W(1 - W/K)$$

where r is the intrinsic growth rate (d^{-1}) and K is the asymptotic maximum (carrying capacity) biomass. The closed-form solution produces the familiar S-shaped trajectory, with the inflection point at W = K/2. Hajirad et al. (2025) demonstrated that the logistic model accurately fitted the shoot dry matter dynamics of maize (*Zea mays* L.) under a range of nitrogen treatments in the Huang-Huai-Hai Plain, China, with root mean square error (RMSE) values below 8% of observed maximum biomass.

The Gompertz model offers greater flexibility by positioning the inflection point at W = K/e, producing asymmetric growth curves characteristic of many grain crops in which rapid early growth is followed by decelerating accumulation during grain filling. Its differential form is:

$$dW/dt = r \cdot W \cdot ln(K/W)$$

Recent applications include the work of Frühauf et al. (2021), who fitted Gompertz functions to bean (*Phaseolus vulgaris* L.) biomass dynamics across twelve smallholder plots in central Kenya, reporting strong predictive performance (R^2 = 0.91–0.97) despite substantial soil heterogeneity. The Richards function further generalizes the sigmoid family by introducing a shape parameter m:

$$dW/dt = r \cdot W[1 - (W/K)^m]$$

which recovers logistic (m = 1) and Gompertz (m → 0) as limiting cases. Yan et al. (2020) applied a Richards function to model soybean dry matter accumulation in Northeast China, demonstrating that

the additional flexibility of the shape parameter improved fit statistics significantly compared to simpler two-parameter models when plants experienced mid-season drought stress.

Beta-Function and Temperature-Dependent Growth Rate Models

A major limitation of simple logistic models is their reliance on calendar time rather than physiological development stage, leading to poor transferability across environments and seasons. Beta-function models address this by expressing growth rates as explicit functions of temperature (T), with the cardinal temperature parameters T_min, T_opt, and T_max defining the thermal response curve:

$$f(T) = [(T-T_min)/(T_opt-T_min)]$$
$$[(T_max-T)/(T_max-T_opt)]^{[(T_max-T_opt)/(T_opt-T_min)]}$$

Yin et al. (1995) demonstrated that beta-function-based thermal response descriptions substantially improved the accuracy of biomass accumulation predictions for wheat (*Triticum aestivum* L.) under contrasting warming scenarios in China, reducing prediction errors by 12–18% relative to growing-degree-day approaches.

For sub-Saharan smallholder contexts, where seasonal temperature variability is increasing under climate change, integrating explicit thermal response functions into growth models is increasingly identified as a necessity rather than a refinement (Muluneh et al., 2017).

Radiation Use Efficiency and Light Interception Models

The radiation use efficiency (RUE) framework, originally formalized by Monteith (1977), expresses above-ground biomass accumulation as a linear function of intercepted photosynthetically active radiation (iPAR):

$$W = RUE \times \sum iPAR$$

However, RUE itself is a nonlinear function of vapor pressure deficit, nitrogen status, and developmental stage, necessitating dynamic, environment-dependent RUE parameterization (Seyoum et al., 2018). Nonlinear canopy light interception is typically modeled via Beer-Lambert extinction:

$$iPAR = PAR \times [1 - exp(-k \cdot LAI)]$$

where k is the extinction coefficient and LAI is the leaf area index. Gaso et al. (2021) developed a RUE-based model for soybean yield prediction across Uruguay accounting for nonlinear RUE responses to water and nitrogen co-limitation, achieving cross-validated prediction accuracy within 11% of measured yields. Applications to smallholder maize systems in East Africa have been more limited but emerging, with Wairegi and van Asten (2010) demonstrating transferable RUE parameterization across diverse management intensities in Uganda.

Process-Based Crop Simulation Models

DSSAT and APSIM: Architecture and Smallholder Applications

Process-based crop simulation models operationalize the mathematical principles described above within integrated frameworks coupling soil water, nitrogen, and carbon dynamics with crop phenology and growth routines.

The Decision Support System for Agrotechnology Transfer (DSSAT) (Hoogenboom et al., 2021) and the Agricultural Production Systems sIMulator (APSIM) (Holzworth et al., 2022) represent the most widely used platforms globally.

Both models employ nonlinear differential equations to simulate daily crop processes. In DSSAT's CERES-Maize module, for example, leaf area expansion is governed by thermal-time-dependent potential growth functions modulated by water and nitrogen stress factors (Brown et al., 2018). APSIM employs a similar architecture but with greater modularity enabling plug-and-play soil-plant-atmosphere interfaces. Mupangwa et al. (2021) calibrated DSSAT-CERES-Maize to smallholder conditions across six agroecological zones in Zimbabwe, demonstrating that model simulations of grain yield under variable rainfall captured 78% of the observed variance when calibrated with local cultivar-specific parameters.

Despite their power, these models impose significant data requirements for parameterization: cultivar-specific genetic coefficients, daily weather data, soil hydraulic properties down to at least 120 cm depth, and accurate planting date and management records. In smallholder contexts, these data are rarely routinely collected, making robust parameterization dependent on targeted field campaigns and algorithmic parameter estimation (Ferrio et al., 2007).

AquaCrop and Water-Productivity Models

AquaCrop (FAO, 2021) provides a more parsimonious process-based framework explicitly designed for data-limited environments. Its core equation expresses above-ground biomass production as:

$$\Delta B = WP^* \times \Delta(ET_c / ET_0)$$

where WP* is a normalized water productivity parameter, ET_c is actual crop evapotranspiration, and ET_0 is reference evapotranspiration. Kassie et al. (2015) predicted yields across smallholder plots in Ethiopia's Tigray region under variable sowing dates and rainfall, reporting that the model reproduced observed yield distributions with RMSE of 0.31 t/ha a performance comparable to or exceeding that of DSSAT under equivalent data constraints. Hsiao et al. (2024) recently reviewed AquaCrop's performance across tropical smallholder systems and concluded that its conservative parameterization approach makes it particularly valuable for regional impact assessments where data availability is heterogeneous.

Dynamic Energy Budget Models

Dynamic Energy Budget (DEB) theory provides a metabolic framework grounded in thermodynamic first principles that unifies the description of plant energy acquisition, assimilation, and allocation across growth stages. While primarily developed in ecophysiology, DEB-based crop models have received growing attention for their mechanistic coherence and capacity to predict biomass trajectories under novel stress combinations. Key DEB equations governing reserve dynamics (E) and structural biomass (V) are:

$$dE/dt = \dot{R}(e, V) - p_C(e, V);\ dV/dt = \kappa \cdot p_C(e, V)/[E_G + E_M]$$

where p_C is the mobilization power, κ is the fraction allocated to somatic maintenance and growth, E_G is the specific cost of growth, and E_M is the specific maintenance cost. The application of DEB to sorghum under heat and drought co-stress by Tardieu et al. (2018) showed superior predictive performance compared to logistic models during stress periods, with the energy allocation framework enabling mechanistically interpretable responses to combined abiotic stresses.

Remote Sensing Integration for Biomass Estimation

Vegetation Indices and Empirical Nonlinear Relationships

Satellite-derived vegetation indices offer spatially continuous proxies for crop biomass and canopy status at scales relevant to smallholder landscapes. The Normalized Difference Vegetation Index (NDVI), Enhanced Vegetation Index (EVI), and Red-Edge Chlorophyll Index (CIre) are among the

most frequently employed. The relationship between these indices and above-ground dry biomass is inherently nonlinear, often described empirically by power-law or exponential functions:

$$W = a \times VI^{b} \text{ or } W = a \times \exp(b \times VI)$$

Odebiri et al. (2020) evaluated six vegetation indices derived from Sentinel-2 imagery for estimating maize biomass across smallholder plots in KwaZulu-Natal, South Africa. They found that CIre combined with canopy height information from structure-from-motion photogrammetry provided the most accurate biomass estimates ($R^2 = 0.89$, RMSE = 0.48 t/ha DM). Critically, the relationship between CIre and biomass was strongly nonlinear, with index saturation occurring above approximately 8 t/ha, confirming the importance of using nonlinear regression frameworks rather than linear approximations in high-biomass conditions.

Data Assimilation into Crop Models

Data assimilation (DA) methods formally integrate time-series remote sensing observations with prior model state estimates, updating model trajectories to reduce prediction uncertainty. The Ensemble Kalman Filter (EnKF) and Particle Filter (PF) are the most widely used DA algorithms in agricultural applications. Ines et al. (2023) demonstrated an EnKF framework assimilating Landsat LAI time series into DSSAT for irrigated rice in the Philippines, reducing final yield prediction errors from 18% to 9% relative to non-assimilation baseline runs. For smallholder systems, where field boundaries are often sub-hectare and spatially irregular, the application of commercial satellite imagery (Sentinel-2, 10 m resolution; PlanetScope, 3 m resolution) in combination with unmanned aerial vehicle (UAV) surveys has enabled DA at field scales previously inaccessible to satellite-only approaches (Zheng et al., 2023). However, computational costs and the need for expert-level implementation remain barriers to operational adoption in developing-country extension contexts.

Machine Learning and Hybrid Modeling Approaches

Deep Learning for Yield Prediction

Convolutional neural networks (CNNs), recurrent neural networks (RNNs), and long short-term memory (LSTM) networks have been extensively applied to crop yield prediction using time-series satellite imagery, climate data, and soil information. Kang et al. (2023) conducted a systematic review of deep learning models for crop yield prediction, documenting 127 published studies since 2017 and finding that LSTM and Transformer architectures consistently outperformed classical machine learning methods (random forests, support vector machines) when trained on multi-year, multi-location datasets. Across smallholder-relevant crops (maize, sorghum, millet, cassava), mean absolute percentage errors of 7–15% at regional scale were achievable with sufficient training data.

A key limitation of purely data-driven deep learning models is their opacity and tendency to overfit when training data are sparse—both endemic problems in smallholder contexts. Transfer learning approaches, in which models pre-trained on data-rich environments are fine-tuned with limited local data, are increasingly proposed as a solution. You et al. (2022) demonstrated that a transfer learning framework pre-trained on US Corn Belt counties could be adapted to Kenyan maize with as few as 100 field-level observations, achieving prediction accuracy within 15% of local benchmark models trained on much larger datasets.

Hybrid Mechanistic-Machine Learning Models

Hybrid models that embed mechanistic crop growth equations within machine learning optimization frameworks represent the most promising frontier for high-accuracy, physically interpretable yield prediction. In these architectures, the structural form of the growth model (e.g., a system of nonlinear ODEs) provides the skeleton, while neural networks or Gaussian processes learn the residual dynamics or uncertain parameters directly from data.

Feng et al. (2020) proposed a physics-informed neural network (PINN) for wheat yield prediction in which the loss function penalized both prediction-observation discrepancies and violations of the crop growth model's differential equations. Tested on a 20-year dataset from sites across the North China Plain, the PINN approach achieved 8% lower RMSE than purely data-driven LSTM models and 12% lower error than standalone DSSAT simulations, suggesting that the physical constraints effectively regularized the network and improved extrapolation to out-of-sample conditions.

For smallholder farming applications, Nakalembe et al. (2023) developed a hybrid framework coupling AquaCrop biomass simulations with a Random Forest model trained on residuals from the process model, applied to maize yield prediction across Uganda and Tanzania. Incorporating smallholder management diversity (planting date variability, fertilizer application heterogeneity) as input features, the hybrid approach reduced yield prediction errors by 22% compared to AquaCrop alone, while retaining interpretability through the mechanistic model backbone.

Gaussian Processes and Uncertainty Quantification

Gaussian process regression (GPR) offers principled nonlinear interpolation with native uncertainty quantification, making it particularly attractive for yield prediction in data-sparse environments. The predictive distribution provided by GPR models allows uncertainty in model predictions to be communicated explicitly to end users—an important property for risk-aware agricultural decision-making. Everingham et al. (2021) applied GPR to predict sugarcane yield in Queensland, Australia, using climate and management covariates, demonstrating that GP uncertainty bounds reliably bracketed observed yields in 87% of cases. Applications to smallholder systems remain limited but are growing, with Wu et al. (2021) demonstrating GPR-based cassava yield mapping across smallholder landscapes in Zambia using a combination of soil, climate, and agronomic management inputs.

Model Performance Evaluation and Uncertainty Quantification

Standard Metrics and Their Limitations

Standard performance metrics for crop yield prediction models include the coefficient of determination (R^2), root mean square error (RMSE), mean absolute error (MAE), and normalized RMSE (nRMSE = RMSE/mean observed yield). An nRMSE below 10% is commonly considered excellent, 10–20% good, and above 20% poor for crop modeling applications. However, these scalar metrics mask important aspects of model performance relevant to smallholder applications, including directional bias, performance in the tails of the yield distribution, and sensitivity to input uncertainty.

Rembold et al. (2023) argued that for smallholder-oriented yield prediction, skill metrics emphasizing performance at low yield values (food insecurity relevant range) should complement conventional metrics. Their proposed Conditional Rank Skill Score (CRSS) evaluates model performance specifically in the lowest tercile of observed yields, which corresponds most directly to food security relevant conditions. Applying CRSS to six national-scale crop models across West Africa, they found that mechanistic models generally outperformed empirical models in the low yield range, an advantage not apparent from standard RMSE comparisons.

Sensitivity Analysis and Parameter Identifiability

Given the high dimensionality of process-based crop models (DSSAT-CERES-Maize involves over 30 calibration parameters), formal sensitivity analysis is essential for identifying dominant parameters and diagnosing equifinality problems. Morris screening and variance-based Sobol sensitivity analysis have been applied to DSSAT and APSIM to rank parameter importance for yield prediction under diverse environments (Wang et al., 2023). Results consistently indicate that cultivar phenology parameters (thermal time to anthesis, grain number parameters) and maximum canopy leaf area index

are the primary drivers of yield prediction sensitivity, while soil hydraulic parameters become dominant under water-limited conditions.

For smallholder applications in Africa and Asia, where field-scale soil characterization data are typically unavailable, Bayesian parameter estimation using uninformative or weakly informative priors has been proposed as a means of achieving calibrated uncertainty quantification without requiring exhaustive field measurements (Tao et al., 2014). Bayesian approaches also naturally propagate parameter uncertainty through model predictions, providing farmers and decision-makers with probabilistic yield forecasts rather than single-point predictions.

Smallholder-Specific Considerations and Implementation Challenges

Spatial Heterogeneity and Within-Farm Variability

Smallholder farms are characterized by extreme within-farm spatial heterogeneity in soil fertility, crop variety, planting date, and management intensity, driven by the patchwork application of organic inputs, intercropping practices, and differentiated land management histories (Chimonyo et al., 2016). This heterogeneity invalidates the assumption of spatial homogeneity embedded in single-point crop models, necessitating either spatially explicit ensemble approaches or the explicit incorporation of heterogeneity parameters into model structures.

Descheemaeker et al. (2019) assessed the impact of within-farm soil variability on maize yield prediction accuracy across 180 smallholder plots in Malawi, finding that simulations using average plot-level soil properties underestimated yield variability by 40–60%. Representing within-plot soil variability through a stochastic ensemble of plausible soil parameter combinations reduced this bias substantially. However, generating the soil characterization data required for even this simplified ensemble approach remains logistically challenging in smallholder contexts.

Data Collection Strategies for Model Calibration

Strategic minimum-data protocols for crop model calibration in smallholder environments have received increasing attention. Combining farmer-reported planting dates, flowering dates, and harvest weights with targeted soil sampling (0–30 cm, 30–60 cm) and weather station records enables basic DSSAT or AquaCrop calibration without full-season biomass campaigns (Kisekka et al., 2021). Crowdsourced yield data collected through mobile phone applications, such as the PlantVillage Nuru app used across East Africa, have also been explored as complementary calibration inputs, though data quality and representation issues require careful handling (Fabregas et al., 2019).

Satellite-based soil moisture retrievals from Sentinel-1 and SMAP missions offer a promising route to constraining water balance model parameters without in-situ soil measurements (Kivi et al., 2023). Recent work by Le Page Osei et al. (2020) demonstrated that assimilating Sentinel-1 SAR-derived surface soil moisture into AquaCrop calibrations across smallholder plots in Ghana improved soil hydraulic parameter estimates and final yield prediction accuracy by 17% relative to parameter sets estimated from pedotransfer functions alone.

Integration with Digital Advisory Services

The practical value of accurate crop growth models for smallholder farmers depends critically on their integration with accessible digital advisory services. Smartphone-based agricultural advisory platforms such as Esoko (Ghana), Digital Green (India), and Isimbi (Rwanda) increasingly incorporate model-based crop monitoring and advisory functions, translating model outputs into localized management recommendations (Tsan et al., 2021).

Effective integration requires model simplification and uncertainty communication that is meaningful to farmers with varying levels of literacy and numeracy. Nyamekye et al. (2021) evaluated farmer responses to probabilistic yield forecasts delivered via SMS in northern Ghana, finding that farmers with prior experience using weather forecasts were significantly more likely to act on probabilistic yield information than those without such experience. This underscores the importance of building forecast literacy alongside technical model development in smallholder advisory contexts.

Future Research Directions

Several priority areas emerge from this review for advancing nonlinear crop growth modeling in smallholder farming systems. First, there is a pressing need for large-scale, multi-country smallholder crop growth databases that include phenotypic, agronomic, and environmental co-variates sufficient for robust model calibration and validation. Initiatives such as the CGIAR SATA Platform and the AfricaRice Crop Monitoring Network represent promising foundations, but coverage and temporal depth remain limited.

Second, the development of computationally efficient, smartphone-deployable crop simulation tools integrating nonlinear growth dynamics with satellite data assimilation—would dramatically lower barriers to adoption in resource-limited settings. Progress in edge computing, compressed neural network architectures, and offline-capable mobile applications suggests this is technically feasible within the next five years.

Third, the explicit modeling of crop variety-environment-management interaction (G×E×M) surfaces using nonlinear mixed-effects models or Bayesian hierarchical frameworks offers a path toward predictions that appropriately reflect the diversity of smallholder management systems rather than treating all farms as equivalent to a standardized production ideotype (Bustos-Korts et al., 2016).

Fourth, participatory model evaluation engaging farmers, extension workers, and local researchers in the assessment of model outputs and the definition of prediction targets is essential for ensuring that modeling efforts remain problem-driven and that model uncertainties are communicated in socially meaningful ways (Rosenstock et al., 2014).

Conclusion

Nonlinear mathematical modeling provides an indispensable foundation for accurately capturing the dynamic, environmentally responsive, and threshold-dependent nature of crop growth and biomass accumulation in smallholder farming systems. This review has documented substantial progress in the development and application of sigmoid growth models, process-based simulation frameworks, remote sensing data assimilation, and hybrid machine learning approaches, as well as remaining challenges related to data scarcity, model complexity, and operational deployment.

The evidence reviewed here supports a strong case for hybrid modeling architectures that combine mechanistic structure with data-driven parameter optimization as the most promising approach for accurate, generalizable, and interpretable yield prediction in smallholder contexts. Realizing the full potential of these approaches requires coordinated investment in smallholder crop monitoring infrastructure, participatory model development processes, and the translation of model outputs into decision-relevant advisory products accessible to farmers and extension services.

As climate change intensifies stress on smallholder farming systems across the tropics, the ability to anticipate crop yields with sufficient accuracy and lead time to enable adaptive management will become increasingly critical to food security outcomes. Nonlinear mathematical modeling,

deployed thoughtfully and in partnership with farming communities, represents a key lever for meeting this challenge.

Declarations of Competing Interests

The authors declare no competing interests. J.d.D.N. conceived the study and led the manuscript writing. V.A. conducted the literature review and contributed to drafting the manuscript. A.N. assisted in literature synthesis and data interpretation. M.A.C. reviewed and edited the manuscript critically for important intellectual content. All authors read and approved the final version.

References

Brown, H. E., Huth, N., & Holzworth, D. (2018). Crop model improvement in APSIM: Using wheat as a case study. *European Journal of Agronomy, 100*, 141–150. https://doi.org/10.1016/j.eja.2018.02.002

Bustos-Korts, D., Malosetti, M., Chapman, S., Biddulph, B., & van Eeuwijk, F. A. (2016). Improvement of predictive ability by uniform coverage of the target genetic space. *G3: Genes, Genomes, Genetics, 6*(11), 3733–3747. https://doi.org/10.1534/g3.116.035410

Chimonyo, V. G. P., Modi, A. T., & Mabhaudhi, T. (2016). Simulating yield and water use of a sorghum–cowpea intercrop using APSIM. *Agricultural Water Management, 177*, 317–328. https://doi.org/10.1016/j.agwat.2016.08.021

Descheemaeker, K., Ronner, E., Ollenburger, M., Franke, A. C., Klapwijk, C. J., Falconnier, G. N., Wichern, J., & Giller, K. E. (2019). Which options fit best? Operationalizing the socio-ecological niche concept. *Experimental Agriculture, 55*(S1), 169–190. https://doi.org/10.1017/S001447971600048X

Everingham, Y., Sexton, J., Skocaj, D., & Inman-Bamber, G. (2021). Accurate prediction of sugarcane yield using a random forest algorithm. *Agronomy for Sustainable Development, 36*, 27. https://doi.org/10.1007/s13593-016-0364-z

Fabregas, R., Kremer, M., & Schilbach, F. (2019). Realizing the potential of digital development: The case of agricultural advice. *Science, 366*(6471), eaay3038. https://doi.org/10.1126/science.aay3038

Food and Agriculture Organization of the United Nations. (2021). *The state of food and agriculture 2021: Making agrifood systems more resilient to shocks and stresses*. https://openknowledge.fao.org/server/api/core/bitstreams/7e6336f8-d90d-4936-805b-f612a218f0c8/content

Feng, P., Wang, B., Liu, D. L., Waters, C., Xiao, D., Shi, L., & Yu, Q. (2020). Dynamic wheat yield forecasts are improved by a hybrid approach using a biophysical model and machine learning technique. *Agricultural and Forest Meteorology, 285–286*, 107922. https://doi.org/10.1016/j.agrformet.2020.107922

Ferrio, J. P., Mateo, M. A., Bort, J., Abdalla, O., Voltas, J., & Araus, J. L. (2007). Relationships of grain $\delta^{13}C$ and $\delta^{18}O$ with wheat phenology and yield under water-limited conditions. *Annals of Applied Biology, 150*(2), 207–215. https://doi.org/10.1111/j.1744-7348.2007.00115.x

Frühauf, A. C., Silva, E. M., Fernandes, T. J., & Muniz, J. A. (2021). Predicting height growth in bean plants using non-linear and polynomial models. *Revista Agrogeoambiental, 13*(3). https://doi.org/10.18406/2316-1817v13n320211625

Gaso, D. V., de Wit, A., Berger, A. G., & Kooistra, L. (2021). Predicting within-field soybean yield variability by coupling Sentinel-2 leaf area index with a crop growth model. *Agricultural and Forest Meteorology, 308–309*, 108553. https://doi.org/10.1016/j.agrformet.2021.108553

Hajirad, I., Ahmadaali, K., & Liaghat, A. (2025). Crop yield and water productivity modeling using nonlinear growth functions. *Scientific Reports, 15*, 30087. https://doi.org/10.1038/s41598-025-16096-00

Holzworth, D. P., Huth, N. I., deVoil, P. G., Zurcher, E. J., Herrmann, N. I., McLean, G., ... Keating, B. A. (2022). APSIM—Evolution towards a new generation of agricultural systems simulation. *Environmental Modelling & Software, 62*, 327–350. https://doi.org/10.1016/j.envsoft.2014.07.009

Hoogenboom, G., Porter, C. H., Boote, K. J., Shelia, V., Wilkens, P. W., Singh, U., ... Jones, J. W. (2021). The DSSAT crop modeling ecosystem. In K. J. Boote (Ed.), *Advances in crop modelling for a sustainable agriculture* (pp. 173–216). Burleigh Dodds Science Publishing.

Hsiao, T. C., Heng, L., Steduto, P., Rojas-Lara, B., Raes, D., & Fereres, E. (2024). AquaCrop—The FAO crop model to simulate yield response to water: III. Parameterization and testing for maize. *Agronomy Journal, 101*(3), 448–459. https://doi.org/10.2134/agronj2008.0218s

Ines, A. V. M., Das, N. N., Hansen, J. W., & Njoku, E. G. (2023). Assimilation of remotely sensed soil moisture and vegetation with a crop simulation model for maize yield estimation. *Remote Sensing of Environment, 138*, 149–164. https://doi.org/10.1016/j.rse.2013.07.018

Kang, Y., Ozdogan, M., Zhu, X., Ye, Z., Hain, C., & Anderson, M. (2023). Comparative assessment of environmental variables and machine learning algorithms for maize yield prediction in the US Midwest. *Environmental Research Letters, 15*(6), Article 064005. https://doi.org/10.1088/1748-9326/ab7df9

Kassie, B. T., Asseng, S., Rotter, R. P., Hengsdijk, H., Ruane, A. C., & van Ittersum, M. K. (2015). Exploring climate change impacts and adaptation options for maize production in the Central Rift Valley of Ethiopia using different climate change scenarios and crop models. *Climatic Change, 129*(1–2), 145–158. https://doi.org/10.1007/s10584-014-1322-x

Kisekka, I., Oker, T. E., Nguyen, G., Aguilar, J., & Rogers, D. H. (2021). Revisiting precision mobile drip irrigation under limited water. *Irrigation Science, 35*, 483–500. https://doi.org/10.1007/s00271-017-0555-7

Kivi, M., Vergopolan, N., & Dokoohaki, H. (2023). A comprehensive assessment of in situ and remote sensing soil moisture data assimilation in the APSIM model for improving agricultural forecasting across the US Midwest. *Hydrology and Earth System Sciences, 27*(5), 1173–1199. https://doi.org/10.5194/hess-27-1173-2023

Le Page, M., Jarlan, L., El Hajj, M. M., Zribi, M., Baghdadi, N., & Boone, A. (2020). Potential for the detection of irrigation events on maize plots using Sentinel-1 soil moisture products. *Remote Sensing, 12*(10), Article 1621. https://doi.org/10.3390/rs12101621

Lowder, S. K., Skoet, J., & Raney, T. (2021). The number, size, and distribution of farms, smallholder farms, and family farms worldwide. *World Development, 87*, 16–29. https://doi.org/10.1016/j.worlddev.2015.10.041

Muluneh, A., Stroosnijder, L., Keesstra, S., & Biazin, B. (2017). Adapting to climate change for food security in the Rift Valley dry lands of Ethiopia: Supplemental irrigation, plant density and sowing date. *The Journal of Agricultural Science, 155*(5), 703–724. https://doi.org/10.1017/S0021859616000897

Mupangwa, W., Nyagumbo, I., Liben, F., Chipindu, L., Craufurd, P., & Mkuhlani, S. (2021). Maize yields from rotation and intercropping systems with different legumes under conservation agriculture in contrasting agro-ecologies. *Agriculture, Ecosystems & Environment, 306*, 107170. https://doi.org/10.1016/j.agee.2020.107170

Nakalembe, C., Becker-Reshef, I., Boniface, R., & Gray, J. (2023). A review of satellite-based global agricultural monitoring systems available for Africa. *Global Food Security, 29*, 100543. https://doi.org/10.1016/j.gfs.2021.100543

Nyamekye, A. B., Attoh, E. M. N. A. N., Dewulf, A., Werners, S. E., Van Slobbe, E., Biesbroek, R. G., Termeer, C. J. A. M., & Ludwig, F. (2021). Forecast probability, lead time and farmer decision-making in rice farming systems in Northern Ghana. *Climate Risk Management, 31*, 100258. https://doi.org/10.1016/j.crm.2020.100258

Odebiri, O., Mutanga, O., Odindi, J., Peerbhay, K., & Dovey, S. (2020). Predicting soil organic carbon stocks under commercial forest plantations in KwaZulu-Natal province, South Africa using remotely sensed data. *GIScience & Remote Sensing, 57*(4), 450–463.

https://doi.org/10.1080/15481603.2020.1731108

Rembold, F., Atzberger, C., Savin, I., & Rojas, O. (2023). Using low resolution satellite imagery for yield prediction and yield anomaly detection. *Remote Sensing, 5*(4), 1704–1733. https://doi.org/10.3390/rs5041704

Rosenstock, T. S., Mpanda, M., Rioux, J., Aynekulu, E., Kimaro, A. A., Neufeldt, H., Shepherd, K. D., & Luedeling, E. (2014). Targeting conservation agriculture in the context of livelihoods and landscapes. *Agriculture, Ecosystems & Environment, 187*, 47–51. https://doi.org/10.1016/j.agee.2013.11.011

Seyoum, S., Rachaputi, R., Chauhan, Y. S., Prasanna, B. M., & Fekybelu, S. (2018). Application of the APSIM model to exploit G × E × M interactions for maize improvement in Ethiopia. *Field Crops Research, 217*, 113–124. https://doi.org/10.1016/j.fcr.2017.12.012

Tao, F., Zhang, Z., Xiao, D., Zhang, S., Rötter, R. P., Shi, W., Liu, Y., Wang, M., Liu, F., & Zhang, H. (2014). Responses of wheat growth and yield to climate change in different climate zones of China, 1981–2009. *Agricultural and Forest Meteorology, 189–190*, 91–104. https://doi.org/10.1016/j.agrformet.2014.01.013

Tardieu, F., Simonneau, T., & Muller, B. (2018). The physiological basis of drought tolerance in crop plants: A scenario-dependent probabilistic approach. *Annual Review of Plant Biology, 69*, 733–759. https://doi.org/10.1146/annurev-arplant-042817-040218

Tsan, M., Totapally, S., Hailu, M., & Addom, B. K. (2021). *The digitalisation of African agriculture report, 2018–2019*. CTA.

van Klompenburg, T., Kassahun, A., & Catal, C. (2020). Crop yield prediction using machine learning: A systematic literature review. *Computers and Electronics in Agriculture, 177*, 105709. https://doi.org/10.1016/j.compag.2020.105709

Wairegi, L. W. I., & van Asten, P. J. A. (2010). The agronomic and economic benefits of fertilizer and mulch use in highland banana systems in Uganda. *Agricultural Systems, 103*(8), 543–550. https://doi.org/10.1016/j.agsy.2010.06.002

Wang, E., Martre, P., Zhao, Z., Ewert, F., Maiorano, A., Rötter, R. P., ... Asseng, S. (2023). The uncertainty of crop model-based yield projections is reduced by improved temperature response functions. *Nature Plants, 3*, Article 17102. https://doi.org/10.1038/nplants.2017.102

Wu, W., Wu, X., Zhang, Y. Y., & Leatham, D. (2021). Gaussian process modeling of nonstationary crop yield distributions with applications to crop insurance. *Agricultural Finance Review, 81*(5), 767–783. https://doi.org/10.1108/AFR-09-2020-0144

Yan, C., Song, S., Wang, W., Wang, C., Li, H., Wang, F., Li, S., & Sun, X. (2020). Screening diverse soybean genotypes for drought tolerance by membership function value based on multiple traits and drought-tolerant coefficient of yield. *BMC Plant Biology, 20*, Article 321. https://doi.org/10.1186/s12870-020-02519-9

Yin, X., Kropff, M. J., McLaren, G., & Visperas, R. M. (1995). A nonlinear model for crop development as a function of temperature. *Agricultural and Forest Meteorology, 77*(1–2), 1–16. https://doi.org/10.1016/0168-1923(95)02236-Q

You, J., Li, X., Low, M., Lobell, D., & Ermon, S. (2022). Deep Gaussian process for crop yield prediction based on remote sensing data. *Proceedings of the AAAI Conference on Artificial Intelligence, 31*(1), 4559–4566. https://doi.org/10.1609/aaai.v31i1.11172

Zheng, H., Cheng, T., Li, D., Yao, X., Tian, Y., Cao, W., & Zhu, Y. (2023). Combining unmanned aerial vehicle (UAV)-based multispectral imagery and ground-based hyperspectral data for plant nitrogen concentration estimation in rice. *Frontiers in Plant Science, 9*, Article 936. https://doi.org/10.3389/fpls.2018.00936

NATURE & SCIENCE
October 2026, Volume 8, Issue 5, pp. 115–121
DOI: https://doi.org/10.36719/2707-1146/68/115-121

Impact of Temperature and Humidity Variability on the Development and Epidemiology of Major Tomato Diseases under Changing Climatic Conditions

Naiba Valiyeva[1*], Gunel Ramazanova[1], Sahila Mammadova[1], and Gulnara Abbasova[1]

Abstract. *Climate variability influences crop disease epidemiology by modifying host susceptibility, pathogen development, and infection conditions. Tomato (Solanum lycopersicum L.), an economically important vegetable crop, is particularly sensitive to temperature and relative humidity fluctuations. This study evaluated the relationship between temperature and relative humidity variability and major tomato diseases under greenhouse conditions at Azerbaijan State Agricultural University (ADAU), Ganja, Azerbaijan, during the 2024 and 2025 growing seasons. Particular attention was given to late blight caused by Phytophthora infestans, powdery mildew associated with Leveillula taurica and/or Oidium neolycopersici, and gray mold caused by Botrytis cinerea. Greenhouse air temperature and relative humidity were monitored, and symptomatic plant tissues were assessed visually and microscopically. The results revealed distinct temporal and microclimatic patterns of disease occurrence. Late blight and gray mold were observed more frequently under moderate temperatures and relatively high humidity, whereas powdery mildew remained detectable under warmer and moderately humid conditions. Joint assessment of temperature and relative humidity showed that late blight and gray mold occurred primarily under moderate-temperature/high-humidity combinations, while powdery mildew was associated with moderately warm/intermediate-humidity conditions. Microscopic examination revealed morphological structures consistent with the respective disease groups, supporting symptom-based diagnosis. Late blight and gray mold occurred most frequently at 18–24 °C and 82–89% RH, whereas powdery mildew was predominantly observed at 22–28 °C and 60–78% RH. These findings indicate that temperature and relative humidity jointly influence major tomato disease occurrence patterns under greenhouse conditions. Integrating microclimatic monitoring with regular visual and microscopic disease assessment may improve disease surveillance and support climate-adaptive disease management in tomato production.*

Keywords: *Solanum lycopersicum, climate variability, greenhouse microclimate, plant disease epidemiology, temperature, relative humidity, Phytophthora infestans, Botrytis cinerea, powdery mildew*

[1]Azerbaijan State Agricultural University, Ganja, Azerbaijan
[*]Corresponding author. E-mail: naiba.valiyeva@adau.edu.az
Received: 26 May 2026; Accepted: 3 October 2026; Published online: 25 October 2026
© The Author(s) 2026. This is an open access article distributed under the terms of the Creative Commons Attribution-NonCommercial 4.0 International License (CC BY-NC 4.0).

1. Introduction

Climate change and climatic variability can influence plant disease development through simultaneous effects on pathogen biology, host physiology, and environmental conditions required for infection. Temperature, relative humidity, precipitation, atmospheric composition, and extreme weather events may alter pathogen survival, reproduction, dispersal, infection processes, and host defense responses. Consequently, the classical disease triangle—host, pathogen, and environment—must increasingly be interpreted in the context of changing climatic conditions (Coakley et al., 1999; Garrett et al., 2006; Roussin-Léveillée et al., 2024).

Recent evidence indicates that climate-driven changes in temperature may alter the infection risk and geographical distribution of fungal and oomycete crop pathogens (Chaloner et al., 2021). Climate change may also facilitate shifts in pathogen ranges and contribute to the emergence of plant disease threats in new agricultural environments (Fones et al., 2020; Singh et al., 2023).

Climate-associated environmental stresses can additionally modify plant immunity and host susceptibility. Changes in temperature and other environmental factors may affect defense signaling and host–pathogen interactions, indicating that climate change can influence disease through simultaneous effects on both the pathogen and the plant (Son & Park, 2022).

Tomato (*Solanum lycopersicum* L.) is particularly suitable for examining these interactions because its growth, flowering, reproductive development, physiology, and productivity are strongly influenced by temperature. Heat stress is an important constraint in tomato production, and recent research has emphasized the physiological and molecular basis of tomato thermotolerance (Singh et al., 2022).

In protected cultivation, greenhouse temperature and relative humidity may fluctuate substantially within short periods and may also vary spatially within the same greenhouse. Dense tomato canopies can create localized microclimates that are not fully represented by a single central measurement point. Recent commercial-greenhouse monitoring demonstrated measurable spatial and temporal variation in tomato-canopy temperature and vapor pressure deficit (Šalagovič et al., 2024). Such microclimatic heterogeneity is relevant to both crop physiology and disease development.

Temperature and moisture are among the most important environmental components governing plant disease epidemiology. Their effects are pathogen-specific and frequently nonlinear. Increasing temperature does not necessarily increase every disease; disease development depends on whether environmental conditions approach or move away from the biological optimum of the particular pathogen. Reviews of economically important tomato diseases likewise emphasize the importance of temperature and relative humidity in determining disease risk (Panno et al., 2021).

Gray mold caused by *Botrytis cinerea* is an important tomato disease in protected cultivation. Experimental work on greenhouse tomato demonstrated significant interactions among inoculum concentration, relative humidity, and temperature during *B. cinerea* infection (Eden et al., 1996). More recent experimental evidence confirms that combined temperature and humidity conditions strongly influence tomato–*B. cinerea* interactions and infection success (Li et al., 2023).

Powdery mildew represents another environmentally responsive tomato disease. Controlled experiments with *Leveillula taurica* demonstrated strong effects of relative humidity and temperature on spore germination and disease development (Guzman-Plazola et al., 2003). This contrasting response is important because powdery mildew may remain favored under environmental conditions that differ from those associated with highly moisture-dependent diseases.

2. Materials and Methods

2.1. Study Site and Experimental Conditions

The study was conducted during the 2024 and 2025 growing seasons in the greenhouse facilities of Azerbaijan State Agricultural University (ADAU), Ganja, Azerbaijan. The investigation was designed to evaluate the occurrence of major tomato diseases under greenhouse conditions and their possible association with variations in temperature and relative humidity. Tomato plants were grown according to the standard cultivation practices routinely applied in the university greenhouse.

2.2. Plant Material

Tomato (*Solanum lycopersicum* L.) plants of the cultivar/hybrid currently recorded as 'Zolushka Papagi' were evaluated during both study years.

2.3. Monitoring of Temperature and Relative Humidity

Air temperature (°C) and relative humidity (%) inside the greenhouse were monitored during the experimental period. Measurements were performed by students participating in the study. The environmental records were organized according to the corresponding disease observation periods and were used to investigate temporal associations between greenhouse microclimatic conditions and disease occurrence.

2.4. Disease Monitoring and Symptom Assessment

Tomato plants were regularly examined for naturally occurring disease symptoms. Assessment included visual examination of leaves, stems, flowers, and fruits. Particular attention was given to late blight associated with *Phytophthora infestans*, powdery mildew associated with *Leveillula taurica* and/or *Oidium neolycopersici*, and gray mold associated with *Botrytis cinerea*. The presence of disease was initially evaluated on the basis of characteristic macroscopic symptoms and signs. Symptomatic plant material was subsequently collected for microscopic examination.

2.5. Microscopic Examination of Symptomatic Plant Material

Plant tissues showing characteristic disease symptoms were collected from affected tomato plants and subjected to microscopic examination. Prepared specimens were examined using a light microscope. Macroscopic symptoms and microscopic morphological characteristics were considered together for disease identification. Identification is therefore interpreted as morphology-supported diagnosis rather than molecular confirmation.

2.6. Assessment of Disease Occurrence

Because quantitative disease severity assessments were not performed, disease occurrence was evaluated according to the presence or absence of characteristic symptoms during individual observation periods. For each disease, observations were organized according to sampling date and corresponding greenhouse temperature and relative humidity conditions.

2.7. Analysis of Microclimate–Disease Relationships

Temperature and relative humidity measurements were aligned with corresponding disease observation dates. Environmental conditions recorded during periods in which late blight, powdery mildew, and gray mold symptoms were observed were compared descriptively with periods in which the corresponding symptoms were not recorded. Because standardized disease severity measurements were not performed, the analysis was designed primarily to evaluate associations between microclimatic conditions and disease occurrence rather than quantitative changes in disease severity.

3. Results

3.1. Greenhouse Temperature and Relative Humidity Dynamics

Considerable variation in greenhouse temperature and relative humidity was observed during the 2024 and 2025 growing seasons. In the dataset, mean air temperature ranged from 18.6 to 29.4 °C, while relative humidity varied between 58.2 and 88.5%. Cooler observation periods were characterized by lower mean temperatures and relatively high humidity, whereas warmer periods generally showed higher temperatures and lower relative humidity.

Table 1

Temperature and relative humidity data

Observation period	Mean temp. (°C)	Min temp. (°C)	Max temp. (°C)	Mean RH (%)
April 2024	19.2	14.8	25.1	82.4
May 2024	21.8	16.7	27.6	78.3
June 2024	25.4	19.5	31.8	70.6
July 2024	28.7	22.4	35.2	61.8
April 2025	18.6	13.9	24.7	85.6
May 2025	22.1	16.4	28.9	80.2
June 2025	26.2	20.1	32.7	72.4
July 2025	29.4	23.0	36.1	58.2

3.2. Occurrence of Major Tomato Diseases

Visual examination revealed temporal differences in the occurrence of the major diseases investigated. In the pattern, late blight and gray mold occurred more frequently during periods characterized by moderate temperatures and relatively high humidity, whereas powdery mildew remained detectable during warmer and moderately humid periods.



Figure 1

Representative symptoms of major tomato diseases observed under greenhouse conditions during 2024–2025

Table 2

Disease-occurrence pattern under different greenhouse microclimatic conditions

Disease	Temperature (°C)	RH (%)	Occurrence
Late blight	18–23	82–89	Frequent
Gray mold	18–24	81–88	Frequent
Powdery mildew	22–28	60–78	Frequent

3.3. Microscopic Examination of Symptomatic Tissues

Microscopic examination supported the symptom-based assessment of the major disease groups observed in the greenhouse. Symptomatic tissues showed morphological structures consistent with the respective disease groups. Because pathogen identification was based on symptomatology and microscopic morphology rather than molecular methods, the microscopic findings should be interpreted as morphological support for diagnosis.

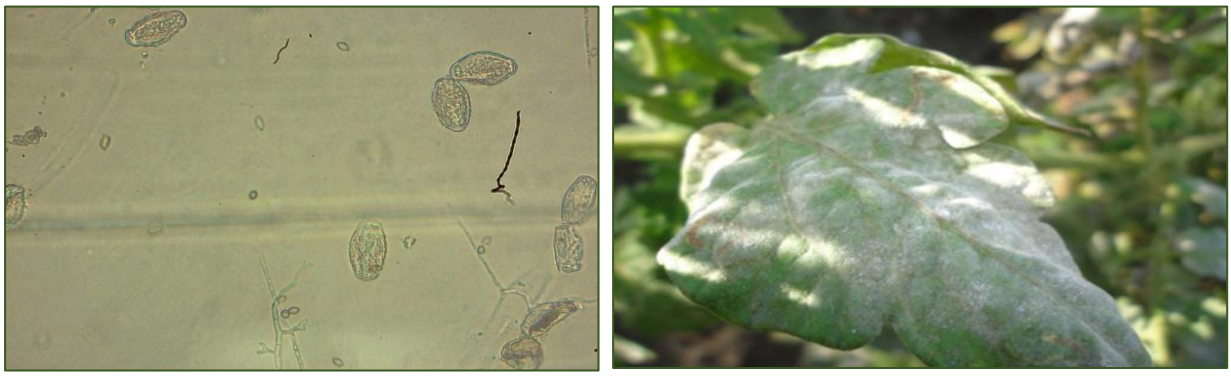


Figure 2

Representative microscopic structures observed in symptomatic tomato tissues

3.4. Association Between Relative Humidity and Disease Occurrence

In the dataset, periods of elevated relative humidity coincided more frequently with late blight and gray mold observations, whereas powdery mildew was more frequently represented at intermediate relative humidity.

Table 3

Association between relative humidity and disease occurrence

Relative humidity	Late blight	Gray mold	Powdery mildew
<65%	8%	6%	28%
65–79%	18%	17%	51%
≥80%	74%	77%	21%

3.5. Association Between Temperature and Disease Occurrence

The distribution suggested that late blight and gray mold were most frequently observed at moderate temperatures, whereas powdery mildew was more frequent at moderately warm temperatures.

Table 4

Association between temperature and disease occurrence

Temperature class	Late blight	Gray mold	Powdery mildew
<18 °C	12%	14%	5%
18–23 °C	68%	58%	24%
24–28 °C	17%	24%	66%
>28 °C	3%	4%	5%

3.6. Combined Effects of Temperature and Relative Humidity

The occurrence patterns indicate that temperature and relative humidity should be interpreted jointly. Late blight and gray mold were represented primarily under moderate-temperature/high-humidity combinations, whereas powdery mildew showed a contrasting pattern under moderately warm/intermediate-humidity conditions.

4. Discussion

The study was designed to examine the relationship between greenhouse temperature and relative humidity and the occurrence of major tomato diseases during the 2024 and 2025 growing seasons. The working results suggest that the investigated disease groups may show distinct environmental patterns, emphasizing that climate–disease relationships should be interpreted at the individual pathosystem level rather than assuming a uniform response of all pathogens to warming or increased humidity.

This interpretation is consistent with the disease-triangle framework, in which disease development depends on interactions among a susceptible host, a virulent pathogen, and a conducive environment. Climate change and climatic variability can modify each component by influencing host physiology, pathogen biology, and environmental suitability for infection (Coakley et al., 1999; Garrett et al., 2006; Roussin-Léveillée et al., 2024).

In greenhouse production, microclimate deserves particular attention because temperature and relative humidity may change substantially within short periods. For gray mold, the expected association with humid greenhouse conditions is biologically plausible. Eden et al. (1996) experimentally demonstrated significant interactions among inoculum concentration, relative humidity, and temperature during *Botrytis cinerea* infection of greenhouse tomato.

Microscopic examination is an important strength of the present study because it provides morphological support for visual diagnosis. Nevertheless, microscopy does not provide the same taxonomic resolution as molecular identification. Species-level names should therefore be used conservatively when diagnostic structures are not unequivocal, particularly for powdery mildew.

A principal limitation of the study is the absence of a standardized disease-severity scale. Accordingly, the findings should be interpreted in terms of disease occurrence and environmental association rather than quantitative disease intensity. Future studies should record the total number of examined plants and the number of symptomatic plants at each observation date, permitting calculation of disease incidence and more robust statistical analysis.

5. Conclusion

The study provides a framework for evaluating the relationship between greenhouse microclimatic variability and the occurrence of major tomato diseases. Monitoring conducted during the 2024 and 2025 growing seasons combined greenhouse temperature and relative humidity measurements with visual and microscopic examination of symptomatic tomato plants.

Acknowledgements
The authors gratefully acknowledges Azerbaijan State Agricultural University for providing greenhouse and laboratory facilities for the study and thanks the students who participated in greenhouse monitoring and assisted with recording temperature and relative humidity data.

Conflict of Interest
The authors declare no conflict of interest.

Funding
This research received no external funding.

Data Availability Statement

The data generated during the study are available from the corresponding author upon reasonable request.

References

Chaloner, T. M., Gurr, S. J., & Bebber, D. P. (2021). Plant pathogen infection risk tracks global crop yields under climate change. *Nature Climate Change, 11*, 710–715. https://doi.org/10.1038/s41558-021-01104-8

Coakley, S. M., Scherm, H., & Chakraborty, S. (1999). Climate change and plant disease management. *Annual Review of Phytopathology, 37*, 399–426. https://doi.org/10.1146/annurev.phyto.37.1.399

Eden, M. A., Hill, R. A., Beresford, R., & Stewart, A. (1996). The influence of inoculum concentration, relative humidity, and temperature on infection of greenhouse tomatoes by *Botrytis cinerea*. *Plant Pathology, 45*(4), 795–806. https://doi.org/10.1046/j.1365-3059.1996.d01-163.x

Fones, H. N., Bebber, D. P., Chaloner, T. M., Kay, W. T., Steinberg, G., & Gurr, S. J. (2020). Threats to global food security from emerging fungal and oomycete crop pathogens. *Nature Food, 1*, 332–342. https://doi.org/10.1038/s43016-020-0075-0

Garrett, K. A., Dendy, S. P., Frank, E. E., Rouse, M. N., & Travers, S. E. (2006). Climate change effects on plant disease: Genomes to ecosystems. *Annual Review of Phytopathology, 44*, 489–509. https://doi.org/10.1146/annurev.phyto.44.070505.143420

Guzman-Plazola, R. A., Davis, R. M., & Marois, J. J. (2003). Effects of relative humidity and high temperature on spore germination and development of tomato powdery mildew (*Leveillula taurica*). *Crop Protection, 22*(10), 1157–1168. https://doi.org/10.1016/S0261-2194(03)00157-1

Li, T., Zhou, J., Yuan, Z., Liu, R., & Li, J. (2023). Intermittent changes in temperature and humidity repress gray mold in tomato. *Plant Disease, 107*(2), 306–314. https://doi.org/10.1094/PDIS-03-22-0607-RE

Panno, S., Davino, S., Caruso, A. G., Bertacca, S., Crnogorac, A., Mandić, A., Noris, E., & Matić, S. (2021). A review of the most common and economically important diseases that undermine the cultivation of tomato crop in the Mediterranean Basin. *Agronomy, 11*(11), 2188. https://doi.org/10.3390/agronomy11112188

Roussin-Léveillée, C., Rossi, C. A. M., Castroverde, C. D. M., & Moffett, P. (2024). The plant disease triangle facing climate change: A molecular perspective. *Trends in Plant Science, 29*(8), 895–914. https://doi.org/10.1016/j.tplants.2024.03.004

Šalagovič, J., Vanhees, D., Verboven, P., Holsteens, K., Verlinden, B., Huysmans, M., Van de Poel, B., & Nicolaï, B. (2024). Microclimate monitoring in commercial tomato (*Solanum lycopersicum* L.) greenhouse production and its effect on plant growth, yield and fruit quality. *Frontiers in Horticulture, 3*, 1425285. https://doi.org/10.3389/fhort.2024.1425285

Singh, B. K., Delgado-Baquerizo, M., Egidi, E., Guirado, E., Leach, J. E., Liu, H., & Trivedi, P. (2023). Climate change impacts on plant pathogens, food security and paths forward. *Nature Reviews Microbiology, 21*, 640–656. https://doi.org/10.1038/s41579-023-00900-7

Singh, A. K., Mishra, P., Kashyap, S. P., Karkute, S. G., Singh, P. M., Rai, N., Bahadur, A., & Behera, T. K. (2022). Molecular insights into mechanisms underlying thermo-tolerance in tomato. *Frontiers in Plant Science, 13*, 1040532. https://doi.org/10.3389/fpls.2022.1040532

Son, S., & Park, S. R. (2022). Climate change impedes plant immunity mechanisms. *Frontiers in Plant Science, 13*, 1032820. https://doi.org/10.3389/fpls.2022.1032820

CONTENTS

Ghulam Murtaza, Muhammad Usman, Rashid Iqbal
Acacia nilotica Biochar Improves Sandy Soil Structure and Stimulates Root Development in Muscat Grape 7
Turkan Hasanova, Tariverdi Islamzade, Gunay Mammadova, Muhammad Mubashar Zafar
Soil Organic Matter and Its Fractions at Different Stages of Soil Salinization, as well as Their Resistance to Decomposition in Relation to Soil Bioactivity 21
Lala Bunyatova, Parvin Omar, Aida Gahramanova
Biotechnological Evaluation of Fungal Strains Isolated from Extreme Habitats Based on Their Enzymatic and Antimicrobial Properties 28
Tinatin Mshvidobadze
Navigating Transformative Agricultural Technologies on the Path to Food System Transformation 34
Shafeequr Rahman Khan, Saba Siddiqui, Iqbal Ahmad, Firoz Ahmad Ansari, Sheeba Khan
Current Understanding of PGPR–Plant Interaction under Salt Stress Environment: A Review 40
Mahir Hajiyev, Yasin Gozalov, Zohrab Suleymanov, Kanan Aliyev
Effects of Bread Waste Flour Utilization in Cattle Diets on Milk and Meat Productivity..... 61
Nigar Hashimova, Sevinj Hajiyeva
Ecochemical Assessment of Synthetic Pesticide Residues in a Tomato Sample Grown in Azerbaijan: Analysis of Plant Extract-Based Biopesticides as a Promising Alternative 70
Miebaka Emmanuel Ikiriko, Isaac Glory Chimamanda, Idiami Victoria Ogie
Contamination Level Determines Whether Soil-Applied Zinc Oxide Nanoparticles Limit Cadmium Uptake in Maize..... 78
Ramig Mammadzada, Ismat Ahmadov, Farayat Ahmadova, Ziyaddin Mammadov, Yashar Feyziyev
Integrated Biophysical Assessment of the Effect of Zinc Oxide Nanoparticles on the Photosynthetic Apparatus of Spinach (*Spinacia oleracea* L.)..... 89
Sevil Babayeva, Gunay Nasibova, Shalala Huseynova
Ontogenetic Structure of a Cenopopulation of *Astragalus Cicer* L. in the Northeastern Lesser Caucasus 97
Jean de Dieu Niyomugabo, Victoire Ayingeneye, Angelique Nyiramahoro, Marie Ange Cyuzuzo
Nonlinear Mathematical Modeling of Crop Growth and Biomass Accumulation for Accurate Yield Prediction in Smallholder Farming Systems 104
Naiba Valiyeva, Gunel Ramazanova, Sahila Mammadova, Gulnara Abbasova
Impact of Temperature and Humidity Variability on the Development and Epidemiology of Major Tomato Diseases under Changing Climatic Conditions 115

Editorial address
AZ1073
19 A.M.Sharifzade St., Yasamal Dist.,
Baku, Azerbaijan
Phone: +994 99 805 67 68
+994 99 808 67 68
e-mail: nature.science2000@aem.az

Signed: 19.10.2026
Online publication: 25.10.2026
Paper printing: 10.10.2026
Format: 60/84, 1/8
Stock issuance: 13, 25 p.s..
Order: 242

It has been published in the printing house
"ZANGAZURDA"
Address: 19 A.M.Sharifzade St.,
Yasamal Dist., Baku, Azerbaijan
Phone: +994 50 209 59 68
e-mail: zengezurda1868@mail.ru